Dissertation

Submitted to the

Combined Faculties for the Natural Sciences and for Mathematics

of the Ruperto-Carola University of Heidelberg, Germany

for the degree of

Doctor of Natural Sciences

Presented by

Rana Roy

Diplom – M.Sc. in Biochemistry from University of Calcutta, India

Born in: Purulia, India

Oral examination:

Thesis Title

Biochemical Analysis of SNARE Protein Interactions – Role of Transmembrane Domain

Referees: Prof. Dr. Dieter Langosch

Dr. Christian Ungermann

This thesis is dedicated to my parents,
My mother Smt. Sunita Roy and My father Sri Saradindu Roy
Without their encouragement I could not have reach this step

Acknowledgements

I am grateful to Prof. Dr. Dieter Langosch for his kindness to offer me such a good opportunity to work in his esteemed laboratory and for his patient, charismatic and perfect guidance and supervision.

I thank Dr. Cristian Ungermann for agreeing to act as my second supervisor.

I would like to thank Walter Stelzer, Dr. Markus Gütlich and Mathias Hofmann for their expertise help in computer.

I would like to thank Dr. Thomas Letzel, Eric Lindner, Dr, Anja Ridder, Dr. Weiming Ruan, Stephanie Unterreitmeier, Bernhard Poschner, Dr. Jan Rohde, Dr. Rolf Gurezka, for the fantastic atmosphere and discussion in lab as well as the technical assistance of Bettina Brosig, Barbara Rauscher and Anna Baller.

Special thanks to Dr. Laura Mascia for continuous support and help to complete this thesis.

I would like to thank all my friends for their continuous encouragement and help.

The final thanks go to my family. I want to thank my brother and sister-in-law for their constant encouragement.

Declaration

I hereby declare that I wrote this thesis independently and used no other sources and aids than those indicated.

…….. ……..

(Rana Roy) (Date)

Contents

List of Figures

List of Tables

1. Abstract

SNARE (soluble NSF attachment protein receptor) proteins comprise distinct families of proteins conserved from yeast to human, which are essential for membrane fusion in cellular processes like vesicle trafficking, neurotransmitter release or yeast vacuole fusion. Prior to membrane fusion, SNARE assemble to form a stable complex, that according to the “zipper” model starts from the cytosolic domain and is propagated to the transmembrane domain (TMD). Previous evidence indicated that the TMD of SNARE proteins has not only the role of anchoring the protein to the membrane but is important for the function. In this work, I investigated the role of TMD in assembly of the neuronal SNARE synaptobrevin II and of the yeast vacuolar SNAREs.

Homodimerization of the neuronal SNARE synaptobrevin II, involved in the neurotransmitter release, previously was shown by different authors to depend on its TMD. Here synaptobrevin II Homodimerization was shown to be preserved better in the presence of urea than in its absence. At the same time, urea is not affecting α-helical structure of its TMD as detected by CD measurement.

The role of TMD in yeast vacuolar SNARE protein assembly is here characterized under native conditions. Sucrose gradients showed that the vacuolar SNARE Vam3p forms a homodimer that is clearly dependent on its TMD, while Nyv1p and Vti1p self-interactions are not dependent on their TMD. The other vacuolar SNARE proteins Vam7p and Ykt6p, lacking a TMD, are detected mainly as monomers.

In vitro assembly of vacuolar full length SNARE complex composed by Vam3p, Nyv1p, Vam7p and Vti1p was studied by sucrose gradient coupled to co-immunoprecipitation. The *in vitro* assembled complex was specifically disassembled by Sec18p and Sec17p in presence of ATP, like native SNARE complexes, demonstrating its biological relevance. Moreover, SNARE complex assembly is modulated by the Vam3p TMD as its deletion leads to partial formation of unspecific multimers. *In vitro* assembly of cytosolic SNARE complex, in which TMD has been deleted from all proteins, is also studied. In comparison with the full length SNARE complex, high molecular weight multimers were detected here. A pentameric SNARE complex with Ykt6p could not be identified in the present experimental condition.

2 Introduction

2.1 Cell membranes and membrane proteins

The boundaries of cells are formed by biological membranes, the barriers that define the inside and the outside of a cell. These barriers prevent molecules, generated inside the cell, from leaking out and unwanted molecules from diffusing in, yet they also contain transport systems that allow specific molecules to be taken up and unwanted compounds to be released from the cell. In order to fulfill this task membranes are dynamic structures of lipid and proteins, where lipid components form the permeability barrier and protein components act as a transport system of pumps and channels that endows the membrane with selective permeability. In addition to an external cell membrane, called plasma membrane, eukaryotic cells also contain internal membranes that form boundaries of organelles such as mitochondria, chloroplasts, peroxisomes, lysosomes etc.

The specific function of a particular membrane is mostly determined by proteins residing in membrane. The importance of membrane proteins can be inferred from the fact that in each organism around 25-30% of all genes code for membrane proteins. Peripheral membrane proteins are associated with the bilayer through electrostatic and/or hydrophobic interactions with the surface of the membrane. In contrast, integral membrane proteins actually traverse the membrane with one or more transmembrane domains. Because the membrane interior is apolar, the peptide bonds, present in polypeptides traversing the bilayer, form hydrogen-bonds with each other, therefore protein segments generally span membrane in two manners: as an α-helix or a β-barrel (Figure 1).

The endoplasmic reticulum (ER) is the site of protein synthesis. Thus the ER is the main machinery to translocate integral membrane proteins to the membrane. The majority of membrane proteins utilize the signal recognition particle (SRP) dependent pathway to be incorporated into membrane (High and Dobberstein, 1992). Cleavable signal peptides or signal anchors mediate the insertion of protein into the membrane. The Sec61 complex, localized on ER, acts as translocation machinery in which a protein complex composed of α,β,γ subunits and TRAM (translocating chain-

associated membrane protein) inserts proteins into the membrane. A special type of membrane protein, known as “tail-anchored” proteins, are synthesized on free ribosomes and inserted into ER membrane post-translationally without SRP and Sec61 involvement. Thus membrane proteins reside on plasma membranes and/or on other many compartments of the cell that are originating from ER, the first compartment of the secretory pathway. The synthesized proteins travel through cargo vesicles from ER to different target compartments and those cargo vesicles fuse to the target membrane to deliver the molecules.

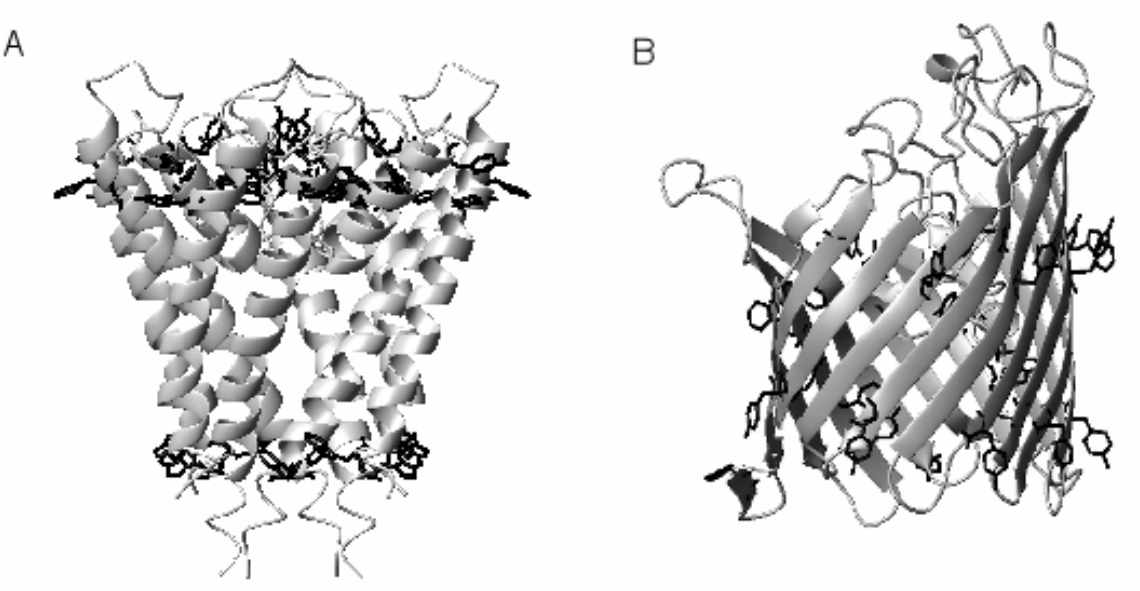

Figure 1. **Structure of two prototypical membrane proteins**. A, the α-helical potassium channel from *Steptomyces lividans*. ((Cowan et al., 1992), PDB access code [1BL8]) B, the β-barrel protein PhoE from *Escherichia coli*. ((Doyle et al., 1998), PDB access code [1PHO])

2.2 Membrane fusion and importance of SNARE proteins

Membrane fusion is essential for the life of eukaryotic cells. At least three types of biological membrane fusion can be distinguished (Jahn et al., 2003):

1. Extra- and intracellular fusion of pathogens with host cells. Among these, fusion of enveloped viruses (influenza virus, HIV), in which the entire reaction is carried out by a single protein, is the best characterized example.
2. Extracellular fusion of eukaryotic cells. Examples are fusion of sperm with oocytes or formation of syncytia of muscle cells.

3. Intracellular fusion of organelles. These reactions are mediated by dynamic supramolecular assemblies involving conserved protein families such as SNARE proteins [Soluble N-ethyl maleimid-sensitive factor (NSF) attachment protein receptor].

Intracellular vesicular transport follows defined routes requiring mechanisms for mutual recognition and attachment of the membrane to be fused. Different members of the SNARE protein family fulfill this function in the secretory and the endocytic pathways (e.g. ER, Golgi, endosomes, lysosomes, transport and secretory vesicles and the plasma membrane) (Guo et al., 2000; Pelham, 2001; Zerial and McBride, 2001). A reconstituted proteoliposome fusion assay demonstrated that SNAREs can act as a minimal machinery of intracellular fusion (Weber et al., 1998). The best characterized SNARE proteins are those mediating neurotransmitter release (exocytosis) from presynaptic vesicles (Sollner et al., 1993a; Sollner et al., 1993b). The three proteins involved in this reaction are syntaxin 1A (Bennett et al., 1992), SNAP-25 (25 kDa synaptosome associated protein) (Oyler et al., 1989) and synaptobrevin II, also known as vesicle associated membrane protein (VAMP II) (Baumert et al., 1989; Trimble et al., 1988). In particular, syntaxin 1A and synaptobrevin II are attached to the membrane by a C-terminus single membrane spanning domain and SNAP-25 is attached to the membrane by palmitoylation of four cysteine residues in the central region of the protein (Hess et al., 1992). SNAREs were originally classified into two groups: v-SNAREs, which are associated with vesicle membranes, and t-SNAREs, which are associated with target membranes. In the above example, synaptobrevin II is a v-SNARE while syntaxin 1A and SNAP-25 are t-SNAREs (Sollner et al., 1993b). However, it was found that v-SNARE and t-SNARE can coexist on vesicles or target membranes (e.g. in homotypic vacuole fusion as shown in Figure 2). Therefore to avoid confusion, SNARE proteins were reclassified as R-SNARE (arginine containing SNAREs, e.g. synaptobrevin II) and Q-SNARE (glutamine containing SNAREs, e.g. syntaxin 1A and SNAP-25), based on a highly conserved glutamine (Q) or arginine (R) residue in their SNARE domain (Fasshauer et al., 1998b). All SNARE proteins share a homologous cytoplasmic domain, termed SNARE motif (Weimbs et al., 1997), that mediates their association in the core complex via formation of parallel coiled-coil (Jahn and Sudhof, 1999). Formation of this structure, starting from the N-termini, may directly precede fusion (Hanson et al., 1997a; Hay and Scheller, 1997).

Membrane fusion mediated by SNARE proteins can be divided into three different steps – priming, docking and fusion (Conradt et al., 1994; Mayer and Wickner, 1997; Mayer et al., 1996; Ungermann et al., 1998a; Ungermann et al., 1998b). Schematic representation of these three steps with comparison of heterotypic (neurotransmitter release) and homotypic fusion (yeast vacuole fusion) are explained in Figure 2.

Two groups of components with their cofactors are involved in the different fusion steps: Rab proteins and SNAREs. Rab proteins constitute a family of conserved GTPases which are localized in different compartments (Novick and Zerial, 1997; Zerial and McBride, 2001). Several large effector complexes have been identified as tethering factor [e.g. EEA1 (involved in early endosome) (Christoforidis et al., 1999; Gorvel et al., 1991), TRAPP (involved in vesicle fusion to Golgi) (Barrowman et al., 2000; Sacher and Ferro-Novick, 2001; Sacher et al., 1998), HOPS (involved in vacuole fusion) (Price et al., 2000a; Price et al., 2000b; Sato et al., 2000; Seals et al., 2000)] for Rab GTPases and those are required for an initial binding of the fusion partners (Figure 2, panel A). Rab GTPases and tethering factors are intimately linked to SNAREs. The localization of Rabs and SNAREs shows significant but not absolute compartment specificity. Therefore, specificity of transport could be achieved in a combinatorial fashion relying on the combination of particular Rab proteins with particular tethering factors and SNAREs for certain trafficking routes (Mayer, 2001; Mayer, 2002).

In homotypic fusion Q- and R-SNAREs are forming complexes in the same membrane (*cis*-complexes) (Figure 2, Panel A). These *cis*-complexes can be disrupted (Fasshauer et al., 2002; Fasshauer et al., 1997a; Fasshauer et al., 1997b; Nichols et al., 1997; Ungermann et al., 1998b; Ungermann et al., 1999a) by the ATP-driven chaperon NSF (Whiteheart et al., 1992; Wilson and Rothman, 1992; Wilson et al., 1992) and its cofactor α-SNAP (Clary et al., 1990; Clary and Rothman, 1990; Whiteheart et al., 1993), yielding activated SNAREs, which are then competent to form trans-SNARE complexes, defined as association between Q- and R-SNAREs from the opposing membranes (Figure 2, panel A) (Banerjee et al., 1996; Hanson et al., 1997b; Hay and Scheller, 1997; Mayer et al., 1996; Ungermann et al., 1998b). In homotypic fusion, formation of *trans*-complexes mediates docking, the second stage of the membrane attachment, thus yielding close and strong apposition of the two

membranes. The last step, lipid mixing of the two adjacent bilayers (fusion) occurs after formation of the *trans*-complexes, and it is triggered by Ca^{2+} ion (Peters and Mayer, 1998; Ungermann et al., 1999b; Wada et al., 1997).

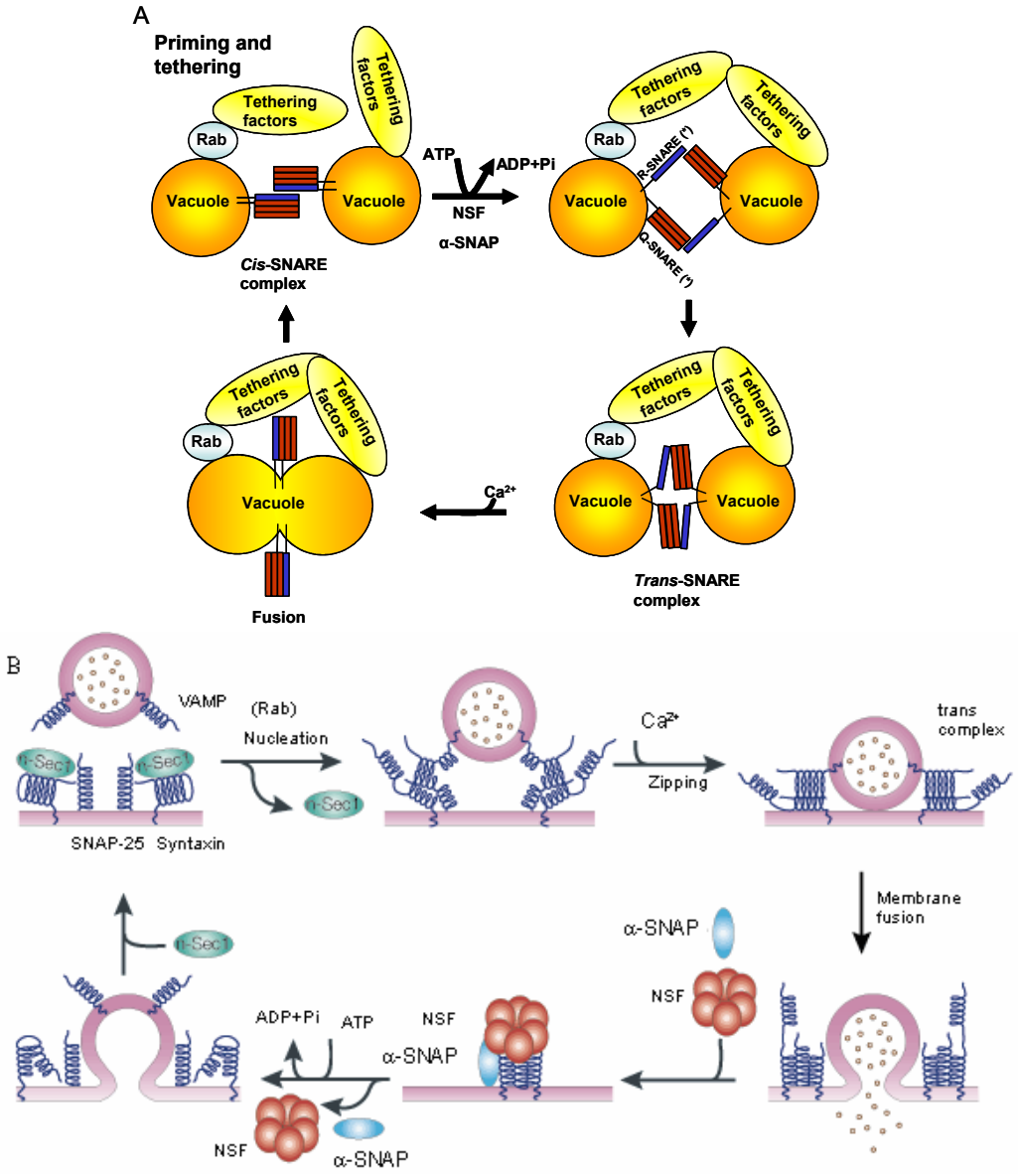

Figure 2. **Mechanism of SNARE-mediated membrane fusion**. A, Homotypic fusion, Mutual recognition and attachment of membranes during fusion depends on Rabs, SNAREs and tethering factors. Rab proteins cooperate with large complexes of the tethering factors to mediate an initial interaction (priming). The ATPase NSF and α-SNAP disrupt *cis*-SNARE complexes (SNARE complexes on the same membrane) by ATP hydrolysis and activate (prime) SNAREs (*) to form *trans*-complexes between the membrane (docking), which probably coincides with close apposition of the membranes. The final step is mixing of lipid bilayer (fusion). Adapted and modified from the reference (Mayer, 2001). B, Heterotypic fusion, Syntaxin 1A is bound to n-Sec1 before formation of the core complex. Rab proteins might facilitate the dissociation of n-Sec1 from syntaxin, allowing subsequent binding between the three neuronal SNAREs; syntaxin, SNAP-25 and VAMP (for simplicity, only one coil is drawn for SNAP-25) (docking). Ca^{2+} triggers the full zipping of the coiled-coil complex (priming), which results in membrane fusion and release of vesicle contents. After the fusion event, recruitment of α-SNAP and NSF from cytoplasm and subsequent hydrolysis ATP by NSF causes dissociation of the SNARE complex. Syntaxin, VAMP and SNAP-25 are then free for recycling and another round of exocytosis (Chen and Scheller, 2001).

Homotypic and heterotypic fusion events share many common steps, but also some typical differences. The two sequential steps: priming and docking of homotypic fusion are inverted in heterotypic fusion (Broadie et al., 1995; Hunt et al., 1994; Schulze et al., 1995). In heterotypic fusion it has not been yet identified a “clear” *cis*-complex, as for homotypic fusion (Figure 2, panel A); thus “true” priming step, where ATP driven NSF/α-SNAP disrupts the *cis*-complex, cannot be described. In heterotypic membrane fusion NSF/α-SNAP are required after the membrane fusion, in order to release individual SNARE proteins from the complex, thus allowing another round of exocytosis (Figure 2, panel B). Calcium ion is playing important role in heterotypic fusion (Chen et al., 1999) as well as in homotypic fusion. The probable mechanism for lipid mixing is described below.

2.3 SNARE hypothesis and membrane fusion

Membranes do not fuse spontaneously because the repulsive energy between two opposing phospholipids membranes in an aqueous environment is very high. These forces need to be overcome in order to reach the metastable transition state that leads to fusion (Jahn and Grubmuller, 2002; Jahn et al., 2003; Jahn and Sudhof, 1999). Two extreme hypotheses of membrane fusion have been proposed. Some authors (Jahn and Sudhof, 1999; Mayer, 2001; Mayer, 2002; Monck et al., 1995) postulate that fusion of membranes is primarily mediated by phospholipids (stalk formation), with the role of proteins restricted to reducing the activation energy and spatially organizing the fusion site. According to this hypothesis, fusion of lipid membranes requires at least five distinct steps: approach to short distance, local perturbation of the lipid structure and merger of proximal monolayers, stalk formation, stalk expansion, known as hemifusion, and finally mixing of second layer or full fusion (Figure 3 panel A) (Chernomordik et al., 1987; Jahn and Grubmuller, 2002; Kozlov and Markin, 1983).

Other authors (Almers and Tse, 1990; Jahn et al., 2003; Jahn and Sudhof, 1999; Lindau and Almers, 1995; Mayer, 1999; Mayer, 2001; Mayer, 2002) propose initial fusion pore formation with transmembrane proteins and lipids. The fusion pore is depicted as a channel that spans two opposing membranes and forms oligomeric ring structure. Thus, the aqueous fusion pore would be initially lined by proteins and only subsequently invaded by phospholipids (Figure 3, panel B). The model implies

that nonbilayer transition states of the fusing membrane are governed by protein-lipid interactions, which may be both hydrophilic and hydrophobic. The proteins could guide the lipids at the contact sites through non bilayer structures that they may not form in the absence of the proteins.

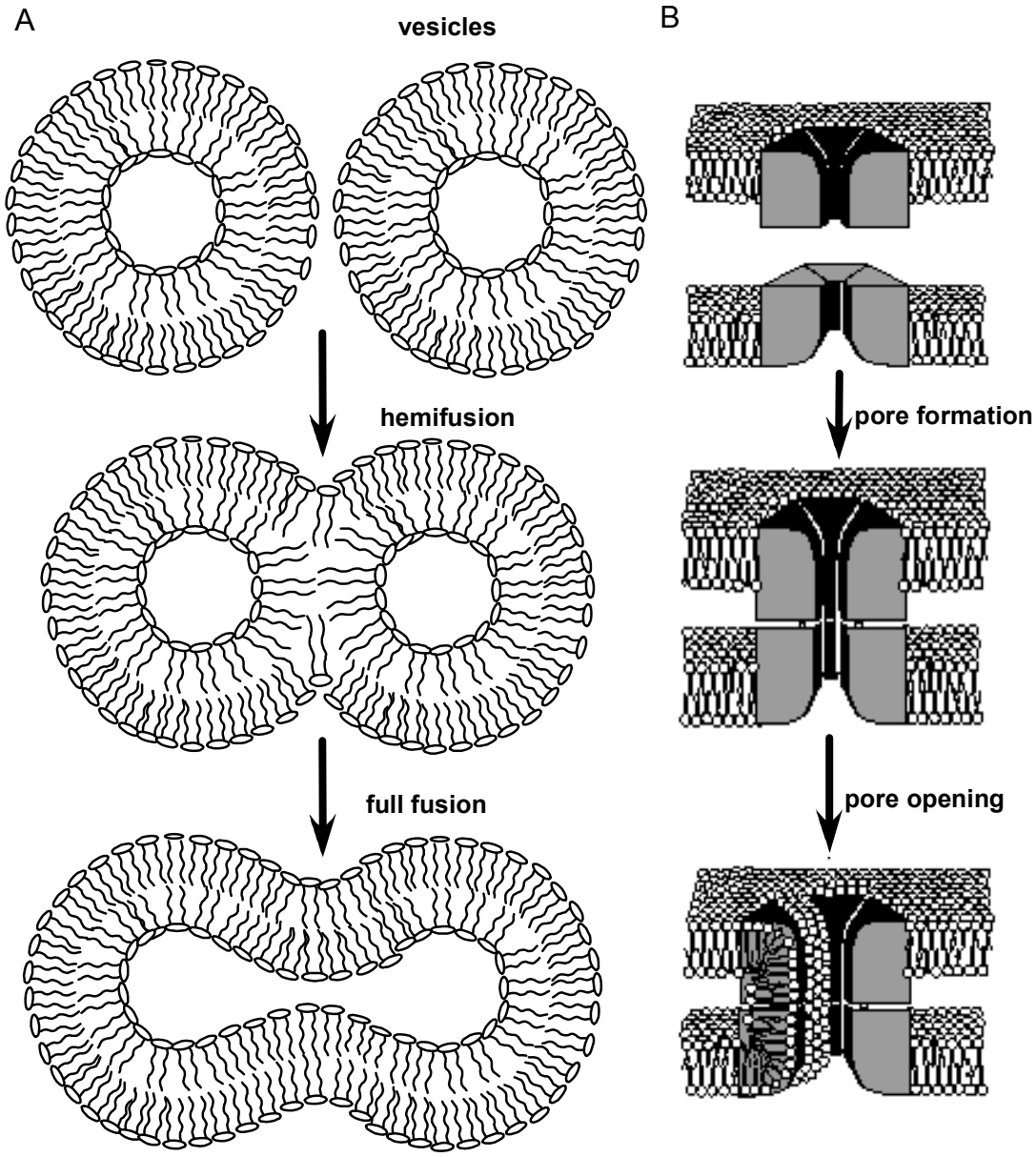

Figure 3. **Models for membrane fusion**. A, Stalk hypothesis, vesicles approach to close contact followed by local perturbation of lipid structure and merger of outer monolayer (hemifusion). Finally, inner monolayer mixing produces the full fusion. B, Fusion pore model. A continuous proteinaceous assembly forms between membranes. The pore subunits partially dissociate in the plane of the membrane, leading to the radial opening of this proteinaceous pore (ROPP). Concomitant with this, lipids invade the amphiphilic clefts between the subunits, enabling their migration between the membranes. Adapted and modified from reference (Mayer, 2002). Other proteins involved in membrane fusion are omitted to simplify the picture.

SNARE hypothesis postulates that the assembly of SNAREs mediates the attachment of membranes before fusion and that NSF-driven disassembly would lead to fusion completion. Furthermore, v-SNARE and t-SNARE interactions determine the specificity of intracellular vesicle traffic, i.e. that a single SNARE would function only in a single trafficking step (Rothman, 1994a; Rothman, 1994b; Sollner et al., 1993a; Sollner et al., 1993b). This hypothesis was the first attempt to intigrate SNAREs membrane localization and the assembly-disassembly cycle of SNAREs with membrane fusion. Later it was discovered that NSF does not participate in fusion itself, as already described (Figure 2) it is required after (in heterotypic fusion (Banerjee et al., 1996; Bittner and Holz, 1992; Littleton et al., 1998)) or before (in homotypic fusion (Mayer and Wickner, 1997; Mayer et al., 1996)) fusion step to release individual SNAREs. Different studies questioned the specificity of SNARE pairing since recombinant cytoplasmic domains of SNARE proteins interacted promiscuously in binding assay (Fasshauer et al., 1999; Yang et al., 1999). On the other hand, in liposome or cellular fusion experiments, recombinant full-length SNAREs interact specifically (Brugger et al., 2000; Scales et al., 2000). These results suggest that SNARE pairing in lipid bilayers may be more specific than in solution. Another hypothesis proposed that the specificity can be determined by a combination of SNARE protein complex with Rab proteins, tethering factors etc (Figure 2) (Mayer, 2001; Mayer, 2002). However it is still matter of debate, whether such activity is sufficient to account for the precise and fast fusion necessary within the cells.

2.4 Structure of SNARE interaction domain

SNARE proteins are typically characterized by the presence of SNARE motif, approximately 60-70 residues length, located immediately adjacent to a C-terminus transmembrane anchor (Weimbs et al., 1997). The SNARE motif consists of heptad repeat pattern of residues, spaced such that the adoption of an α-helical structure places all the relevant side chains on the same face of the helix (Ungar and Hughson, 2003). In *trans*-SNARE complex formation the SNARE motifs assemble into parallel four helix bundles (3 Q-SNAREs and 1 R-SNARE), stabilized by the burial of these helix faces in the bundle core (Figure 4) (Antonin et al., 2002; Poirier et al., 1998b; Sutton et al., 1998). Investigators have visualized two different SNARE complexes (the synaptic SNARE and endosomal SNARE) at high resolution using X-

ray crystallography. This landmark structure revealed that an arginine (R) and three glutamine (Q) residues compose a polar layer by forming a hydrogen-bonded network sequestered from the solvent (Antonin et al., 2002; Sutton et al., 1998).

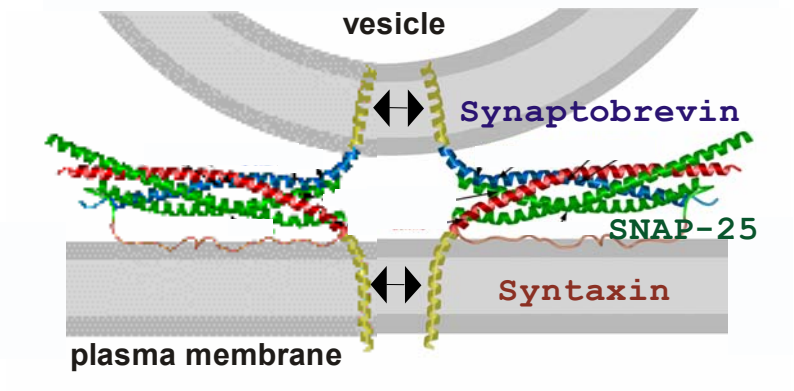

Figure 4. **Neuronal SNARE core complex with SNARE domain**. Synaptic SNARE proteins form a four helix bundle via a parallel coiled-coil structure. Synaptobrevin II (blue) and syntaxin 1A (red) contribute one helix each to the complex whereas SNAP-25 (green) contributes two helices. TMDs are presented in yellow. This picture is adapted and modified from the reference (Sutton et al., 1998)

In addition to the SNARE motif, several SNAREs, such as syntaxin 1A, have an N-terminus domain that can back fold onto the SNARE motif and thus exist in closed or open form (Dietrich et al., 2003; Fasshauer, 2003; Ungar and Hughson, 2003). In the isolated syntaxin 1A, N-terminus H_{abc} domain (see Figure 6 for comparison), a three helix bundle, is bound intramolecularly to the coiled-coil domain of SNARE motif in the closed conformation (Fasshauer, 2003; Fernandez et al., 1998; Lerman et al., 2000; Margittai et al., 2003). Munc 18-1 binding with syntaxin 1A converts the closed form to open form via unknown mechanism, allowing the formation of the *trans*-complexes with synaptobrevin II and SNAP-25 (Dietrich et al., 2003; Fasshauer et al., 1998a; Poirier et al., 1998a). A similar behavior was described also in case of Sso1p (Munson et al., 2000), a syntaxin 1A homolog on yeast plasma membrane; interestingly assembly of SNARE complex formation *in vitro* is accelerated 2000-fold in the absence of Sso1p N-terminus domain (Nicholson et al., 1998). In the late endocytic pathway the interaction between the N-terminus domain of the syntaxins, Vam3p and Pep12, is not important, since these proteins do not adopt a closed conformation with N-terminus three helix bundle (Dietrich et al., 2003), even if the N-terminus domain mutant of Vam3p vacuoles fuse with markedly reduced efficiency

(Laage and Ungermann, 2001). This is probably due to its poor interaction with NSF and α-SNAP proteins, required for the disruption of *cis*-complexes (Dietrich et al., 2003).

The amino terminus of the synaptobrevin family is of different length, ranging from a few up to 150 residues. Recent studies revealed significant sequence homology of this N-terminus domain of synaptobrevins, allowing further classifications of synaptobrevin family as longins (Dietrich et al., 2003). Two studies, addressing the longin domains of VAMP7 and Ykt6p, suggest an autoinhibitory mechanism (Martinez-Arca et al., 2000; Tochio et al., 2001), that is reminiscent of the closed syntaxin conformation. A hydrophobic patch in longins of Ykt6p can bind with the SNARE motif. The mutation in a crucial residue F42E of the hydrophobic patch is sufficient to break this interaction in an *in vitro* assay (Martinez-Arca et al., 2000). In contrast to Sec22p, which contains similar hydrophobic patch in a similar spatial orientation, an interaction between longins and SNARE motif was shown to be unlikely (Gonzalez et al., 2001).

The SNAP-25 (Q-SNARE) does not contain a TMD, but is attached to the membrane via lipid anchor (Hess et al., 1992). The yeast vacuolar protein, Vam7p, or the yeast plasma membrane SNARE Sec9p and its homolog Spo20p, shows homology to SNAP-25 family, but these proteins are not bound to membrane via lipid anchor (Dietrich et al., 2003). The yeast vacuolar SNARE Vam7p is found both in cytosol and on the vacuole (Sato et al., 1998). Vam7p contains an N-terminus PX domain (named after the NADPH oxidase subunits $p40^{phox}$ and $p47^{phox}$). PX domains were identified as novel phosphatidylinositol phosphate binding proteins, most of them having a preference for phosphatidylinositol 3-phosphate (Cheever et al., 2001; Sato et al., 2001; Wishart et al., 2001). PX-domain consists of a module of three β-strands and three to four α-helices (Lu et al., 2002) that bind to phosphatidylinositol 3-phosphate, thus probably inserting part of the PX domain into lipid bilayer (Cheever et al., 2001). During exocytosis, Sec9p, the SNAP-25 homologue in the yeast plasma membrane, acts together with the syntaxin like t-SNARE Sso1p (Dietrich et al., 2003). During spore formation, Sec9p is replaced by Spo20p, which is 40% homologous to Sec9p and essential for sporulation (Neiman, 1998). Interestingly, despite the substantial overall homology of these proteins, the N-terminus domains

appear to have distinct functions. Replacement of Sec9p N-terminus by the one of Spo20p inhibits vegetative growth, while surprisingly removal of the Sec9p N-terminus does not affect fusion (Neiman et al., 2000).

2.5 Structure – function analysis of yeast vacuolar SNAREs

The yeast vacuole is critical for yeast viability. The vacuole is analogous to the mammalian lysosome and is required for the turnover of selected proteins (Hicke, 1999; Klionsky et al., 1990). It is the site of storage of phosphate, selected amino acids, metals and selected toxins. In addition, the yeast vacuole helps in buffering the pH of the cytoplasm and it is important in water and ion homeostasis, thus playing multiple roles in the response to cellular stresses (Catlett and Weisman, 2000; Weisman, 2003).

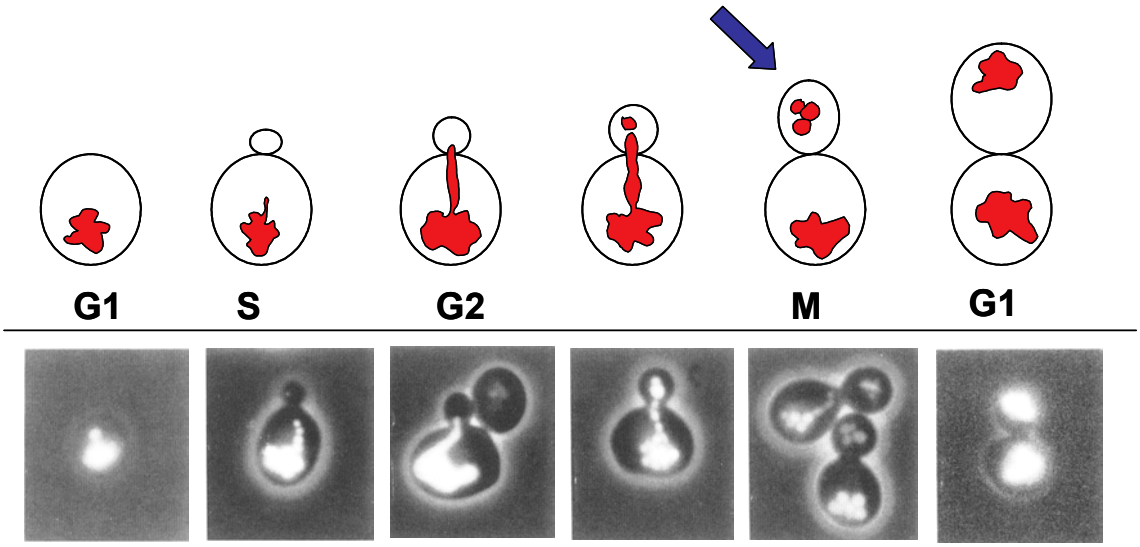

Figure 5. **Vacuole inheritances in budding yeast**. Vacuole begins to migrate into budding daughter cell early in G1 phase. After cell division segregated vacuoles fuse among themselves to form one to two organelles per cell. Vacuoles were visualized with the fluorescent FM4-64 (Vida and Emr, 1995). This picture is adapted and modified from reference (Conradt et al., 1992).

The vacuole of the budding yeast is actively divided between mother and daughter cells. Vacuole inheritance initiates early in the cell cycle, prior to the bud emergence and ends in G2, just prior to nuclear migration (Figure 5). The process begins with a portion of the vacuole extending into an emerging bud (Conradt et al., 1994). This tubular-vesicular entity, called the segregation structure, enables continued exchange of the vacuole contents between mother and daughter vacuoles (Catlett

and Weisman, 2000; Weisman, 2003). The segregation of vacuole from mother to daughter cell in budding yeast is known as vacuole fission. In mating cells, segregated structures fuse rapidly in the zygote bud, allowing the exchange of membranes and lumen contents via bud vacuole (Wang et al., 1998; Weisman et al., 1987; Weisman et al., 1988). Vacuole fusion is also required for normal vacuolar morphology, as mutants that are defective in fusion often have highly vesiculated vacuoles (Price et al., 2000b). Vacuole fusion also takes place in response to hypo-osmotic stress, enabling a rapid increase in vacuole volume (Catlett and Weisman, 2000).

Homotypic (self) fusion of yeast vacuoles, which is essential for the low copy number of this organelle, is mediated by SNARE proteins. Studies of homotypic vacuole fusion suggested a modified paradigm of membrane fusion, in which SNARE proteins form stable *cis*-complexes as well as *trans*-complexes (Figure 2). Chaperons as NSF/Sec18p and α-SNAP/Sec17p disassemble *cis*-complexes to prepare for the docking of organelles rather than driving fusion. The specificity of organelle docking resides in a cascade of *trans*-interactions (involving Rab-like GTPases), “tethering factors”, and trans-SNARE pairing. Fusion itself, the mixing of the membrane bilayer and the organelle contents, is triggered by calcium signaling (Wickner and Haas, 2000). Five SNARE proteins are involved in yeast vacuole fusion: Vam3p, Nyv1p, Vti1p, Vam7p and Ykt6p (Darsow et al., 1997; Nichols et al., 1997; Ungermann et al., 1998b; Ungermann et al., 1999a; Ungermann and Wickner, 1998).

Figure 6 shows a schematic representation of the different domains of the yeast vacuole SNARE proteins studied in this thesis.

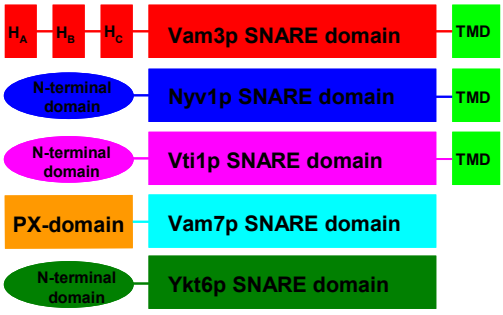

Figure 6. **Schematic representation of yeast vacuolar SNARE proteins.**

In the yeast vacuole the syntaxin homolog Vam3p (Wada et al., 1997) has a single membrane spanning domain at the C-terminus end (Darsow et al., 1997; Dulubova et al., 2001). At the functional level, complete deletion of Vam3p from yeast strain does not interfere with the viability of the cell, but prevent vacuole-vacuole fusion. Jones et al. observed that when Vam3p is deleted from yeast cell, alkaline phosphatase, a vacuolar membrane hydrolase, accumulates in the precursor form and the maturation of pro-aminopeptidase I, a hydrolase precursor delivered to vacuole from the cytoplasm, is blocked due to fusion defects (Srivastava and Jones, 1998). Recent studies revealed that the C-terminus TMD is very important for the vacuole fusion, since its deletion and replacement with a prenyl anchor at the C-terminus causes a reduced vacuole fusion efficiency up to 4 fold compared to wild type. This deletion of C-terminus TMD of Vam3p also reduces the palmitoylation of Vac8p, a reaction required beyond *trans*-SNARE complexes (Rohde et al., 2003) (Figure 7).

The yeast vacuole R-SNARE, Nyv1p is a synaptobrevin analog that contains an integral membrane spanning domain at the C-terminus (Fischer von Mollard and Stevens, 1999; Nichols et al., 1997). In functional studies, deletion of Nyv1p is associated with less pronounced defects in the *in vitro* fusion that can be rescued by adding extra recombinant Vam7p (Thorngren et al., 2004). The authors suggested that recombinant Vam7p could mediate fusion, in absence of Nyv1p, employing Ykt6p as the R-SNARE. A similar situation is also observed in yeast ER-to-Golgi transport, where Ykt6p can substitute for the R-SNARE Sec22p (Liu and Barlowe, 2002; Thorngren et al., 2004) (Figure 7).

The SNAP-25 analog in yeast vacuole is Vam7p, a Q-SNARE. Vam7p does not contain any TMD and it is attached to the membrane via PX-domain, which binds the phosphatidylinositol 3-phosphate (Cheever et al., 2001; Sato et al., 1998) (Figure 7). At the functional level, deletion of Vam7p from yeast cells does not affect cell viability, but creates fragmented vacuole. Vam7p is distributed in cytosol and on the vacuolar membrane (Boeddinghaus et al., 2002; Sato et al., 1998; Sato et al., 2001). Recent *in vivo* studies show that inhibition of Sec18p, an NSF protein required for yeast vacuole fusion, shifts most of Vam7p to the vacuole (Sato et al., 1998), thus suggesting that Vam7p cycles between the vacuolar membrane and the cytosol:

during Sec18p/ATP dependent priming, up to 90% of Vam7p is released from the vacuolar membrane as monomer (Dietrich et al., 2003) (Figure 7). The released Vam7p is a functional intermediate, as it can rescue fusion of vacuoles depleted of Vam7p; and the PX domain is important for this rescue, since the C-terminus coiled-coil domain of Vam7p or a Vam7p proteins mutated in its PX-domain, do not rescue fusion (Boeddinghaus et al., 2002; Cheever et al., 2001). It is likely that association of the PX-domain to phosphoinositide target is a prerequisite for the migration of Vam7p to the fusion site ((Dietrich et al., 2003)).

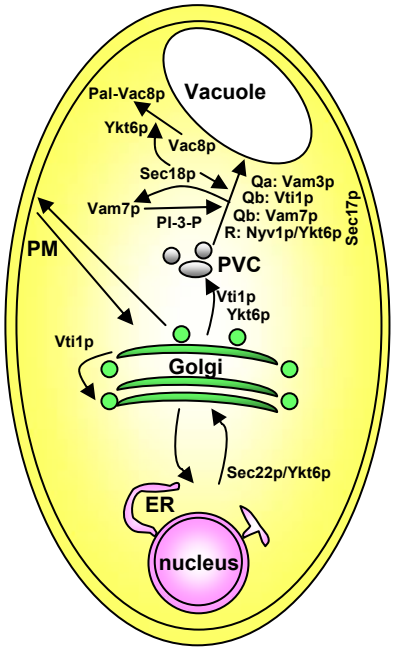

Figure 7. **Yeast vacuolar SNARE proteins**. The five SNARE proteins of yeast vacuole are presented as Qa, Qb, Qc and R. Among these Vti1p is involved in other vesicle trafficking pathway like *trans*-Golgi network to prevacuolar compartment and retrograde trafficking to *cis*-Golgi. Ykt6p is also involved in vesicle trafficking between ER to *cis*-Golgi and *trans*-Golgi to PVC. Ykt6p is also involved in Vac8p palmitoylation (Pal-Vac8p) which is Sec18p dependent. Vam7p is recruited to vacuolar membrane from cytosol by phosphatidylinositol 3-phosphate (PI-3-P); Sec18p driven *cis*-complex disruption release majority of Vam7p in cytosol. Sec17p is α-SNAP analog in yeast vacuolar fusion. Other proteins, required for vacuolar fusion, are omitted for the simplicity of the picture. This picture is adapted and modified from reference (Burri and Lithgow, 2004)

Vti1p is a Q-SNARE, containing a single membrane spanning domain at C-terminus. *In vivo* studies show that deletion of Vti1p leads yeast cell to death (Dilcher et al., 2001). This protein is involved in vesicle transport from *trans*-Golgi network to pre-vacuolar compartment, in retrograde trafficking to *cis*-Golgi and in vacuolar

membrane fusion (Fischer von Mollard and Stevens, 1999; Fischer von Mollard et al., 1997) (Figure 7).

Ykt6p is an R-SNARE without any TMD. It is attached to the membrane via prenylation at the C-terminus. The yeast cell can not survive if Ykt6p is deleted (McNew et al., 1997). This protein is involved in trafficking vesicles from ER to Golgi and in vacuole fusion where it interacts with Vti1p (Dilcher et al., 2001; Fischer von Mollard et al., 1997; McNew et al., 1997; Ungermann et al., 1999a). Ykt6p also shows weak interaction with COPII coat component (Springer and Schekman, 1998). Recent studies showed that Ykt6p is involved in the palmitoylation of Vac8p, described to be essential for vacuole fusion (Dietrich and Ungermann, 2004; Fukasawa et al., 2004) (Figure 7).

2.6 The importance of TMD in SNARE interactions and membrane fusion

Membrane fusion is the fundamental step for the transfer of proteins and lipids between different compartments, for exocytosis and for the structural integrity of the organelles. The components required for membrane fusion and the specificity for the selection of the correct target membrane are discovered, but the precise mechanism of lipid mixing is still unknown yet. Investigators are discussing several scenarios of TMDs, how it might promote lipid bilayer mixing. According to the “zipper” model, assembly of the SNARE ternary complex begins at the N-terminus SNARE domains and progresses towards the membrane anchors, gradually bringing membrane into close proximity where interaction between the TMDs may be associated with the formation of a fusion stalk (Margittai et al., 1999).

Exocytosis in yeast requires the assembly of the vesicular membrane Snc1p (v-SNARE) and the plasma membrane Sso2p and Sce9p (t-SNAREs). Grote et al. showed that when Snc1p and Sso2p were incorporated via geranylgeranylation at the C-terminus instead of their TMD, yeast exocytosis is blocked, even if a successful docking of vesicles to the plasma membrane was observed (Grote et al., 2000). Thus the TMDs appear to play a vital role in the fusion process.

Synaptobrevin II, an essential SNARE protein for neurotransmitter release, is forming homodimer in synaptic vesicle membrane (Calakos and Scheller, 1994; Edelmann et al., 1995; Washbourne et al., 1995) and as a recombinantly expressed protein in detergent solution, a membrane mimicking condition (Laage and Langosch, 1997). Dimerization is strongly dependent on the specific TMD sequence of synaptobrevin II since its mutation can disrupt it and this sequence motif is conserved for heterophilic interaction with syntaxin 1A (Laage et al., 2000). Synaptobrevin II and syntaxin 1A dimerization was also observed by other methods such as ToxR (Laage et al., 2000; Roy et al., 2004) and liposome fusion assay where these proteins were reconstituted in liposomes (Margittai et al., 1999). TMD-TMD interactions may play a role at different stages of SNARE protein interaction. First, the affinity of homophilic TMD-TMD assembly can regulate the *trans*-SNARE complex formation. Second, the heterophilic interaction by TMD can lead to multimerization of SNARE complexes (Poirier et al., 1998b), as it was observed by electron microscopy, where dimers and multimers of native or recombinant SNARE complexes are associated at the sites of the TMDs; on the contrary multimerization was absent with SNARE complexes composed of cytoplasmic domains only (Hohl et al., 1998). Though the functional relevance for SNARE complex multimerization is not known, but it could be possible that these multimers can stabilize the *cis*-complex. Third, heterophilic TMD-TMD interaction may stabilize the *trans*-SNARE complex by complete zipping of SNARE proteins (Laage et al., 2000; Margittai et al., 1999); this can facilitate the lipid mixing by structural flexibility of TMD. Langosch et al. showed that incorporation of the TMD peptides of synaptobrevin II or syntaxin 1A into the synthetic liposomes strongly increase their ability to fuse, thus suggesting a potential fusogenic activity of the TMDs. Structural studies of synaptobrevin II TMD peptide revealed a co-existence of α-helical and β-sheet conformations. The authors suggested that the conformational plasticity of TMD may be important for the SNARE protein function at a late step in membrane fusion, since fusogenic activity significantly decreases if the α-helical property of synaptobrevin II TMD peptide is stabilized by mutation (Langosch et al., 2001). When full length syntaxin and synaptobrevin are anchored to liposome via short fatty acid chain, the liposome fusion is prevented, whereas fatty acid lipid anchors that potentially span lipid bilayers allowed for fusion, suggesting a particular length of transmembrane segment requirement for membrane fusion (McNew et al., 2000). Experiments on

C.elegans revealed that mutations that affect synaptobrevin or syntaxin TMDs result in severe neurotransmission defect (Nonet et al., 1998; Saifee et al., 1998) and syntaxin isoforms in *C.elegans* (Saifee et al., 1998) and vertebrates were identified that are only distinguished by their TMD sequence (Bennett and Scheller, 1993; Ibaraki et al., 1995). Rohde et al showed that deletion or mutation of Vam3p TMD, a syntaxin analog in yeast vacuole; affect the efficiency of membrane fusion as described in the previous section (Rohde et al., 2003). In conclusion, SNARE-TMDs seem to act as autonomous domains.

3 Aim of the work

In the first part of the thesis the TMD dependent homodimerization of synaptobrevin II is presented. Homodimerization of synaptobrevin II was previously shown by different authors to depend on its single TMD, and the crucial residues forming helix–helix interface have been mapped. Since another recent study challenged these results, we re-examined this under different experimental conditions.

Rohde et al revealed by functional analysis that the deletion of the Vam3p TMD or mutation in TMD does not affect the localization of the Vam3p in yeast vacuole, but the vacuole fusion is severely affected. Considering the importance of TMD in vacuole fusion and the established role of TMD–TMD interaction in presynaptic SNARE interactions, the main aim of this work was to clarify whether TMD of Vam3p would contribute to homo- or heterophilic yeast SNARE interactions *in vitro*. Thus, we wished to clarify, whether the functional effect of the TMD alteration could be correlated to its interactions.

4. Materials and methods

4.1 Chemicals

4.1.1 General chemicals

Unless specified otherwise, the standard chemicals have been obtained from the following companies: Roth (Karlsruhe), J.T.Baker (Holland), Merck (Darmstadt), Sigma (Munich), Applichem (Darmstadt). All solutions were prepared with deionised water (Millipore filter unit).

4.1.2 Detergent

CHAPS (3-[3-cholamidopropyl-dimethylammonio]-1-propansulfonat), Triton® X-100 and sodium dodecyl sulfate (SDS) were from Applichem. Thesit® (dodecylpoly[ethyleneglycolether]$_n$) was obtained from Fluka.

4.1.3 DNA-modifying enzyme

DNase I was from Roche (Mannheim). Restriction endonucleases, T4 DNA ligase and *Taq* polymerase were obtained from MBI Fermentas. Turbo *Pfu* polymerase and *Dpn* I were obtained from Stratagene.

4.1.4 Antibodies

Polyclonal antibodies, α-Vam3p, α-Nyv1p, α-Vti1p, α-Vam7p and α-Ykt6 were a gift of Dr. Christian Ungermann (BZH, Heidelberg). Myc monoclonal antibody 9E10 was extracted from the supernatant of hybridoma cells. Enzyme-conjugated secondary antibodies: Goat-anti-mouse HRP conjugated and Goat-anti-rabbit HRP conjugated were obtained from Promega.

4.1.5 Kits

PCR purification kit, Plasmid purification kit and DNA isolation from agarose gel kit were obtained from Macherey Nagel (Düren). DNA sequencing was performed with SequiTherm EXCEL™ II DNA sequencing kit (BioZyme).

4.1.6 Synthetic Oligonucleotides

Synthetic oligonucleotides for PCR and mutagenesis were obtained from Invitrogen (Scotland). Sequencing primers were obtained from MWG-Biotech (Ebersberg). Longer oligonucleotides (100mers) were obtained as PAGE purified from ThermoHybaid.

Primer DNA sequencing

T7 promoter primer

IRD700-TAATACGACTCACTATAGGG

T7 terminator primer

IRD800-GCTAGTTATTGCTCAGCGG

Vam3pΔTM primer

CAGGGTCTCGAGACCGCATTTGTTACGGTCCCT

Nyv1pΔTM primer

AATTTTGGATCCTTCTGCCACCACATTATTTC

Vti1pΔTM primer

ATTAGCGAATTCCCTTCTAGTCATTGTTTTTAG

Vam3p Ala20 primer

CAGGGTCTCGAGACTGGCGGCTGCTGCTGCTGCGGCTGCGGCTGCGGCGGCT
GCGGCTGCGGCTGCTGCTGCTGCGCATTTGTTACGGTCCCTCTGATGC

Nyv1pAla21primer

CAGGGTGGATCCCAGGCGGCGGCTGCTGCTGCTGCTGCGGCTGCGGCG
GCTGCGGCTGCGGCTGCTGCTGCTGCATTTTTGACCTTCTGCCACCACATTATT
TC

Vti1pAla23primer

CAGGGTGAATTCTTTAAACTTTGAGGATGCTGCGGCGGCGGCTGCTGCTGCTG
CGGCTGCGGCTGCGGCGGCTGCGGCTGCGGCTGCTGCTGCTGCCCTTCTAGT
CATTGTTTTTAGTGTC

Vam3pC274A I

CATTATAATAGTTGTGGCCATGGTGGTATTGC

Vam3pC274A II

GCAATACCACCATGGCCACAACTATTATAATG

4.1.7 Vectors

Synaptobrevin II (from *R. norvegicus*) was cloned in pSNiR-series vectors (Laage and Langosch, 1997; Laage and Langosch, 2001). Vam3p, Vti1p and Vam7p were cloned in pET28a, and Nyv1p was cloned in pET15b. Ykt6 protein was cloned in pGEX4T-1 and Ykt6p was subcloned into pET28a vector. We are thankful to Dr. James Rothman for providing these cloned yeast genes in different vectors. Vam3pA4 and Vam3pA4bb mutants are generous gift from Dr. Jan Rhode and these mutants were subcloned into pET28a.

4.1.8 Bacterial strains

All bacterial strains used are modifications of *Escherichia coli*. The BL21, BL21(DE3)pLysS and Rosetta (DE3) strains were obtained from Novagen. The M15 strain was obtained from Quiagen for expression of Sec17p and Sec18p. The strain DH5α was used for normal cloning procedure and DNA-plasmid preparations.

4.2 Preparative and analytical DNA-techniques.

4.2.1 Plasmid DNA MINI preparation

Single bacterial colonies were inoculated into LB-medium containing appropriate antibiotic and grown overnight at 37^{o}C in a shaker. The grown cultures were centrifuged for 10 min at 14000xg, the supernatant was discarded and the pellet was resuspended in 150 µl Sol I. After 5 min incubation at room temperature (RT), 200 µl Sol II was added and the solutions were mixed by inverting the tubes fro 5-10 times. The mixture was incubated 5 min at RT, thereafter 150 µl of cold sol III was added, and the tube was inverted for 5-10 times and then incubated on ice for 5 min and centrifuged at 4^{o}C with 14000xg for 15 min. The supernatant was collected from the tube and mixed with phenol:chloroform:isoamyl alcohol (25:24:1) by vortexing for 10-30 sec. The aqueous layer and organic layer were separated by centrifuging the mixture at RT for 15 min at 14000xg. The aqueous layer was carefully collected from the upper part and 1/10th volume of 5 M sodium acetate pH 5.2 was added to that. Equal volume of iso-propanol was added and incubated at RT for 5-10 min to precipitate plasmid DNA. Subsequently the DNA was precipitated via centrifugation at 4^{o}C 14000xg for 30 min., the precipitated DNA was washed with 70% ethanol and

dried at RT. The precipitate was then resuspended into 30 µl TE (10 mM Tris pH 8.0), 1 mM EDTA or H_2O.

Sol I

50 mM Tris-HCl; pH 8.0

10 mM EDTA

100 mg/ml RNase

Sol II

0.2 N NaOH

1% SDS (w/v)

Sol III

3 M potassium acetate

2 M Acetic acid

4.2.2 Agarose gel electrophoresis of DNA

DNA and fragments after restriction digestion were analysed by agarose gel electrophoresis, using electrophoresis chamber TypM100 from EMBL, Heidelberg. 0.8-1.5% (w/v) Ultrapure agarose solutions in TBE (45 mM Tris-borate; 1 mM EDTA, pH 8.0) were heated in a microwave oven to dissolve the agarose and 2 µl ethidiumbromide (10 mg/ml) was added when the solution was cold but not solidified. TBE was used as running buffer.

4.2.3 Restriction digestion

Vector DNA or PCR DNA fragments were digested with restriction endonucleases to generate DNA fragment for cloning. The calculation of the amount of enzyme was done according to the following formula:

$$\frac{(\mu g\ DNA \times number\ of\ cuts \times 50)}{(kb \times cuts\ in\ \lambda)} = units\ enzyme$$

Digestion mix

0.1-5 µg DNA

+ 0.1 vol digestion buffer

+ H_2O to final volume

+ max 0.1 vol enzyme

incubation from1h till overnight at 37°C

4.2.4 Analysis and isolation of DNA fragments from agarose gels

Gel pieces with the desired DNA fragment were cut out from the agarose gel with a sterile scalpel and transferred into a 1 ml tubes. The DNA was extracted from the gel piece according to the protocol described in the Macherey Nagel kit protocol. The isolated DNA was visualized again on agarose gel.

4.2.5 Amplification of specific DNA sequences

Specific DNA fragment was amplified by polymerase chain reaction (PCR). *Taq* DNA polymerase was used in all PCR reaction. The reaction was made according to the MBI Fermentas protocol sheet. For 100 µl reaction mixture, the composition was as follows:

DNA template	1 µl (25-100 ng)
Taq DNA polymerase buffer with 15 mM $MgCl_2$	10 µl (10x from MBI)
Sense primer	1 µl (100 pmol/µl stock)
Antisense primer	1 µl (100 pmol/µl stock)
dNTP mix	2 µl (10 mM stock)
Taq DNA polymerase	1 µl (1 unit/µl)
H_2O	84 µl

Amplification was performed on an Eppendorf Robocycler. The reaction protocol was as follows:

94°C	5 min	
55°C	2 min	
94°C	40 sec	35 cycles
55°C	40 sec	
72°C	1 min	
94°C	1 min	
55°C	40 sec	
72°C	20 min	
4°C	Hold	

The PCR products were purified by PCR purification kit from Macherey Nagel and detected by agarose gel electrophoresis.

4.2.6 DNA fragment ligation

DNA ligation was performed in a 10 µl reaction mixture. The protocol was as follows:

Vector DNA	1 µl (100 ng)
Insert DNA	5-10 times molar amount of vector DNA
Ligase buffer	1 µl (5 Weiss unit/µl)
H_2O	to add up 10 µl

4.2.7 Preparation of chemical competent cells (according to Inoue method)

The production of competent *E.coli* strain DH5α, BL21, BL21(DE3)pLysS, Rosetta(DE3) and M15 was done according to the method of Inoue (Inoue et al., 1990). One colony was inoculated with or without appropriate antibiotic and 1% glucose from a fresh plate. The cells were grown for min 6-8 hrs at 37^{o}C, thereafter 1-2 µl culture was inoculated into 100 ml SOB medium with 2.5 ml of 2 M $MgCl_2$ and incubated at 25^{o}C until the OD_{600} reached 0.45-5 (approximately 13-15 hours). The culture was then cooled on ice for 10-30 min. The cells were then harvested at 4^{o}C at 4000xg and resuspended with 16 ml HTB buffer, centrifuged again and finally resuspended in 4 ml HTB buffer and 300 µl DMSO (or 6-7% of the total volume) was added to the cell suspension. The bacterial suspension was then aliquoted in different tubes and immediately frozen in liquid nitrogen and stored at -80^{o}C.

SOB medium:
- 2% Bactotrypton
- 0.5% Bacto yeast extract
- 9 mM NaCl
- 2.5 mM KCl
- 10 mM $MgCl_2$

HTB:
- 10 mM HEPES
- 15 mM $CaCl_2$
- 250 mM KCl
- dissolved in 150 ml H_2O, adjust pH to 7.0 with KOH
- add water to make 200 ml
- 55 mM $MnCl_2$
- (filtered sterile)

4.2.8 Transformation of *E.coli* cells with plasmid DNA

Competent bacterial cells were quickly thaw (by hand warming) and 1-2 µl of DNA or ligation mixture was added in the suspension and incubated for 30 min on ice. Then the cells were subjected to heat shock for 90 sec at 42^{o}C in a water bath, followed by a cold shock on ice for 3 min. 800 µl LB medium was added to the cells and incubated at 37^{o}C for 1hr to develop the antibiotic resistance. Finally the cells were plated on LB-agar plate with appropriate antibiotic.

4.2.9 Site-directed mutagenesis

The exchange of one amino acid to another was performed by using synthetic oligonucleotides. The plasmid, containing the desired gene, was purified by according to protocol mentioned in Macherey Nagel kit. Two designed oligonucleotides containing the desired mutation were used to introduce mutation in the gene, as described in the scheme (Figure 8).

The protocol used for this mutation is as follows:

Plasmid DNA	5-50 ng
Primer 1	125 ng
Primer 2	125 ng
dNTPs	1 µl
buffer	5 µl (10x reaction buffer)
Pfu turbo polymerase	1 µl (2.5 units/µl)
H_2O	to add up 50 µl

Then the mixture was placed in an Eppendorf Robocycler with a program as follows:

95^{o}C	1 min	
95^{o}C	30 sec	(12-18 cycles)
55^{o}C	30 sec	
68^{o}C	1 min/kb DNA length	

After the reaction the mixture was then cooled on ice for 10 min, thereafter 1 µl *Dpn* I (10 unites/µl) was added in order to cut the parental DNA and incubated for 1 hr in 37^{o}C. 1-2 µl of the mixture was transformed into DH5α competent cells with appropriate antibiotic. The plasmids were isolated from the single colonies as

mentioned before with phenol-chloroform treatment. The mutations were identified with DNA sequencing.

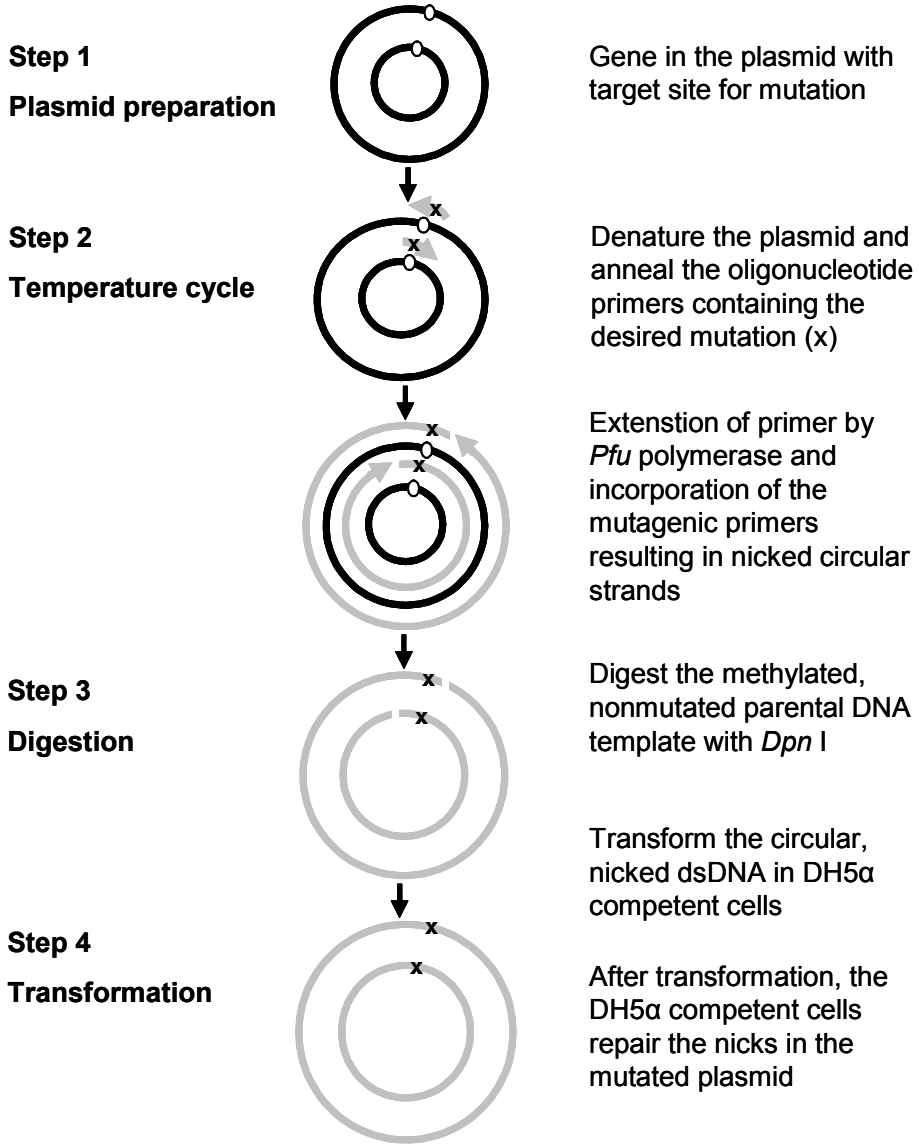

Figure 8. **Site-directed mutagenesis**. The parental plasmid was purified as described in text. The second step consists in the denaturation of the plasmid followed by annealing of two primers, which contain the mutation. Next extension of primers by *Pfu* polymerase (12-18 cycles) incorporates the mutation and produces nicked circular strands. In the last step the reaction mixture was incubated at 37°C for 1 hr with *Dpn* I, in order to digest the methylated (Gm6A↓TC) nonmutated parental plasmid. The mixture was transformed into *E.coli* DH5α strain, where the nicked circular product would be repaired. The mutation was characterized by sequencing as mentioned in the text. This Figure is adapted and modified from www.stratagene.com.

4.2.10 Sequencing

Analysis and identification of cloned PCR-fragments and site-directed mutagenesis products were performed (MWG LI-COR 4000L DNA sequencer) by dideoxy chain

terminating sequencing using fluorescence labeled (IRD700 or IRD800) primers. The sequencing method used is based on cycle PCR method and analysis on LI-COR DNA sequencer. The protocol followed is described in the SequiTherm EXCEL™ DNA sequencing kit. 17 µl of premix was prepared for each DNA template:

Labeled primer	2 pmol
DNA	100 - 250 fmol
Buffer	7.5 µl (10x stock buffer)
DNA polymerase	1 µl
Water to add up to	17 µl

Then 2 µl of each termination mix (ddATP, ddCTP, ddGTP and ddTTP) was added in four different tubes. 4 µl of premix was added in to each tube and the tubes were place into Eppendorf Robocycler with a program:

95°C	5 min	
95°C	30 sec	(30 cycles)
50°C	15 sec	
70°C	1 min	

After the PCR 3 µl of stop (loading) buffer was added to each tube, which were heated to 95°C for 3-4 min and immediately placed on ice to denature the sample before loading. The gel (0.2 cm thick and 66 cm long) was prerun for 10 min before loading the 2 µl of sample. The running condition was 2800 V, 40 mA, 55 W, 45°C with a scan speed 3 and frame 30. The gel was run for 7-8 hours. The scanned bands were analyzed by software (v 4.0 image analysis).

4.3 Preparative and analytical biochemistry

4.3.1 Expression and purification of synaptobrevin II in BL21(DE3)pLysS

Synaptobrevin II was recombinantly expressed in the vector pSNiR. The vector with synaptobrevin II gene was transformed into BL21 (DE3) pLysS competent cells and plated on a LB-agar plate containing 200 µg/ml ampicillin and 30 µg/ml chloramphenicol and incubated overnight at 37°C. One single colony was inoculated in 100 ml LB medium (containing 200 µg/ml ampicillin and 30 µg/ml chloramphenicol)

and incubated at 37°C until the OD_{600} was ~ 0.2. Then the bacterial cells were induced with 1 mM IPTG and grown further for 3 hrs at 37°C. The cells were then harvested and frozen at -20°C. Frozen pellets were resuspended in 4 ml lysis buffer (25 mM HEPES pH 7.6; 100 mM NaCl; 1 mM EDTA; 1 mM PMSF; 0.025% [w/v] NaN_3). The bacterial cell suspension was freezed and thawed three times in liquid N_2 and 37°C. The lysis was performed by the lysozyme expressed from the low copy number plasmid pLysS present in the BL21 (DE3) cells. 10 mM $MgCl_2$ was added to the lysed suspension to activate the nuclease function of the fusion protein and incubated at room temperature 5 min. The suspension was kept on ice (~1hr) for complete digestion of DNA. The soluble part was separated from the insoluble part of the cell lysate by centrifugation at 14000xg at 4°C for 20 min. The supernatant was kept for SDS-PAGE analysis. The pellet was resuspended with solubilization buffer (25 mM HEPES pH 7.6; 1 M NaCl; 2% [w/v] Thesit; 1 mM EDTA; 1 mM PMSF; 0.025% [w/v] NaN_3) and incubated at 4°C in an Eppendorf shaker for 1 hr. Non solubilized part was separated via ultracentrifugation in Beckman Optima TL at 4°C for 1 hr at 100000xg. Finally the supernatant and pellet fractions were visualized by Coomassie staining of SDS-PAGE.

4.3.2 Expression of vacuolar SNARE proteins

4.3.2.1 Expression of Vam3p, Vti1p, Vam7p and Ykt6

Vam3p and its mutants, Vti1p and its mutants, Ykt6p and Vam7p were expressed in pET28a vector, whereas GST-Ykt6p was expressed in pGEX-4T-1. The respective clones were transformed in Rosetta (DE3) competent cells and plated on LB-agar plate with kanamycine (35 µg/ml), chloramphenicol (30 µg/ml), and 1% (w/v) glucose and incubated at 37°C overnight. A single colony was inoculated into 3 ml LB medium (containing kanamycine [35 µg/ml], chloramphenicol [30 µg/ml] and 1% [w/v] glucose) and incubated at 37°C overnight. Cells were collected from 1 ml of the overnight culture and resuspended with fresh LB medium and inoculated in 1 liter LB medium with the antibiotics mentioned before but without glucose. The cells were incubated at 37°C until the OD_{600} reached 0.6-0.8 (~4 hrs) and then cooled on ice (for 30-45 min). The cells were then induced with 1 mM IPTG and incubated overnight (~20 hrs) at 16°C (at 150 rpm shaking). The cells were harvested, washed with PBS and then frozen in -80°C.

4.3.2.2 Expression of Nyv1p

Nyv1p and its mutant, cloned in pET15b, were transformed in Rosetta (DE3) competent cells and plated on LB-Agar medium containing ampicillin (50 µg/ml), chloramphenicol (30 µg/ml), 1% (w/v) glucose and incubated for overnight at 37^{o}C. A single colony was then inoculated in 100 ml LB medium containing ampicillin (200 µg/ml) and chloramphenicol (30 µg/ml) and incubated at 37^{o}C, until the OD_{600} reached 0.5. The cells were induced with 1 mM IPTG and incubated further 3 hrs at 37^{o}C. Finally the cells were harvested and frozen in -80^{o}C. Sec17p (pQE9/M15) and Sec18p (pQE9/M15) were also expressed by similar procedure.

4.3.3 Purification of vacuolar SNARE proteins

The SNARE proteins were expressed with GST-tag or histidine-tag either N-terminal or C-terminal. The frozen cells were thawed on ice (10-20 min) and resuspended with 20 ml (for 1 liter culture) buffer (25 mM HEPES pH 7.6; 1 M NaCl; 10 mM β-mercaptoethanol; 2% [v/v] Triton X-100 and 2% [v/v] Thesit, 500 µg α2-macroglobulin; 20% [v/v] glycerol and lysozyme [5-8 mg]). Cells were kept on ice for 30 min with occasional mixing by inverting the tube and thereafter sonicated with 7 sec pulse of 60% amplitude and 20 sec off for 12 min on a Branson digital sonifier W-250 D. Prior to sonication 1 mM PMSF was added to the cell suspension. The sonication was carried out on ice-cold condition. After sonication 1 mM PMSF and 500 µg of α2-macroglobulin were added to the mixture again, then 10 mM $MgCl_2$ and 1 mg DNase I were added and incubated at room temperature (5-10 min). The lysate was incubated at 4^{o}C with gentle shaking for maximum solubilization (1-2 hr). The soluble proteins were separated from non soluble proteins by centrifugation at 4^{o}C at 14000Xg for 30 min. The supernatant was applied on a Ni-NTA column or GST column.

4.3.3.1 Purification by immobilized metal ion affinity chromatography (IMAC)

Two principle buffers were prepared for immobilized metal ion affinity chromatography. Buffer A: 25 mM HEPES pH 7.6, 1% Thesit (v/v), 1 M NaCl, 10 mM β-mercaptoethanol, 10% glycerol (v/v) and buffer B: 25 mM HEPES pH 7.6, 1% Thesit (v/v), 1 M imidazole, 1 M NaCl, 10 mM β-mercaptoethanol, 10% glycerol (v/v). The other buffers of different imidazole concentrations (e.g. 50 mM, 80 mM, 100 mM

and 500 mM imidazole buffer) were prepared mixing buffer A and B. The HiTrap™ Chelating HP column first wash with 5 column volumes of water and then 1 ml of 0.1 M $NiCl_2$ was applied on the column and washed again with 5 column volumes of water. Then the column was equilibrated with 5 column volumes of buffer A at a speed of 1 ml/min and then with 5 column volumes of elution buffer (500 mM imidazole) and again with 5 column volumes of buffer A. The sample was loaded on the equilibrated column at a speed of 0.5 ml/min. After loading the sample, the column was washed with imidazole buffer at a speed of 1 ml/min and with a gradient from 0–100 mM imidazole. 5 column volumes of each imidazole buffer were used for washing the column. The His_6-tag protein was eluted with 5 column volumes of 500 mM imidazole buffer. The column was washed with 50 mM EDTA for removing nickel ions from the column. Eluted fractions were visualized by Coomassie staining on SDS-PAGE.

4.3.3.2 Purification by affinity chromatography on immobilized glutathione column

Two principal buffers were prepared for affinity chromatography on immobilized glutathione column – binding buffer (PBS + 1% [v/v] Thesit) and elution buffer (50 mM Tris pH 8.0, 1 M NaCl, 10 mM reduced glutathione, 1% [v/v] Thesit). The column was washed first with water (5 column volumes) and equilibrated at a speed of 1 ml/min with 5 column volumes of binding buffer, then with 5 column volumes of elution buffer and again with 5 column volumes of binding buffer. The sample was loaded on the equilibrated column at a speed of 0.5 ml/min. The column was washed with 5 column volume of binding buffer with a speed of 1 ml/min. The GST tagged protein was then eluted with 5 column volumes of elution buffer. Eluted samples were visualized by Coomassie staining on SDS-PAGE.

4.3.4 Protein storage

The eluted fractions after purification were dialyzed against buffer containing 25 mM HEPES pH 7.6, 1% Thesit (v/v), 1 M NaCl, 10 mM β-mercaptoethanol, 10% glycerol (v/v) to remove imidazole or glutathione. Purified SNARE proteins were stored at 4^{o}C after dialysis. The dialyzed proteins were further used for protein-protein interaction studies.

4.3.5 Protein precipitation according to Wessel-Flügge

The purification according to Wessel-Flügge (Wessel and Flugge, 1984) is based on the precipitation of proteins with methanol and subsequent extractions of lipids and detergents with chloroform. 400 µl methanol, 300 µl H_2O and 100 µl chloroform were added to 100 µl of protein solution, mixed by vortexing and centrifuged for 5 min at 14000xg room temperature. The upper layer was removed carefully and mixed with 300 µl methanol and centrifuged for 5 min at 14000xg at room temperature. After drying the pellet was dissolved in SDS sample buffer.

4.3.5 Protein precipitation with TCA

Large volume of protein solution was precipitated with trichloro acetic acid (TCA). Equal volume of 20% (w/v) TCA was mixed with protein solution and incubated on ice for 30 min. The solution was centrifuged at 4^{o}C at 14000xg for 10 min to collect the protein precipitate. The supernatant was removed and the precipitate was washed 3 times with 1 ml of ice-cold acetone. The precipitate was dried and resuspended in SDS sample buffer.

4.3.6 SDS-polyacrylamide gel electrophoresis (Laemmli, 1970)

SDS-gel electrophoresis allows protein separation according to their molecular weights. The anionic detergent SDS denatures the proteins and binds at a ration of approximately 1.4 gm SDS per gram of protein, thus conferring a net negative charge to the polypeptide in proportion to its length. The separation occurs in an electric field. Minigels were run with the Vertical Minigel Unit (Sigma Techware, St. Louis. USA). Depending on the molecular weight of the proteins, 7.5–15% acrylamide gels were casted as follows (ratio acrylamide: bis-acrylamide 30: 0.8):

Stacking gel buffer “Upper Tris”: 0.25 M Tris, pH 6.8 0. 0.2% (w/v) SDS

Separating gel buffer “Lower Tris”: 1 M Tris, pH 8.5, 0.26% (w/v) SDS

Running buffer: 25 mM Tris pH 8.3, 250 mM glycine, 0.1% (w/v) SDS

Sample buffer (standard): 50 mM Tris pH 6.8, 3% (w/v) SDS, 10% (v/v) Glycerol, 0.02% (w/v) bromophenol blue.

For reducing conditions, 10% (v/v) β-mercaptoethanol or 100 mM DTT were added. Protein interaction analysis was done in the presence of only 1% (w/v) SDS (ultrapure). Gels were subsequently subjected to Western blot or stained with Coomassie brilliant blue.

Molecular weight standard

Low molecular weight markers (LMW): Bovine serum albumin – 66 kDa, ovalbumin – 45 kDa, glyceraldehyd-3-phosphatedehydrogenase – 36 kDa, carbonic anhydrase – 29 kDa, trypsinogen – 24 kDa, trypsin inhibitor – 20 kDa, lactalbumin – 14 kDa.
High molecular weight markers (HMW): Myosin – 205 kDa, β-galactosidase – 116 kDa, phosphorylase b – 97.4 kDa, bovine serum albumin – 66 kDa, ovalbumin – 45 kDa, carbonic anhydrase – 29 kDa.

4.3.7 Interaction analysis with SDS-PAGE (mild SDS-PAGE or urea SDS-PAGE)

Protein-protein interaction studies were carried by mild SDS-PAGE or urea SDS-PAGE. In mild SDS-PAGE gels were prepared without SDS. Samples were not boiled and the SDS concentration in the sample buffer was 2% (w/v). The running buffer was Lämmli buffer as described before. Samples were run at 4^{o}C overnight (Bowen et al., 2002; Roy et al., 2004).

Alternatively, when urea SDS-PAGE was performed, the gels were made with SDS and 6 M urea and they were dissolved in sample buffer containing 1% (w/v) SDS plus 6 M urea and samples were not boiled. The SDS concentration in the gel and the running buffer was same as Lämmli SDS-PAGE as described before. Samples were run at 4^{o}C overnight (Laage and Langosch, 1997; Roy et al., 2004).

4.3.8 Coomassie staining of proteins

Coomassie staining is required to visualize proteins separated by SDS-PAGE. The gels were incubated for 30 min in Coomassie solution (0.25% [w/v] Coomassie brilliant blue [G-250], 50% [v/v] Methanol, 10% [v/v] acetic acid), and destained with solution containing 30% (v/v) Methanol, 10% (v/v) acetic acid, until the protein bands were visible and the background was fully destained.

4.3.9 Western Blot

Antibody detection of electrophoretic separated proteins requires the transfer of the proteins from the gel onto a membrane. Separated proteins were blotted with a semi dry CTI-blotter for 1 – 2 hr onto nitrocellulose membrane (Amersham Biosciences). The gel and nitrocellulose membrane were placed between 5 layers of Whatman 3

MM paper soaked in blot buffer (25 mM Tris pH 8.3, 250 mM glycine, 0.1% [w/v] SDS, 20 % [v/v] Methanol). Protein bands were visualized in 0.2% (w/v) PonceauS, 3% (w/v) TCA. Unspecific binding sites were blocked by incubating the blot in TBB (5% [w/v] milk powder in TWB) for overnight. The membrane was incubated in primary antibody (1:5000 in TBB) for 2 hrs. The blot was washed extensively (20 min TBS, 20 min TWB and 20 min TBB) to remove unbound antibody. Blot was then incubated with HRP-enzyme coupled secondary antibody (1:50000 in TBB) for 1 hr and washed again (20 min TBS, 20 min TWB and 20 min TBS). Finally the blot was developed using enhanced chemiluminiscence (ECL).

TBS: 50 mM Tris-HCl, pH 8.0, 150 mM NaCl

TWB: 50 mM Tris-HCl, pH 8.0, 150 mM NaCl, 0.1% Triton X-100

TBB: 5% non fat dried milk in TWB buffer.

4.3.9.1 Antibody detection through Enhanced Chemiluminiscence (ECL)

The ECL method is a very sensitive, non-radioactive and fast method to detect antigens on blots. Antigens are directly or indirectly detected with horseradish peroxidase (HRP) coupled antibodies. The peroxidase itself reacts with a chemiluminiscent substrate and the resulting light signals can be detected via autoradiography on ECL films. Development of the blots was done by incubation for 1 min in ECl-substrate solution that was prepared directly before usage.

ECL-substrate solution:

Stock solution: 250 mM Luminol (5-amino-2, 3-dihydro-1, 4-phthalazinedione) and 90 mM p-Coumaric acid (4-hydroxycinnamic acid) solutions were prepared in DMSO and aliquots were stored at -20^{o}C.

Solution A: 50 µl of 250 mM Luminol and 25 µl of 90 mM p-Coumaric acid were added to 5 ml of TBS

Solution B: 3 µl of 30% (w/w) H_2O_2 was added to 5 ml of TBS solution.

Solution A and B were mixed in a ratio 1:1 and added on the blot drop by drop to cover the total membrane area and incubated for 1min.

4.3.9.2 Western blot re-probing

Immobilized proteins on membrane were reprobed with other antibodies by stripping the membrane. After developing the membrane with ECL substrate solution, the

membrane was stripped with a stripping solution containing 62.5 mM Tris-HCl pH 6.8, 2% SDS (w/v), 100 mM β-mercaptoethanol. The membrane was soaked into stripping solution inside a plastic bag and incubated at 50^{o}C in a water bath with occasional shaking for 30 min. The membrane was washed 3 times with TWB buffer. Unspecific binding sites were blocked with TBB buffer (5% non fat milk in TBS) before incubating with primary and secondary antibody, as described in the previous section. Finally the membrane was developed with ECL substrate solution.

4.3.10 Coupling of IgG to ProteinA-Agarose

Rabbit polyclonal antisera (1 ml) or affinity purified antibody solutions (rabbit anti Vam3p) (10 mg/ml) were loaded onto 500 µl ProteinA-Agarose (Roche) beads, which were prewashed with 0.1 M glycine, pH 2.5 and neutralized subsequently with 0.1 Tris-HCl pH 7.4. Coupling reaction occurred at 4^{o}C on an Eppendorf shaker overnight. The beads were washed twice with 10 volume of 0.2 M sodium borate buffer pH 9.0 and collected by sedimentation (10 min, 6000xg 4^{o}C in an Eppendorf centrifuge). The beads were resuspended in 10 volumes of the same buffer. The equivalent of 10 µl beads was removed for the control of coupling reaction efficiency. Crosslinking of the antibodies to the beads was done by the addition of solid dimethylpimelimidate (DMP) (Perbio Science) to final concentration 20 mM. Samples were incubated with gentle shaking for 30 min at room temperature and equivalent of 10 µl of the cross-linked beads was removed. The reaction was stopped by washing the beads with 0.2 M ethanolamine pH 8.0 and the beads were then incubated for 2 hrs at room temperature in 0.2 M ethanolamine on shaker. After the final wash beads were resuspended in TBS supplemented with 0.025% NaN_3 as preservative. The efficiency of the coupling reaction was analyzed with the beads taken before and after addition of the cross-linker DMP. Samples were resuspended with SDS-PAGE sample buffer and run on 10% SDS-PAGE and subsequently stained with Coomassie brilliant blue. 55 kDa heavy chain protein band of the antibody was detected by SDS-PAGE when the cross-linker was not added, while after addition of the cross-linker this band was not present, thus showing the complete antibody cross-linkage with agarose beads.

4.3.10.1 Co-immunoprecipitation

SNARE protein complexes were analyzed by co-immunoprecipitation. The fractions, collected from sucrose gradient, were incubated with rabbit anti Vam3p antibody coupled with ProteinA-Agarose for 2 hrs or overnight at 4^{o}C. The beads were re-isolated after brief centrifugation and washed 3 times with buffer containing 25 mM HEPES pH 7.6, 1% Thesit (v/v), 1 M NaCl. The bound proteins were eluted with 1 ml of 0.1 M glycine pH 2.5, 0.5 % Thesit. Eluted proteins were TCA precipitated for further analysis on SDS-PAGE and Western blot.

4.3.11 Sucrose gradient analysis

Vacuolar SNARE protein interactions were analyzed on sucrose gradient. A linear gradient of 15–60% sucrose was prepared for the analysis. 60% sucrose was prepared in a buffer containing 25 mM HEPES pH 7.6, 1 M NaCl, 10 mM β-mercaptoethanol and 15% sucrose was prepared in buffer containing 25 mM HEPES pH 7.6, 1% Thesit (v/v), 1 M NaCl, 10 mM β-mercaptoethanol. In a 4 ml Beckman centrifuge tube 3.6 ml of 15% sucrose solution was added and 300 µl 60% sucrose solution was put at the bottom of the tube slowly through a syringe. The tube was preserved at -20^{o}C or -80^{o}C overnight for complete freezing of the solution. The frozen solution was melted (6 – 8 hrs) slowly at 4^{o}C in order to form a linear gradient. The single SNARE protein or overnight SNARE protein mixture were added on the top carefully and centrifuged for 15 hrs at 4^{o}C at 240,000xg in a SWTi 60 rotor in Beckman centrifuge. Twelve fractions were collected from the bottom with a syringe and further analyzed by co-immunoprecipitation or TCA precipitation.

4.3.12 SNARE protein complex assembly

The SNARE protein assembly was carried out by mixing the equimolar mixture of purified SNARE proteins and incubated at 4^{o}C overnight. Complex formation was detected by loading the mixture on sucrose gradient after a brief centrifugation.

4.3.13 SNARE protein complex disassembly

Overnight SNARE protein mixture (50 µl) was incubated with 10 µg of Sec17p, 10 µg Sec18p, 2 mM $MgCl_2$, and 0.5 mM ATP or 0.5 mM ATPγS in a final volume of 100 µl for 1 hr at 4^{o}C in an Eppendorf shaker (Horsnell et al., 2002; Sollner et al., 1993a).

After a brief centrifugation, the reaction mixture was loaded on sucrose gradient for further analysis.

4.3.14 Protein and peptide estimation

Protein concentration was estimated by Bradford assay (Bradford, 1976) by using BSA as a standard protein. The interference of detergent was corrected by preparing the calibration curve with equal amount of Thesit.

Peptides were synthesized by standard solid phase methods (F-moc) by PSL, Heidelberg, Germany. Mass spectrometry showed that the peptides were more than 90% pure. Molar extinction co-efficient of the peptides was determined from the software available on website (http://www.basic.nwu.edu/biotools/proteincalc.html). Concentration of the peptides was determined with the help of this calculated molar extinction coefficient.

4.3.15 Circular Dichroism spectroscopy

Linear polarized light can be viewed as a superposition of opposite circular polarized light of equal amplitude and phase. A projection of the combined amplitudes perpendicular to the propagation of direction thus yields a line (Figure 9 panel A). When this light passes through an optically active sample with a different absorbance for the two components, the amplitude of the stronger absorbed component will be smaller than that of the less absorbed component. The consequence is that a projection of the resulting amplitude now yields an ellipse instead of the usual line, but the polarization direction has not changed (Figure 9 panel B). The occurrence of ellipticity is called Circular Dichroism. Rotation of the polarization plane (or the axes of the dichroic ellipse) by a small angle α occurs when the phases for the 2 circular components become different, which requires a difference in the refractive index *n*. This effect is called circular birefringence.

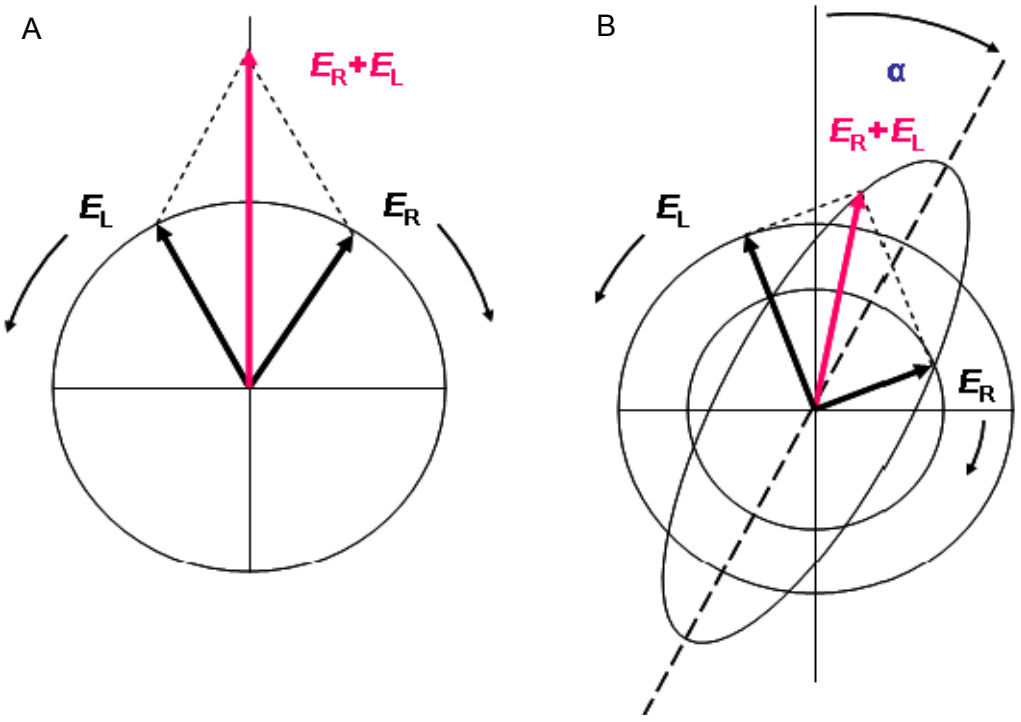

Figure 9. **Circular Dichroism (CD) is observed when optically active matter absorbs left and right hand circular polarized light slightly differently.** A. Linear polarized light can be viewed as a superposition of opposite circular polarized light of equal amplitude and phase. B Different absorption of the left- and right hand polarized component leads to ellipticity (CD) and optical rotation (OR). The actual effect is minute and using actual numbers the ellipse would still resemble a line. This Figure is adapted from http://www-structure.llnl.gov/cd/cdtutorial.htm.

CD measurement gives the data recorded as ellipticity θ_{obs} in degrees or millidegrees. To be able to compare these ellipticity values we need to convert into a normalized value. The unit most commonly used in protein and peptide work is the mean molar ellipticity per residue. The molar ellipticity or mean residue ellipticity is calculated by using the equation presented below:

$$[\theta]_{MRE} = \frac{(\theta_{obs} \times 100 \times M_r)}{(c \times l \times N_A)}$$

Where θ_{obs} is the measured ellipticity in degrees, c is the protein concentration in mg/ml, l is pathlength in cm, and M_r is the protein molecular weight, N_A is the number of amino acids per protein, $[\theta]_{MRE}$ is the mean residue ellipticity or molar ellipticity.

Mean residue ellipticity have the units degrees X cm^2 X $dmol^{-1}$. The factor 100 in equation originates from the conversion of the molar concentration to the $dmol/cm^3$ concentration unit. Standard curves of different secondary structures of protein are presented in Figure 10.

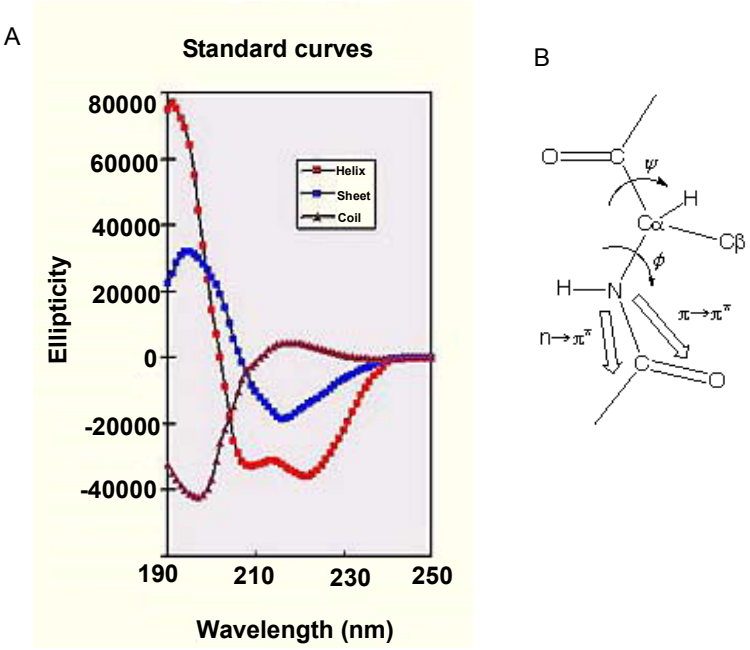

Figure 10. **Standard curve for different secondary structures of proteins.** A, The curve represents α-helix when molar ellipticity at 193 nm (π→π*) is positive and negative at 209 nm (π→π*) and 222 nm (n→π*). The curve represents β-sheet when molar ellipticity is positive at 196 nm (n→π*) but negative at 218 nm (π→π*). Molar ellipticity value positive at 212 nm (π→π*) but negative at 195 nm (n→π*) indicates the random coil structure of the protein. B, The intensity and energy of these transitions depends on Φ and Ψ (i.e., secondary structure). This Figure is adapted from http://www-structure.llnl.gov/cd/cdtutorial.htm and http://www.newark.rutgers.edu/chemistry/grad/chem585/lecture1.html.

All CD spectra were recorded on JASCO J-715 model CD spectrometer with a scan speed 50 nm/min and an average of 10-20 scans per sample. The spectra were recorded at 20°C. For CD experiment full length proteins were dialyzed in buffer 10 mM Tris-HCl pH 7.4, 150 mM NaCl and 1% (v/v) Thesit. When peptides were used for CD experiments, they were first dissolved in TFE. TFE was evaporated under N_2 and then the peptides resuspended in detergent solution: 10 mM Tris-HCl, pH 6.8 (for synaptobrevin II) or pH 7.4 (for Vam3p TMD peptides), 1% (v/v) Thesit. Synaptobrevin II TMD peptides were resuspended in 6M urea with 10 mM Tris-HCl pH 6.8 and 1% (v/v) Thesit for further CD measurement. Samples dissolved in Thesit buffer were incubated for 2 hrs to equilibrate. All samples were centrifuged for 30

min at 14000xg before recording spectra. CD measurements were done at a concentration ~0.100mg/ml and with 0.1 cm path length quartz cuvette. The spectrum of the synaptobrevin II peptide dissolved in 6M urea was measured at a concentration of ~0.500 mg/ml and with 0.02 cm path length cuvette. Similar data were obtained when CD spectra in the absence or presence of urea were recorded at the same peptide concentration (~0.100mg/ml) (Roy et al., 2004). Molar ellipticity of the spectra were calculated by using the formula mentioned above and those were fitted using standard software CDNN ((Bohm et al., 1992), http://www.imtech.res.in/pub/pspt/cdnn/win/) and the average secondary structures were calculated.

5 Results

5.1 Expression and purification of SNARE protein

To understand the role of TMD in SNARE protein interaction the wild type proteins and its mutants were expressed recombinantly in *E.coli*. This will provide good amount of proteins for the further experiments. The details of protein expression and purification are discussed in this section.

5.1.1 Expression and purification of synaptobrevin II

Synaptobrevin II is a v-SNARE or R-SNARE protein, of synaptic vesicles. Previous studies from our laboratory showed that synaptobrevin II has two interaction domains – cytosolic domain and C-terminal transmembrane domain (TMD) (Laage and Langosch, 1997). In this study synaptobrevin II was cloned in pSNiR2 under T7 promoter and expressed in *E.coli* BL21(DE3)pLysS, as described in methods (Laage and Langosch, 1997; Laage and Langosch, 2001; Roy et al., 2004). Figure 11 shows the expression and purification of synaptobrevin II as nucleaseA fusion protein.

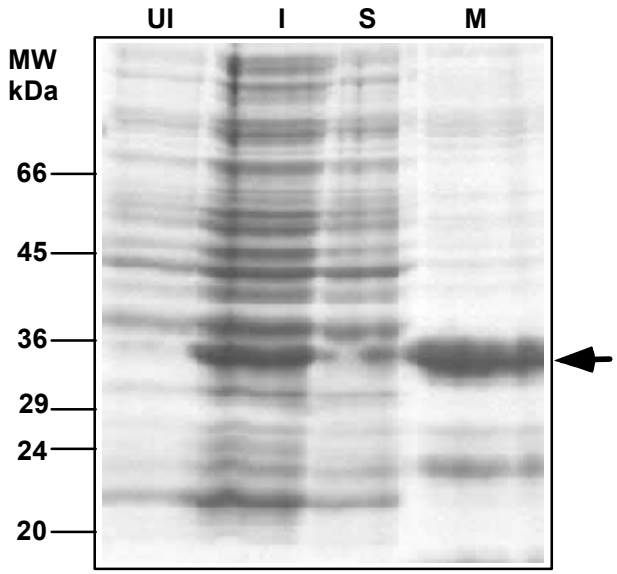

Figure 11. **Expression and purification of synaptobrevin II**. Proteins were visualized by Coomassie staining in 12.5% SDS-PAGE. Lane UI represents the total protein from uninduced host cells, lane I represents the total protein from induced host cells, lane S represents the soluble protein fraction obtained after cell lysis, and lane M represents the detergent soluble protein fraction from membrane and other insoluble material obtained from the host cell after cell lysis. In the M fraction the arrow shows the enriched nucleaseA synaptobrevin II fusion protein.

5.2 Expression and purification of yeast vacuolar SNARE proteins

Yeast vacuole membrane fusion is a homotypic fusion in which five SNARE proteins Vam3p, Nyv1p, Vam7p, Vti1p and Ykt6p are involved. The corresponding genes were directly amplified from yeast genome and cloned into different expression vectors in *E.coli*, therefore the codons of these genes are not optimized for *E.coli* expression host. In order to clarify the possibility of the expression of these eukaryotic genes in *E.coli* host, the codon degeneracy of the amino acids of these proteins was analyzed with the software available on internet (*E.coli* codon usage analyzer 2.1 http://faculty.ucr.edu/~mmaduro/codonusage/usage.htm).

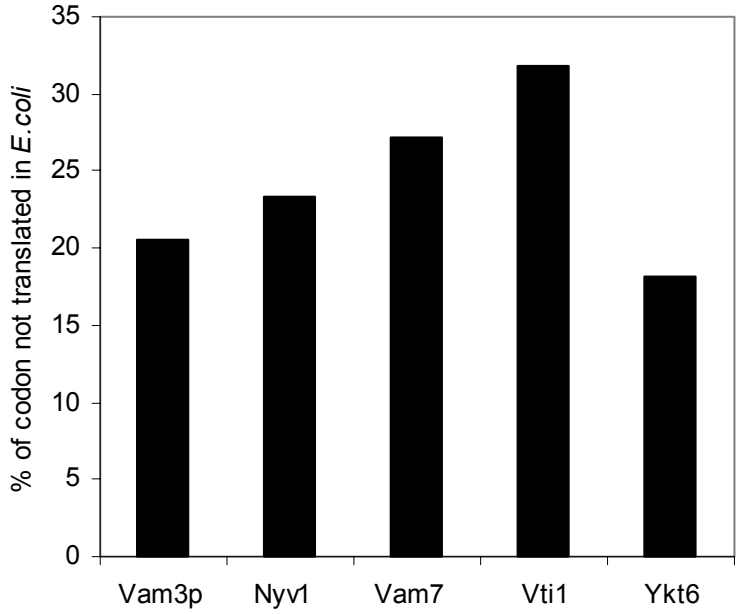

Figure 12. **Analysis of codon by *E.coli* codon analyzer 2.1.** The codon analyzer shows the percentage of the codons that can not be translated in *E.coli* host. Yeast vacuole SNARE proteins have on average 20-30% codons that can not be translated in *E.coli*.

Codon degeneracy analysis (Figure 12) shows that the vacuolar SNARE proteins contain certain percentage of codons, which can not be translated efficiently, due to the low frequency of the corresponding tRNAs in *E.coli*. Therefore a special host strain Rosetta(DE3) was used for the expression of these yeast proteins in prokaryote. Rosetta host strains are BL21 derivatives, designed to enhance the expression of eukaryotic proteins that contain codons rarely used in *E. coli*. These strains supply tRNA genes for AGG (Arg), AGA (Arg), AUA (Val), CUA (Leu), CCC (Pro), GGA (Gly) on a Col-E1 compatible chloramphenicol-resistant plasmid. Thus

the Rosetta strains provide for "universal" translation, which is otherwise limited by the codon usage of *E. coli*. Transcription of the tRNA genes is driven by their native promoters.

The use of this strain did not solve the entire problem of expression, e.g., Vam3p did not express at all when induction was done at 37°C, whereas good yield of proteins was obtained in cold condition at 16°C. In case of Vam7p, expression and induction at 37°C gave low amount of protein; moreover a ladder of low molecular weight proteins was visible, thus suggesting degradation or truncation of the protein during synthesis. Vam7p and Vti1p expression and induction in cold condition at 16°C gave good amount of proteins. For yeast protein expression in prokaryotic host, the cold condition increased the stability of the protein as shown for other proteins (Brugger et al., 2000; Mujacic et al., 1999; Qing et al., 2004).

Different studies report that expression of membrane proteins or eukaryotic proteins in *E.coli* host cells can lead to the production of insoluble inclusion bodies, in which the foreign protein is not in the native folding state. To overcome this problem, the above mentioned proteins were expressed and induced in cold condition at 16°C; in particular the cells were first grown at 37°C till the OD_{600} was about 0.5 and then incubated on ice to cool down the temperature of the culture (as described in method section and Figure 13). Induction was done by adding IPTG to the cold cultures and cells were grown further for expression of the desired protein at 16°C. It has been shown that temperature changes can induce in the bacterial cells the production of cold shock proteins, which can act as chaperons for protein folding (Dougan et al., 2002; Hartl and Hayer-Hartl, 2002; Walter and Buchner, 2002; Wegele et al., 2004).

After obtaining good expression the next task was to purify the proteins. Proteolysis of the proteins was avoided by using a combination of protease inhibitor: PMSF, α_2-macroglobulin and EDTA free protease inhibitor cocktail tablets (Roche). The conventional membrane protein purification protocol is commonly based on two sequential steps: cell lysis followed by separation of soluble part from insoluble part, where in this last step the membrane proteins are solubilized from the insoluble part in presence of detergent. Here we introduced few modifications (Figure 13) in order to avoid proteolysis and to improve membrane protein solubilization. In particular we

lysed the bacterial cells in the presence of 2% Triton X-100 (v/v) and 2% Thesit (v/v) with HEPES buffer and 1 M NaCl, thus allowing complete solubilization of the membrane fraction under the optimal conditions (pH, detergent and salt) for the stabilization of vacuolar SNARE proteins. The lysate was applied on column for purification. The expression and purification of each vacuolar SNARE proteins are discussed below.

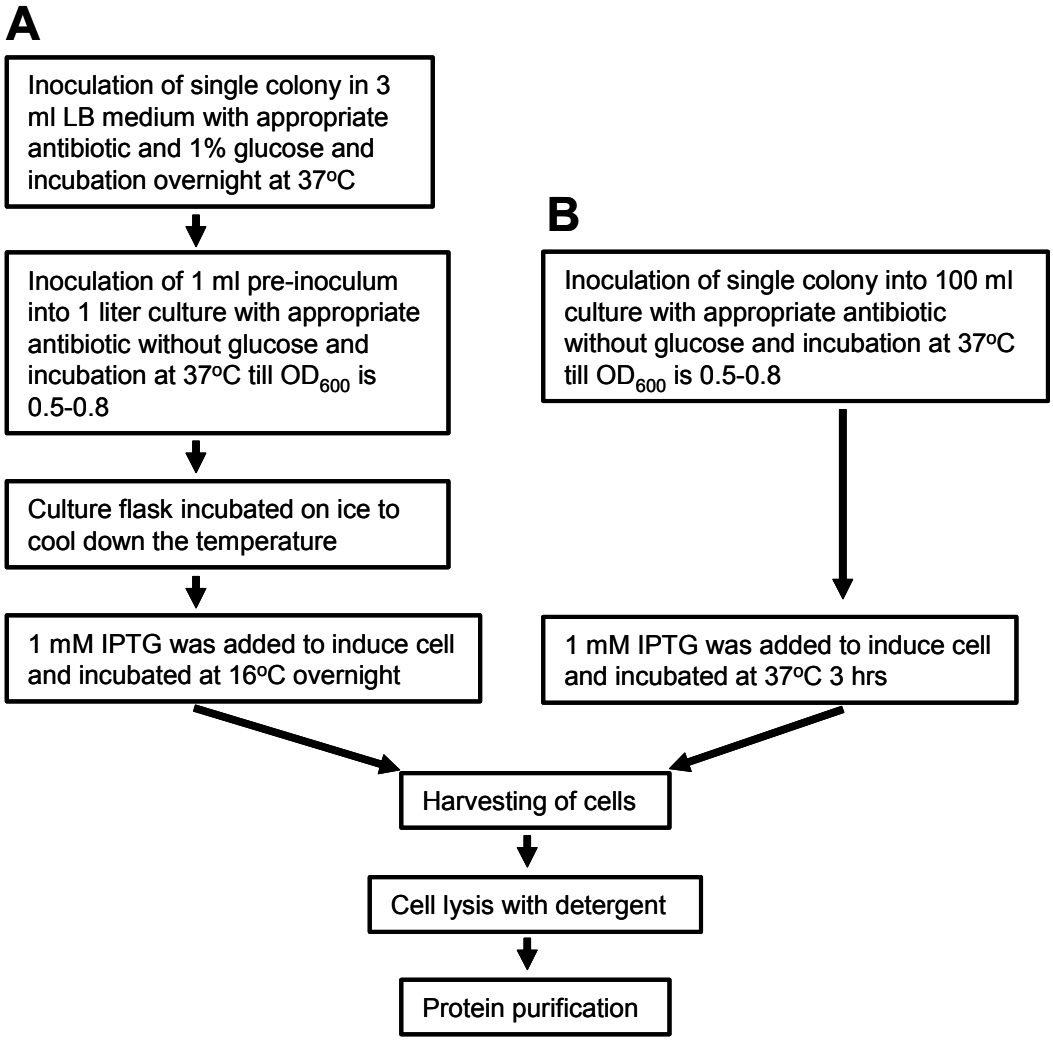

Figure 13. **Schematic representation yeast SNARE protein expression in *E.coli*.** Protein was produced following either pathway A or B as mentioned in the method section.

5.2.1 Expression and purification of Vam3p and the its mutants

Vam3p is a Q-SNARE that participates in the yeast vacuolar membrane fusion. This protein contains a single membrane spanning domain. Previous studies from our laboratory showed that TMD of Vam3p is very important for vacuolar membrane fusion, since deletion of its TMD reduces the efficiency of vacuolar membrane fusion (Rohde et al., 2003). Vam3p was cloned in pET28a under T7 promoter. The mutants Vam3pΔTMD (amino acid residues 1–263) and Vam3p Ala20 (amino acid residues 264–283 were changed to alanine stretch) (Figure14, panel H) were produced by PCR and cloned in the same vector between the *Nco*I and *Xho*I sites, like the wild type Vam3p. The mutant Vam3pC274A was prepared by site-directed mutagenesis, as described in the methods section. Mutations were confirmed by sequencing. All these mutants have a C-terminal $(His)_6$-tag for purification. The Vam3p TMD mutants Vam3pA4 (where amino acid residues 265, 269, 273 and 277 were mutated to alanine) and Vam3pA4bb (where amino acid residues 267, 271, 275 and 279 were mutated to alanine) are cloned between the *Bam*HI and *Xho*I sites of the same vector (Figure14, panel H). These two mutants have an N-terminal $(His)_6$-tag for purification. Expression of these proteins was carried out in cold condition (16^oC) for 20 hours. Vam3p and its mutants were purified by Ni-NTA column, as described in the methods section. After purification the purified proteins were visualized by Coomassie staining on SDS-PAGE (Figure 14). The purified proteins were dialyzed to remove imidazole (Figure14, panel G) and the dialyzed proteins were stored at 4^oC for further usage.

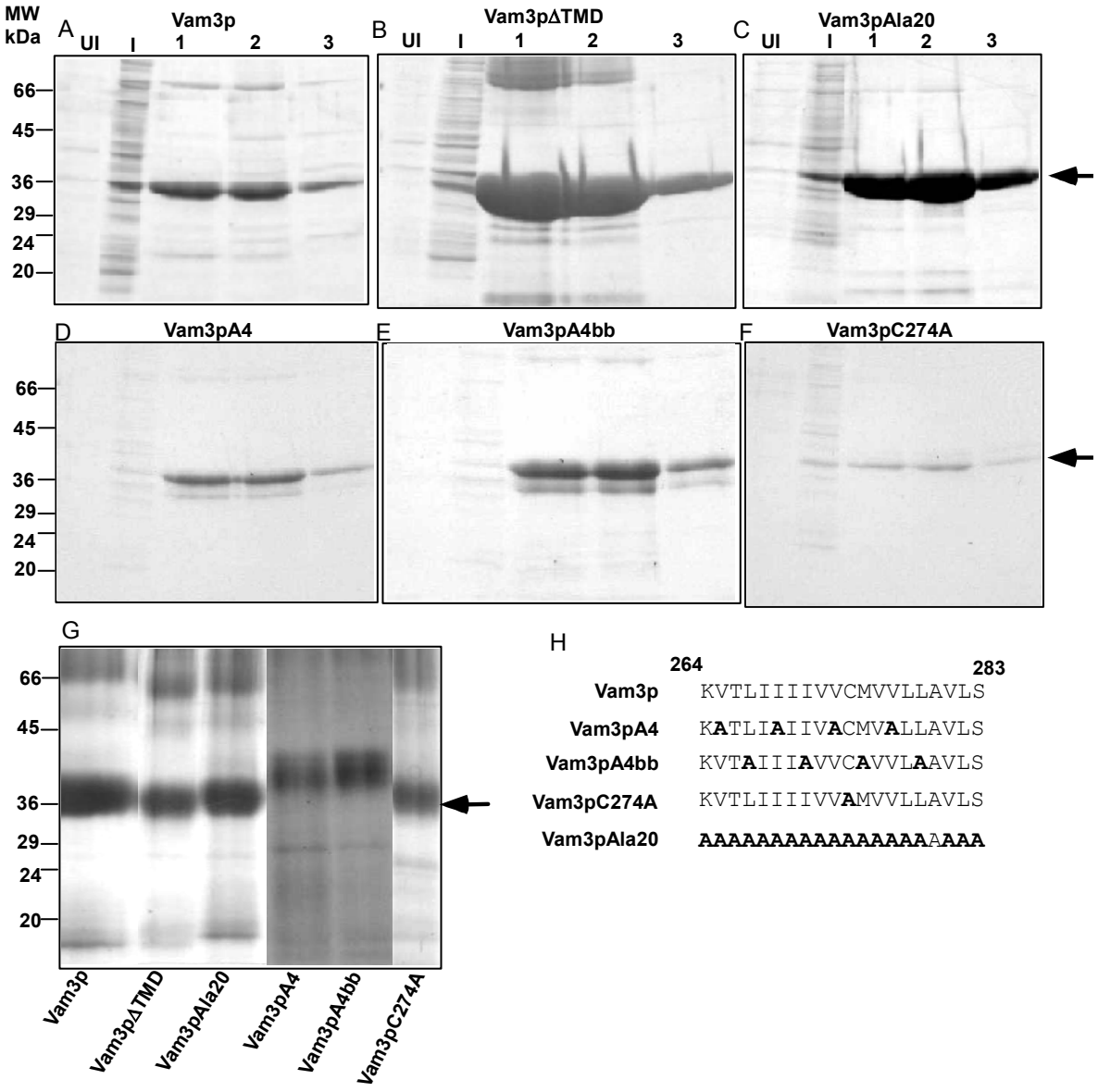

Figure 14. **Expression and purification of Vam3p and its mutants**. Proteins were visualized by Coomassie staining in 12.5% SDS-PAGE. A, Vam3p; B, Vam3pΔTMD; C, Vam3pAla20; D, Vam3pA4; E, Vam3pA4bb; F, Vam3pC274A; G, dialyzed Vam3p and its mutants; H, sequence of the Vam3p wild type TMD and its mutants. Lane UI represents the total proteins of the uninduced host cells, lane I represents the total proteins of the induced host cells, lane 1 represents the first fraction of the purified protein from the column, lane 2 represents the second fraction of the purified protein from the column, lane 3 represents the third fraction of the purified protein from the column. Proteins were eluted with 500 mM imidazole concentration. Arrows indicate the enriched protein fraction of Vam3p and its mutants.

5.2.2 Expression and purification of Nyv1p and mutants

Nyv1p is an R-SNARE, participating in the vacuolar membrane fusion. This protein contains a single membrane spanning domain. Nyv1p was cloned in pET15b under T7 promoter between the *Nde*I and *Bam*HI sites. The mutants Nyv1pΔTM (amino

acid residues 1–226) and Nyv1pAla21 (amino acids residues 229–249 were changed to alanine stretch) (Figure 15, panel E) were prepared by PCR, cloned in the same vector between the same restriction sites as the wild type. Mutations were confirmed by sequencing. All these proteins contain N-terminal $(His)_6$-tag for purification by Ni-NTA column. Nyv1p and its mutants were induced and expressed at 37°C for 3 hours, as described in the methods section. Purified proteins were visualized by Coomassie staining in SDS-PAGE (Figure 15). The purified proteins were dialyzed to remove imidazole (Figure 15, panel D) and the dialyzed proteins were stored at 4°C for further usage.

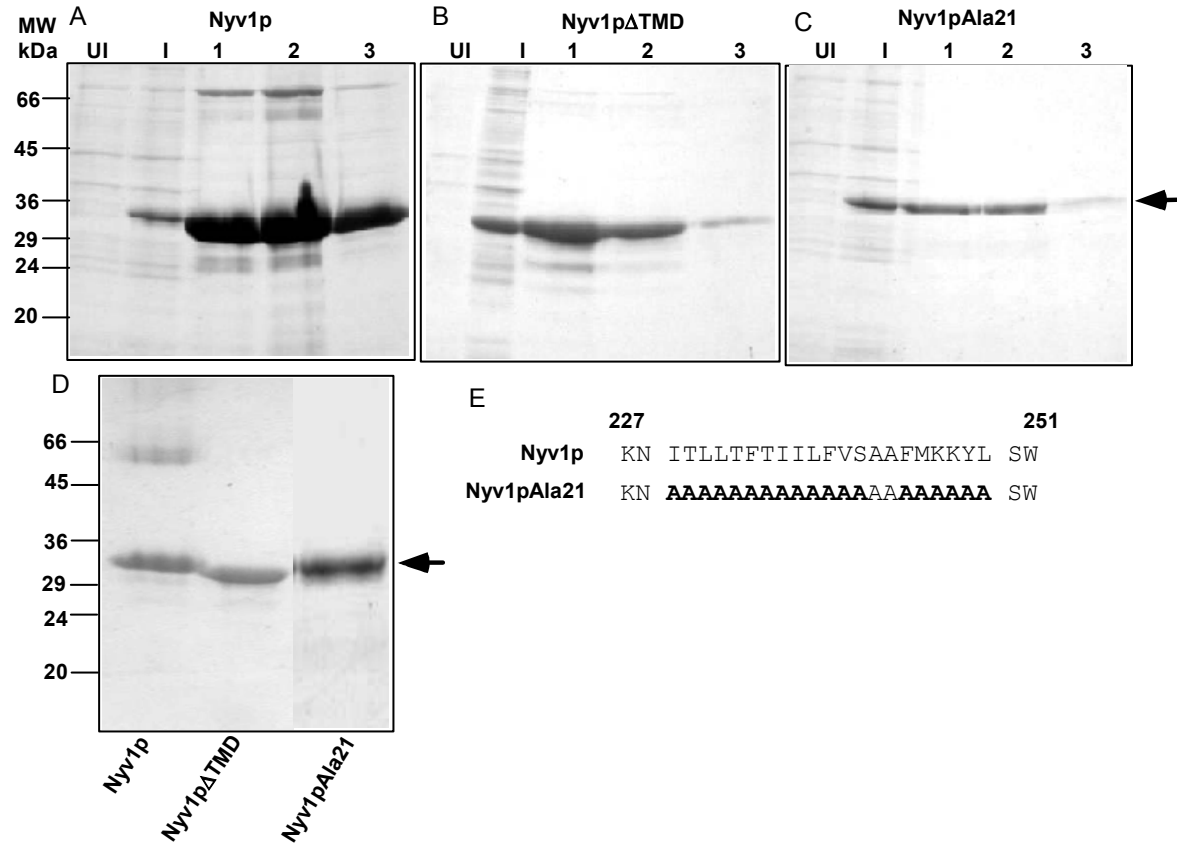

Figure 15. **Expression and purification of Nyv1p and its mutants**. Proteins were visualized by Coomassie staining in 12.5% SDS-PAGE. A, Nyv1p; B, Nyv1pΔTMD; C, Nyv1pAla21; D, dialyzed Nyv1p and its mutants; E, sequence of wild type Nyv1p and its mutants. Lane UI represents the total proteins of the uninduced host cells, lane I represents the total proteins of the induced host cells, lane 1 represents the first fraction of the purified protein from the column, lane 2 represents the second fraction of the purified protein from the column, lane 3 represents the third fraction of the purified protein from the column. Proteins were eluted with 500 mM imidazole concentration. Arrows indicate the enriched protein fraction of Nyv1p and its mutants.

5.2.3 Expression and purification Vti1p and mutants

Vti1p is a Q-SNARE with a single membrane spanning domain. This protein was cloned into pET28a under T7 promoter between the *Bam*HI and *Eco*RI sites. The mutants Vti1pΔTM (amino acid residues 1–188) and Vti1pAla23 (amino acid residues 190–212 were changed to alanine stretch) (Figure 16, panel E) were prepared by PCR and cloned into same vector between the same restriction sites as the wild type. The mutations were characterized by sequencing. These proteins were cloned with N-terminal $(His)_6$-tag for purification by Ni-NTA column. Expression and induction was done in cold condition at 16°C for 20 hours. Purified proteins were visualized by Coomassie staining upon SDS-PAGE (Figure 16). The purified proteins were dialyzed to remove imidazole (Figure 16, panel D) and the dialyzed proteins were preserved at 4°C for further usage.

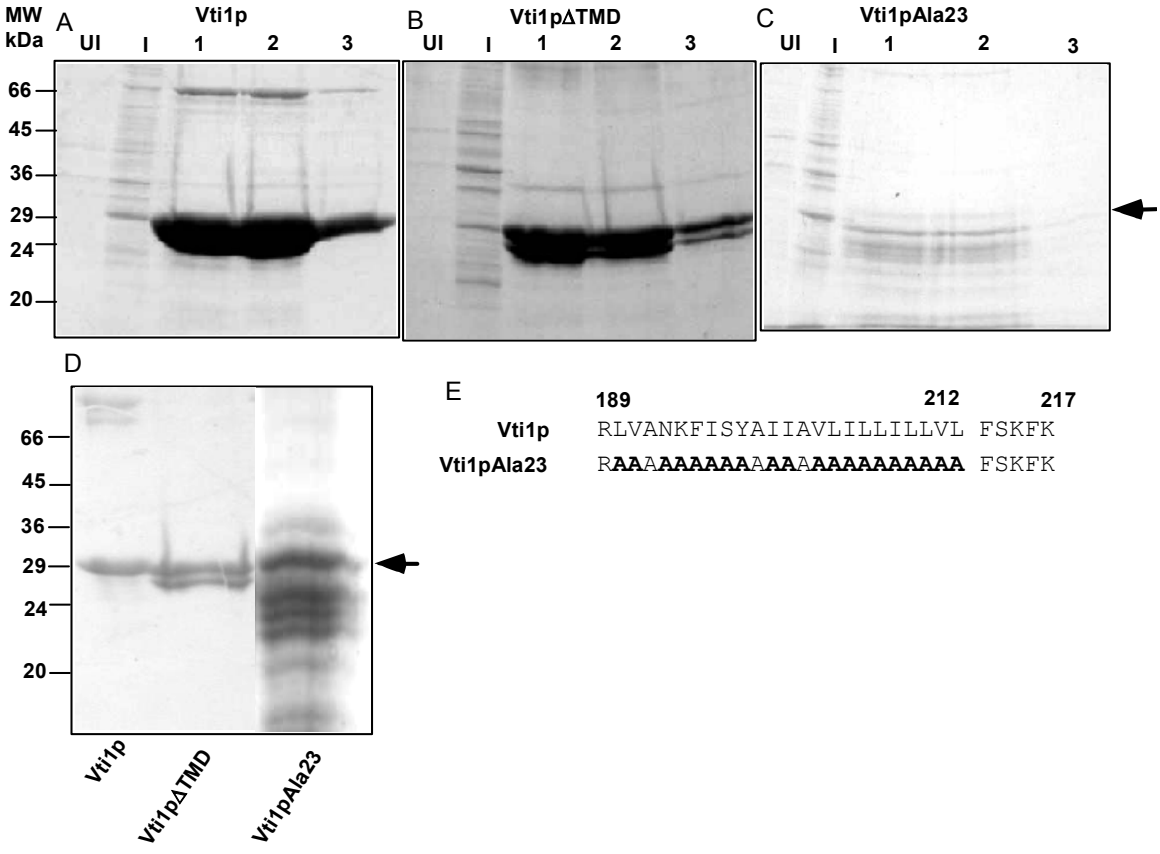

Figure 16. **Expression and purification of Vti1p and its mutants**. Proteins were visualized by Coomassie staining in 12.5% SDS-PAGE. A, Vti1p; B, Vti1pΔTMD; C, Vti1pAla23; D, dialyzed Vti1p and its mutants; E, sequence of Vti1p and its mutants. Lane UI represents the total proteins of the uninduced host cells, lane I represents the total proteins of the induced host cells, lane 1 represents the first fraction of the purified protein from the column, lane 2 represents the second fraction of the purified protein from the column, lane 3 represents the third fraction of the purified protein from the column. Proteins were eluted with 500 mM imidazole concentration. Arrows indicate the enriched protein fraction of Vti1p and its mutants.

5.2.4 Expression and purification of Vam7p

Vam7p is a Q-SNARE that does not contain any membrane spanning domain. It is localized in vacuolar membrane as well as in cytoplasm. This protein was cloned into pET28a under T7 promoter between the *Bam*HI and *Eco*RI sites. It was expressed and induced in cold condition at 16^{o}C. Vam7p was expressed with N-terminal $(His)_6$-tag for purification by Ni-NTA column. The purified protein was visualized by Coomassie staining in SDS-PAGE (Figure 17). The purified protein was dialyzed to remove imidazole (Figure 17, panel B) and stored at 4^{o}C for further usage.

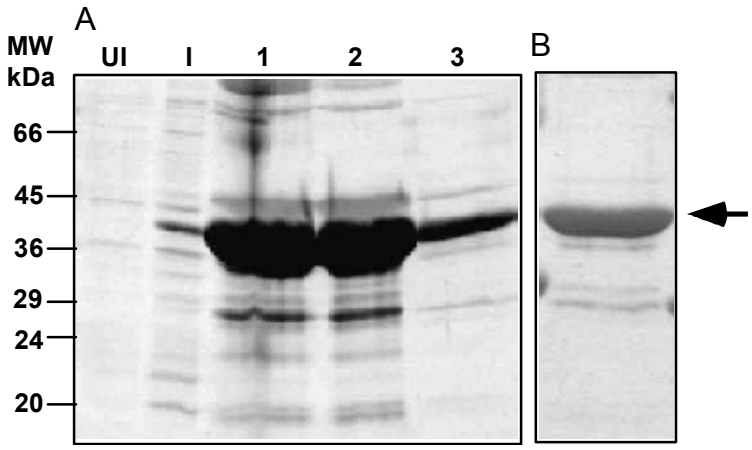

Figure 17. **Expression and purification of Vam7p**. Proteins were visualized by Coomassie staining in 12.5% SDS-PAGE. A, Lane UI represents the total proteins of the uninduced host cells, lane I represents the total proteins of the induced host cells, lane 1 represents the first fraction of the purified protein from the column, lane 2 represents the second fraction of the purified protein from the column, lane 3 represents the third fraction of the purified protein from the column. Proteins were eluted with 500 mM imidazole concentration. B, dialyzed Vam7p. Arrows indicate the enriched protein fraction of Vam7p.

5.2.5 Expression and purification of Ykt6p

Ykt6p is an R-SNARE in vacuolar membrane fusion and it does not contain any membrane spanning domain. It is attached to membrane by prenylation at the C-terminus. This protein was obtained in pGEX 4T-1 vector under *tac* promoter between the *Bam*HI and *Xho*I sites. Ykt6p was expressed and purified as a GST fusion protein (Figure 18, panel A). The same Ykt6p gene was again subcloned in pET 28a under T7 promoter between the *Bam*HI and *Xho*I sites, expressed with N-terminal $(His)_6$-tag for purification and purified by Ni-NTA column (Figure 18, panel

C). The purified proteins were dialyzed to remove imidazole and glutathione (Figure 18, panels B & D) and was stored at 4°C for further usage.

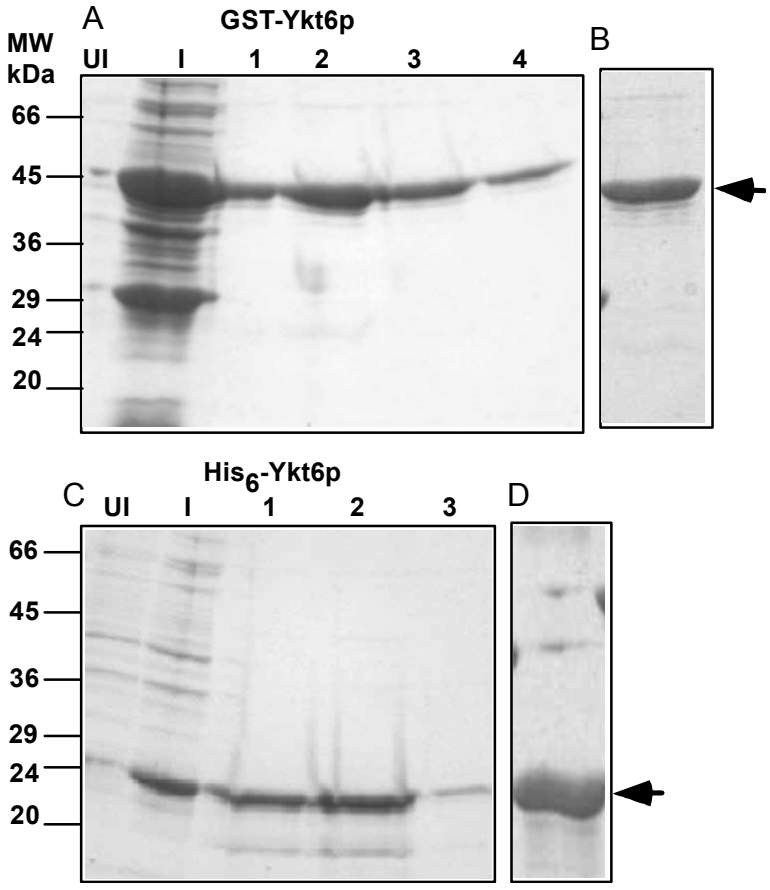

Figure 18. **Expression and purification of Ykt6p**. Proteins were visualized by Coomassie staining upon 12.5% SDS-PAGE. A, GST-Ykt6p; B, dialyzed GST-Ykt6p; C, His_6-tagged Ykt6p; D, dialyzed His_6-Ykt6p. Lane UI represents the total proteins of the uninduced host cells, lane I represents the total proteins of the induced host cells, lane 1 represents the first fraction of the purified protein from the column, lane 2 represents the second fraction of the purified protein from the column, lane 3 represents the third fraction of the purified protein from the column, lane 4 represents the fourth fraction of the purified protein from the column. Proteins were eluted with 500 mM imidazole concentration or 10 mM reduced glutathione concentration. Arrows indicate the enriched protein fraction of Ykt6p.

5.2.6 Expression and purification of Sec17p and Sec18p

Sec17p and Sec18p are α-SNAP and NSF homologous of yeast respectively. These proteins were cloned into vector pQE9 under T5 promoter. Both proteins were expressed in M15 *E.coli* host cells and were induced at 37°C. $(His)_6$-tag purified proteins were visualized by Coomassie staining in SDS-PAGE (Figure 19 panel A &

C). The purified proteins were dialyzed to remove imidazole (Figure 19 panel B & C) and the dialyzed proteins were stored at 4^{o}C for further usage.

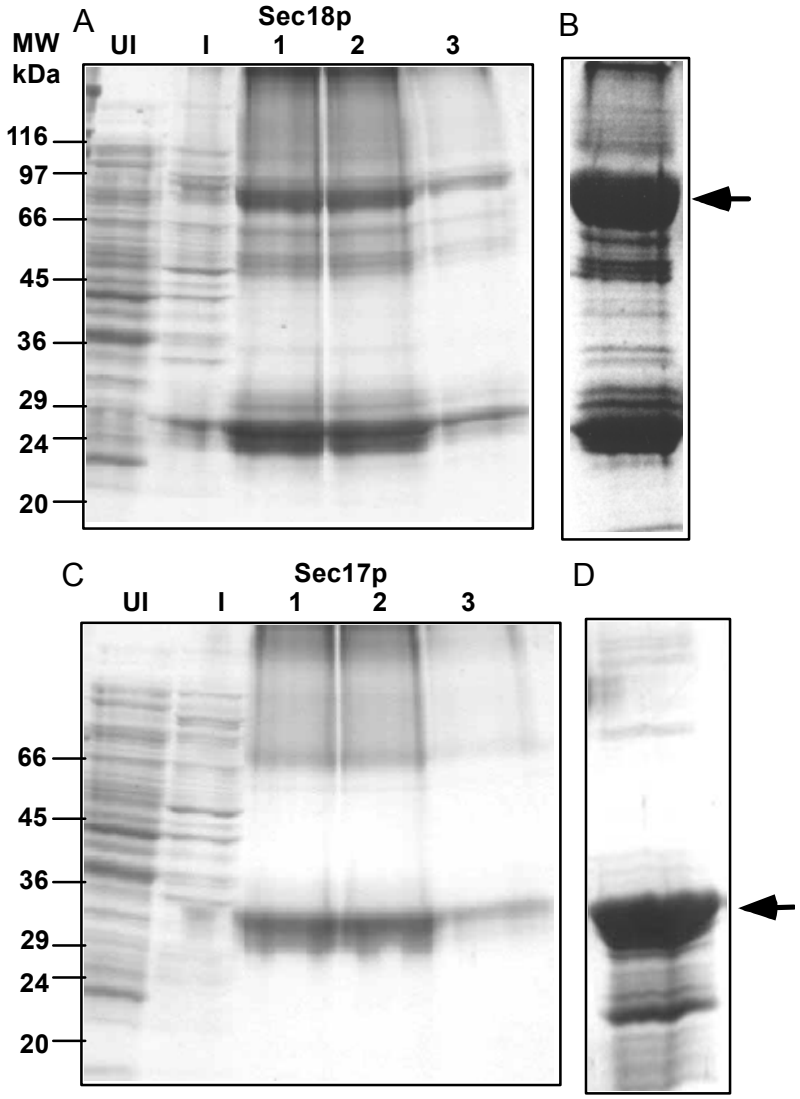

Figure 19. **Expression and purification of Sec17p and Sec18p**. Proteins were visualized by Coomassie staining in 12.5% SDS-PAGE. A, Sec18p; B, dialyzed Sec18p; C, Sec17p; D, dialyzed Sec17p. Lane UI represents the total proteins of the uninduced host cells, lane I represents the total proteins of the induced host cells, lane 1 represents the first fraction of the purified protein from the column, lane 2 represents the second fraction of the purified protein from the column, lane 3 represents the third fraction of the purified protein from the column. Proteins were eluted with 500 mM imidazole concentration. Arrows indicate the enriched protein fraction of Sec17p and Sec18p.

5.2.7 Storage and stability of vacuolar SNARE proteins

After obtaining good expression of vacuolar SNARE proteins, another task was optimizing the stability and storage of these proteins. It was not possible to store these proteins at -80^{o}C, due to their insolubility when thawed from -80^{o}C, therefore these proteins were stored at 4^{o}C. Different detergents were used for solubilizing the vacuolar proteins as shown in Table 1. In particular Nyv1p and its mutants are stable only in HEPES buffer with Thesit, whereas in Triton X-100 and CHAPS oligomers are formed, as determined by sucrose gradient separation (data not shown). Particularly when Nyv1p was solubilized in phosphate buffer with Triton X-100, the protein showed very high oligomer in sucrose gradient (data not shown). Ykt6p without any soluble tag is forming unspecific aggregates, as demonstrated by sucrose gradient separation, in which the protein is present in the entire twelve fractions collected (Figure 30). In case of Vti1p and its mutants solubilization with Triton X-100 or CHAPS is at first successful, but after one week of storage the proteins were precipitated. Moreover, Vam7p and Vti1p were stable only in the presence of 1 M NaCl; therefore all the proteins were stored in 1 M NaCl for uniformity.

In summary, vacuolar SNARE proteins were stored in buffer containing 25 mM HEPES pH 7.6, 1 M NaCl, 10 mM β-mercaptoethanol as reducing agent, 1% (v/v) Thesit as detergent and 10% (v/v) glycerol at 4^{o}C.

Table 1: Stability of vacuolar SNARE protein in different detergent

		Detergent	
Protein	**Thesit**	**Triton X-100**	**CHAPS**
Vam3p	stable	stable	stable
Vam3pΔTMD	stable	stable	stable
Vam3pAla20	stable	stable	stable
vam3A4	stable	visible precipitation	stable
vam3A4bb	stable	visible precipitation	stable
Vam3pC274A	stable	stable	stable
Nyv1p	stable	aggregation[1]	aggregation
Nyv1pΔTMD	stable	aggregation	aggregation
Nyv1p Ala21	stable	aggregation	aggregation
Vti1p	stable	visible precipitation	visible precipitation
Vti1pΔTMD	stable	visible precipitation	visible precipitation
Vti1p Ala23	stable	visible precipitation	visible precipitation
Vam7p	stable	stable	stable
His-ykt6	aggregation	aggregation	aggregation
GST-ykt6	stable	stable	stable

[1]aggregation as detected by sucrose gradient centrifugation.

5.3 Structural analysis of SNARE proteins

Previous studies on neuronal and endosomal SNAREs, revealed a high α-helical conformation of proteins in the complex. Moreover the crystal structure of neuronal SNARE complex demonstrated a typical coiled-coil pattern of interaction of the SNARE domains (Antonin et al., 2002; Sutton et al., 1998). The Secondary structure of vacuolar SNARE proteins, its mutants and the corresponding TMD peptides was examined by CD spectroscopy to understand how deletion of TMD or mutation in TMD influences the structure of the full length protein. CD spectroscopy measurement and calculations of secondary structure were carried out as described in methods section.

5.3.1 Secondary structural analysis of synaptobrevin II TMD peptide

As shown in the next chapter synaptobrevin II exists as monomer and dimer, as detected especially in the presence of urea SDS-PAGE (Laage and Langosch, 1997; Roy et al., 2004). Because urea normally denatures proteins, we tested whether it influences the secondary structure of synaptobrevin II TMD in the detergent solution with and without 6 M urea or TFE (Figure 20). The calculated secondary structure of synaptobrevin II TMD (Table 2) shows higher α-helical content in TFE than in detergent solution or in detergent solution with 6 M urea. The α-helical content of the peptide in detergent solution with or without 6 M urea is almost similar; showing that synaptobrevin II TMD can preserve its secondary structure in 6 M urea.

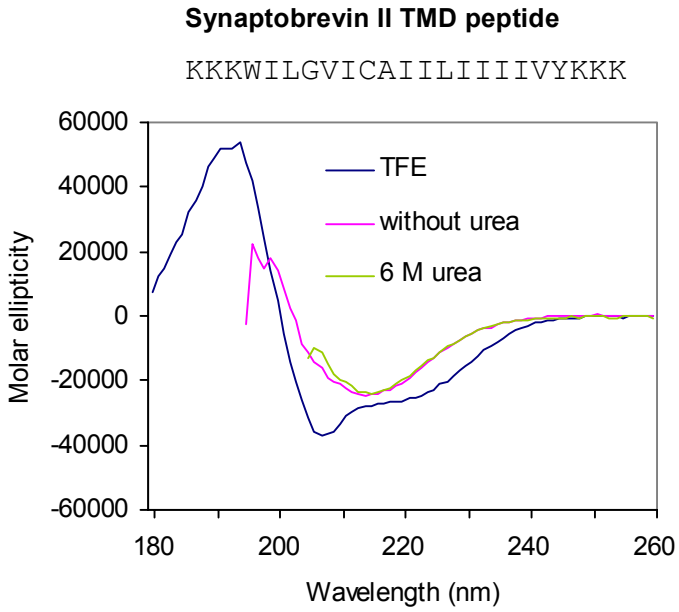

Figure 20. **CD spectra analysis of synaptobrevin II TMD peptide.** The synaptobrevin II TMD peptide was first dissolved in TFE and then different portions were dried under N_2 gas and resuspended in buffer containing 10 mM Tris-HCl, pH 6.8, 1% (v/v) Thesit with and without 6 M urea. Spectra were recorded from 180-260 nm (TFE), 193-260 nm (Thesit without urea) and 205-260 nm (Thesit with 6 M urea). The downward deflection of the spectra below 200 nm for peptides in Thesit is an artifact due to high optical density of the sample in this region.

Table 2: **Spectral analysis of synaptobrevin II TMD peptide**

Calculation was carried out from the spectra obtained between 205-260 nm to treat all the data equally. In the Table percentage of α-helix and β-sheet content were presented and residual secondary structure were accounted by random coil and β-turn conformations.

	Secondary structure	
Solvent	**%of α-helix**	**% of β-sheet**
TFE	85	2
1% Thesit without urea	69	6
1% Thesit with 6M urea	65	7

5.3.2 Secondary structure of Vam3p recombinant proteins and synthetic TMD peptides

Before CD analysis, these proteins were dialyzed against buffer containing 10 mM Tris-HCl, pH 7.4, 150 mM NaCl and 1% (v/v) Thesit in order to stabilize them in solution. After dialysis, proteins were centrifuged briefly before performing CD spectroscopy experiment. Figure 21 shows the different spectra of Vam3p and its mutants. In Figure 21, panel A the spectra of full length Vam3p and its mutants are shown for comparison. Wild type and mutant proteins show similar spectra, suggesting similar secondary structure, confirmed by calculation of the secondary structure percentage (Table 3). Results obtained show that recombinantly expressed Vam3p is mainly in α-helical conformation and mutation in TMD did not destabilize the helical property of the protein. Secondary structure of the Vam3p wild TMD peptide and its TMD mutant peptides was also determined to understand the effect of mutations on the TMD structure. CD spectra of Vam3p wild type TMD (Figure 21, panel B), Vam3pA4 (Figure 21, panel C) and Vam3pA4bb (Figure 21, panel D) peptides were determined in TFE and in detergent solution. Figure 21, panel E shows the molar ellipticity of Vam3p TMD peptide and its mutant in 1% (v/v) Thesit while Figure 21, panel F shows the same in TFE for better comparison. The TMD peptides showed stronger α-helical properties in TFE than in detergent solutions (Table 3). Calculated results show that in detergent solution Vam3pA4bb lose α-helical content with increased percentage of the β-sheet content, while all the other peptides in the detergent solution retained high amount of α-helical structure and negligible amount of β-sheet structure.

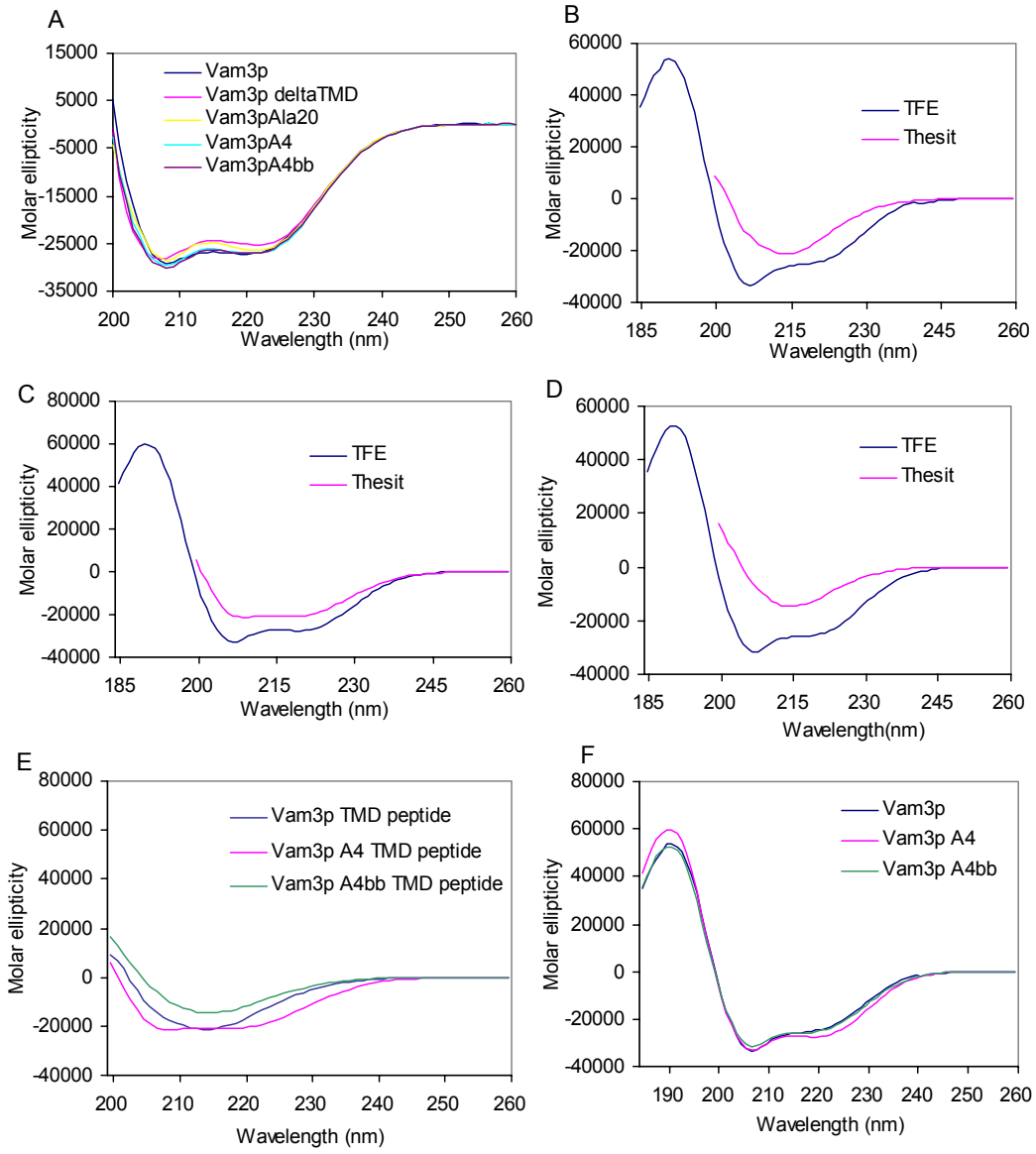

Figure 21. **CD spectra of Vam3p and mutants.** A. Recombinant purified proteins were dialyzed against 10 mM Tris-HCl, pH 7.4 150 mM NaCl, 1% (v/v) Thesit before CD analysis. The spectra were measured between 200-260 nm. B, Vam3p wild type TMD synthetic peptide (KKKWVTLIIIIVVCMVVLLKKK); C, Vam3pA4 TMD synthetic peptide (KKKW**A**TLI**A**IIV**A**CMV**A**LLKKK) and D, Vam3pA4bb TMD synthetic peptide (KKKWVT**A**III**A**VVC**A**VVL**A**KKK). CD spectra were recorded in TFE and in 10 mM Tris-HCl pH 7.4, 1% (v/v) Thesit solution; E, molar ellipticity of Vam3p TMD synthetic peptides and its mutant in 10 mM Tris-HCl, pH 7.4 1% Thesit (v/v). F, molar ellipticity of Vam3p TMD synthetic peptide and its mutant in 100% TFE. The spectra were measured between 185-260 nm.

Table 3 **CD spectral analysis of Vam3p full length protein and TMD peptides**

Calculations were carried out using the spectra obtained between 200-260 nm to treat all the data set equally. Full length Vam3p protein is mostly α-helical. Buffer represents 10 mM Tris-HCl, pH 7.4, 150 mM NaCl, 1% (v/v) Thesit (for peptides 150 mM NaCl is omitted). In the Table percentage of α-helix and β-sheet content are presented and residual secondary structure was accounted by random coil and β-turn conformations.

		Secondary structure	
Protein/peptide	**Solvent**	**%of α-helix**	**% of β-sheet**
Vam3p (full length)	buffer	81	3
Vam3pΔTMD (full length)	buffer	78	3
Vam3pAla20 (full length)	buffer	78	3
Vam3pA4 (full length)	buffer	80	3
Vam3pA4bb (full length)	buffer	81	3
Vam3p 16 (TMD peptide)	TFE	81	3
Vam3p 16 (TMD peptide)	buffer	59	8
Vam3p 16 A4 (TMD peptide)	TFE	82	2
Vam3p 16 A4 (TMD peptide)	buffer	68	6
Vam3p 16 A4bb (TMD peptide)	TFE	80	3
Vam3p 16 A4bb (TMD peptide)	buffer	39	14

5.3.4 Secondary structural analysis of Nyv1p

In Figure 22 CD spectra analysis shows that Nyv1p and its mutants are highly α-helical. Secondary structure calculations show (Table 4) that deletion or mutation in TMD does not modify the α-helix content.

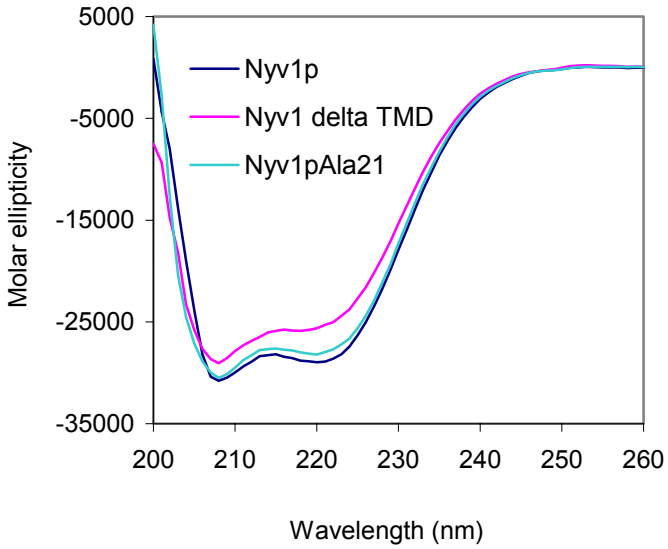

Figure 22. **CD spectral analysis Nyv1p and mutants**. The spectra were measured between 200-260 nm as described in Figure 21.

Table 4 **CD spectral analysis of Nyv1p full length protein and TMD mutant**

Calculations were carried out from the data obtained between 200-260 nm as described in Table 3

		Secondary Structure	
Protein	**Solvent**	**%of α-helix**	**% of β-sheet**
Nyv1p (full length)	buffer	83	2
Nyv1pΔTMD (full length)	buffer	78	3
Nyv1p Ala21 (full length)	buffer	83	2

5.3.5 Secondary structure analysis Vti1p

Figure 23 shows that Vti1p proteins have a high amount of α-helical structure. Secondary structure calculations show (Table 5) that deletion or mutation in TMD has no effect on the percentage of α-helix content.

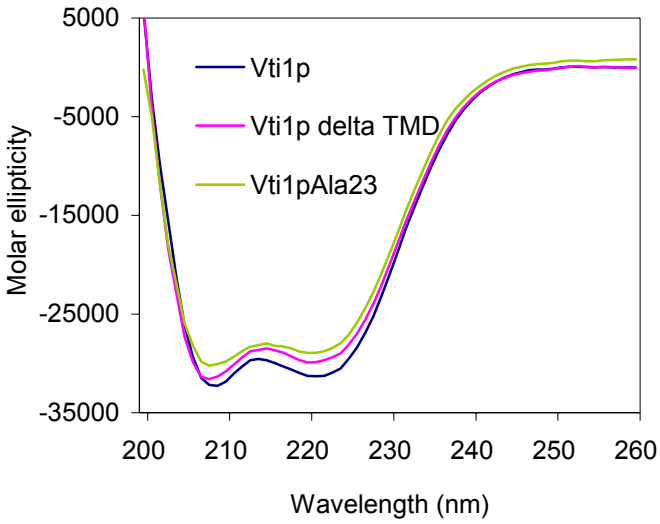

Figure 23. **CD spectral analysis Vti1p and mutants**. The spectra were measured between 200-260 nm as described in Figure 21.

Table 5 **CD spectral analysis of Vti1p full length protein and TMD mutants**

Calculations were carried out from the spectra obtained between 200-260 nm as in Table 3

		Secondary Structure	
Protein	**Solvent**	**%of α-helix**	**% of β-sheet**
Vti1p (full length)	buffer	85	2
Vti1pΔTMD (full length)	buffer	84	2
Vti1p Ala23 (full length)	buffer	83	2

5.3.6 Secondary structure analysis of Vam7p and Ykt6p

CD spectra of Vam7p and Ykt6p were shown in Figure 24. Figure 24, panel A shows that the full length Vam7p is highly α-helical, while Ykt6p (Figure 24, panel B) has the lowest α-helical content and the highest percentage of β-sheet content of all vacuolar SNARE proteins tested here (Table 6).

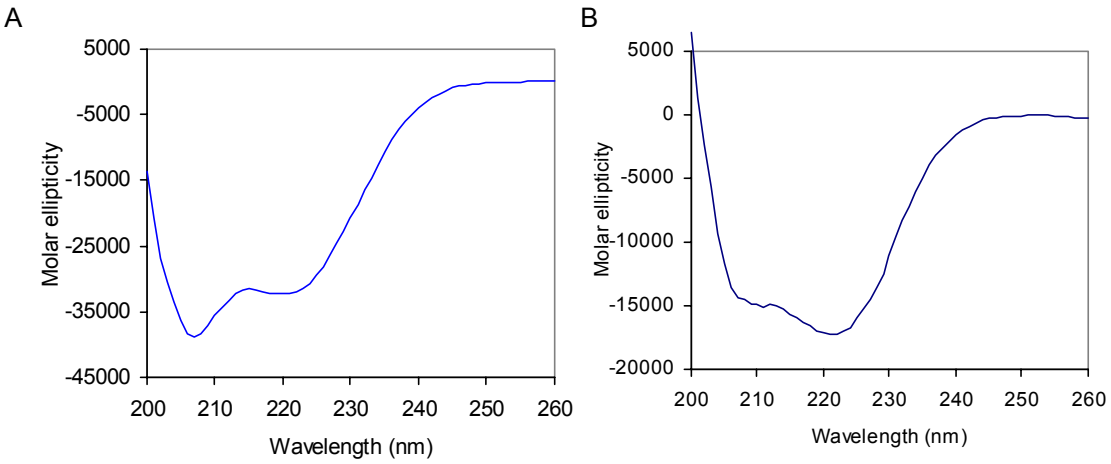

Figure 24. **CD spectral analysis Vam7p and Ykt6p**. The spectra were measured between 200-260 nm as described in Figure 21. A Vam7p showed typical α-helical property. B Ykt6p revealed different amount of α-helical and β-sheet structure.

Table 6 **CD spectral analysis of Vam7p and Ykt6p full length protein**

Calculations were carried out from the spectra obtained between 200-260 nm as described in Table 3

		Secondary Structure	
Protein	**Solvent**	**%of α-helix**	**% of β-sheet**
Vam7p (full length)	buffer	86	2
Ykt6 (full length)	buffer	53	10

5.4 Self-interaction of SNARE proteins

SNARE proteins mediate membrane fusion of vesicles to target membranes (Sollner et al., 1993a; Sollner et al., 1993b). The homotypic yeast vacuole fusion is dependent on the transition from the *cis*-complex, made by SNARE proteins, on the same membrane, to the *trans*-complex, where the SNARE proteins from opposing membranes interact (Figure 2 in introduction) (Jahn, 1999; Jahn, 2000; Jahn, 2004; Jahn et al., 2003; Jahn and Sudhof, 1999; Mayer, 2002; Mayer et al., 1996; Wickner, 2002). The stability of the *cis*-complex may be one parameter that regulates SNARE function. In light of the functional significance of the TMD (Rohde, 2002; Rohde et al., 2003) its role in homophilic interaction and SNARE complex formation was studied.

5.4.1 Homo-oligomerization of synaptobrevin II

Previous studies from our laboratory showed that synaptobrevin homodimerization is mediated by the TMD, as its cytoplasmic domain does not show any dimerization (Laage and Langosch, 1997). Self-interaction of recombinant synaptobrevin II was analyzed by:

1. “mild” SDS-PAGE, without urea, in which low SDS concentration were used to preserve protein-protein interaction and sample boiling was omitted (Figure 25, panel A),
2. “urea” SDS-PAGE, in presence of 6M urea (Figure 25, panel B), since it is known that urea decreases the unspecific aggregation of membrane proteins in SDS-PAGE (Soulie et al., 1996).

The results obtained, (Figure 25) showed that the dimer is far less stable in “mild” SDS-PAGE than in urea. In the absence of urea the dimer was barely visible and only at higher concentration of synaptobrevin II, whereas it was prominent in urea SDS-PAGE. As shown in the previous section, the secondary structure of the synaptobrevin II TMD is not affected by 6 M urea, as determined by CD spectra analysis. Therefore urea affects protein-protein interaction rather than secondary structure formation.

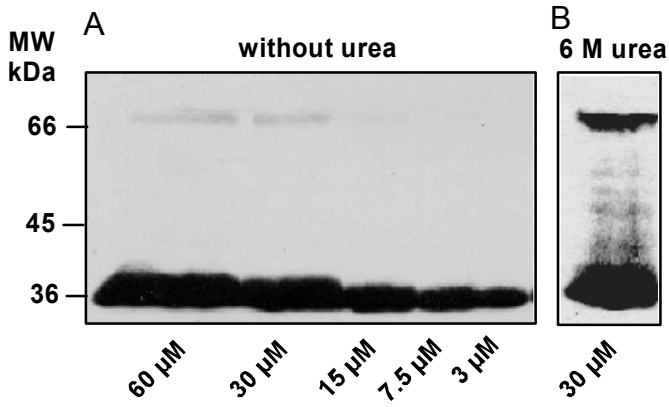

Figure 25. **Dimerization of solubilized recombinant synaptobrevin II**. Synaptobrevin II fusion protein homodimerization was analyzed by SDS-PAGE. In panel A, the protein was dissolved in sample buffer with 2% (w/v) SDS at the indicated concentrations and incubated at 37 °C as in Bowen et al. (Bowen et al., 2002) prior to electrophoresis in a gel without urea. In panel B, the protein was dissolved in sample buffer with 1% (w/v) SDS plus 6 M urea at a concentration of 30 µM and electrophoresed at 4 °C in a gel containing 6 M urea as described by Laage et al. (Laage and Langosch, 1997). Significant homodimer is visible only in the presence of urea.

5.5 Homo interaction of vacuolar SNARE proteins

To characterize homophilic interactions of vacuolar SNARE proteins, SDS-PAGE in mild condition and urea SDS-PAGE, were also tried. Unfortunately it was not possible to clearly detect homodimers in these cases (data not shown). Probably vacuolar SNARE proteins homophilic interactions are too unstable under denaturing conditions, even at very low SDS concentration, at which most of neuronal SNARE homophilic interactions are stable. Therefore methods were used, where native conditions are preserved. In particular homophilic interactions of vacuolar SNARE proteins (Vam3p, Nyv1p, Vti1p, Vam7p and Ykt6p) were studied by sucrose gradient at non-denaturing conditions.

5.5.1 Homo oligomerization of Vam3p and its TMD mutants

Vam3p is a Q-SNARE protein. For better understanding of the involvement of the TMD in self-interaction of Vam3p, the mutants Vam3pA4 and Vam3pA4bb were produced. Vam3pA4 is a mutant in which four important amino acids (residues 265, 269, 273 and 277) were mutated to alanine, whereas in Vam3pA4bb four amino acids (residues 267, 271, 275 and 279) at the opposite side of the helix were mutated to alanine (Figure 14, panel H & Figure 26, panel B). The gap of four residues was chosen because 3.6 amino acid residues make one helix turn. Another

Vam3p TMD mutant was produced, in which the cysteine residue at position 274 is mutated to alanine, (Figure 14, panel H) by site-directed mutagenesis. The other mutant Vam3pΔTMD, that represents the cytoplasmic domain (amino acid residues 1–263), was produced to analyze the self-interaction of Vam3p without TMD. In the Vam3pAla20 mutant, the TMD is replaced by a stretch of 20 alanines (amino acid residues 264–283). Sucrose gradient analysis of Vam3p and the series of its TMD mutants shows that Vam3p is mostly in dimer form (Figure 26 panel A), since the 36 kDa protein co-migrates with the 66 kDa BSA, used as marker in a parallel gradient. Dimerization is not an artifact of disulfide bridge formation between cysteine 274, since Vam3pC274A, where the cysteine at 274 position is replaced by alanine, is also dimer. Interestingly the mutant Vam3pΔTMD and vam3A4 are mostly monomer in sucrose gradient. Vam3pA4bb and Vam3pAla20 are in equilibrium between monomer and dimer forms in sucrose gradient. The results show that dimerization of Vam3p is mediated by TMD. It was surprising to find that mutating both putative helix-helix interfaces abolished dimerization. This will be discussed below in the light of the findings on secondary structure described in the previous section.

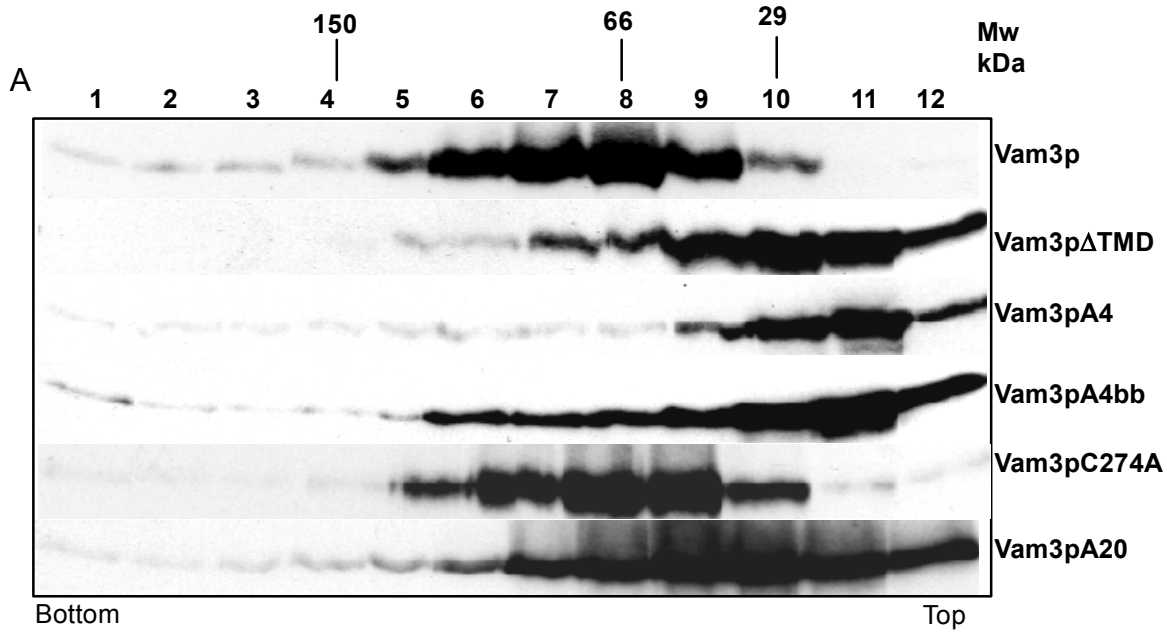

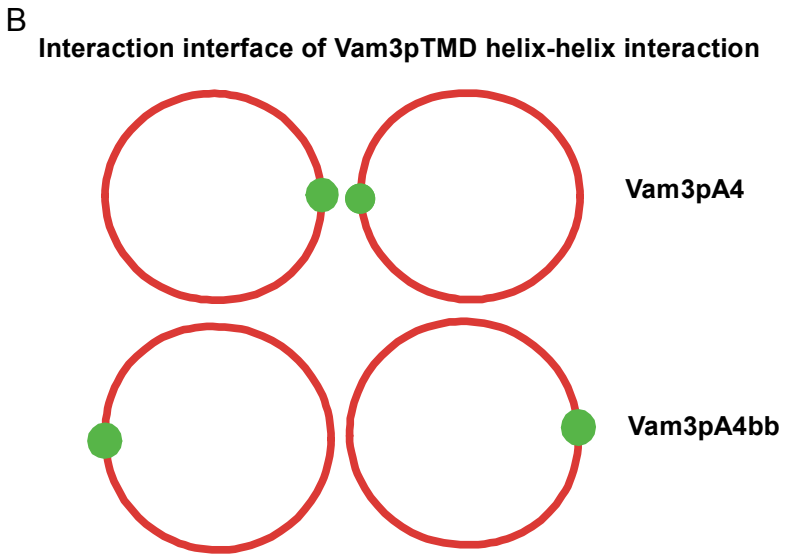

Figure 26. **Self-interaction of Vam3p and its TMD mutants**. A Vam3p analysed in 15-60% linear sucrose gradient. Sucrose gradient was prepared in 25 mM HEPES pH 7.6, 1 M NaCl, 10 mM β-mercaptoethanol and 1% (v/v) Thesit. Fractions were collected from the bottom to top. Molecular weight estimation was done by loading single protein markers on the sucrose gradient in same condition. B schematic representation of interaction interface of Vam3p TMD. As shown the sequence in Figure 14, the gap of two amino acid residue between Vam3pA4 and Vam3pA4bb leads the mutation in the back side of the helix in case of Vam3pA4bb.

5.5.2 Homooligomerization of Nyv1p and its TMD mutants

Nyv1p is an R-SNARE protein. The two mutants Nyv1pΔTMD (amino acid residues 1–226), lacking the full TMD and Nyv1pAla21, in which the TMD is replaced by oligo alanine (amino acid residues 229–250) were produced. These mutants were created to study the self-interaction of Nyv1p without TMD and with altered TMD sequence. Self-interaction of Nyv1p and its TMD mutants were studied by sucrose gradient. The results obtained (Figure 27) show that Nyv1p (34 kDa) and Nyv1pΔTMD are present as monomer and possibly accompanied by a small amount of dimer, whereas for Nyv1pAla21 the equilibrium seems to be shifted to the monomer form. From this result it seems that Nyv1p homooligomerization is not mediated by TMD.

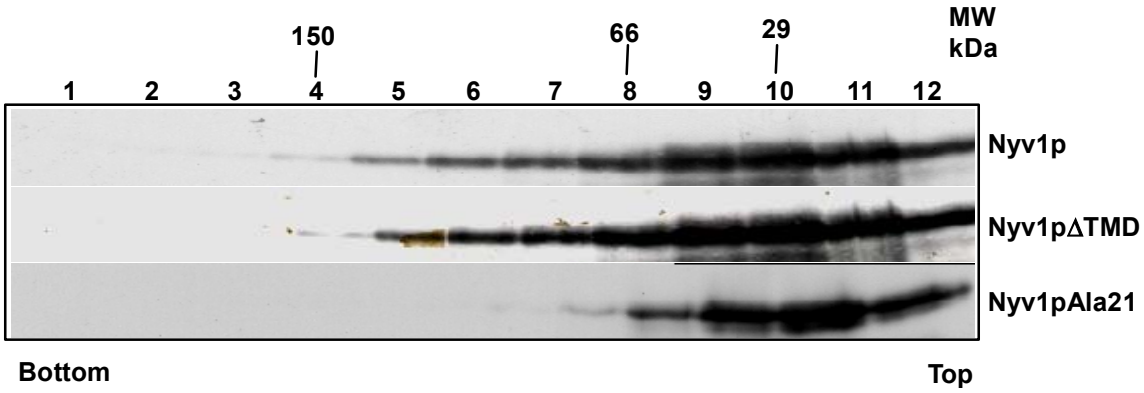

Figure 27. **Self-interaction of Nyv1p and its TMD mutants**. Nyv1p analyzed in 15-60% linear sucrose gradient. Sucrose gradient was prepared in 25 mM HEPES, pH 7.6, 1 M NaCl, 10 mM β-mercaptoethanol and 1% (v/v) Thesit. Fractions were collected from the bottom to top. Molecular weight estimation was done by loading single protein markers on the sucrose gradient in same condition.

5.5.3 Homo oligomerization of Vti1p and its TMD mutants

Vti1p is a Q-SNARE protein. The two mutants Vti1pΔTMD (amino acid residues 1–189), lacking the full TMD and Vti1pAla21, in which the TMD is replaced by oligo alanine (amino acid residues 190–212) were produced. These mutants were created to study the self-interaction of Vti1p without TMD and with altered TMD sequence. Self-interaction of Vti1p and its TMD mutants were studied by sucrose gradient separation. The results obtained (Figure 28) show that Vti1p (29 kDa) and Vti1pΔTMD are present as dimer but with an equilibrium with monomeric form,

whereas for Vti1pAla23 the equilibrium seems to be shifted to the monomeric form. This result is suggesting that Vti1p homo oligomerization is not mediated by TMD.

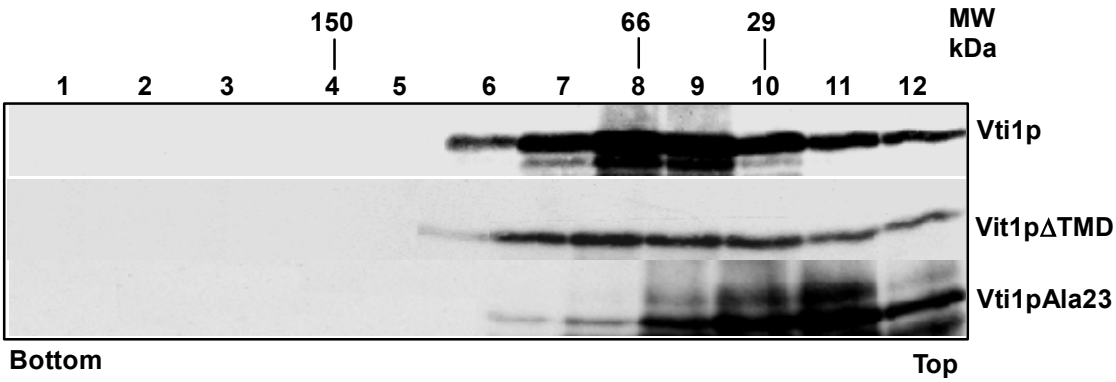

Figure 28. **Self-interaction of Vti1p and its TMD mutants**. Vti1p analyzed in 15-60% linear sucrose gradient. Sucrose gradient was prepared in 25 mM HEPES, pH 7.6, 1 M NaCl, 10 mM β-mercaptoethanol and 1% (v/v) Thesit. Fractions were collected from the bottom to top. Molecular weight estimation was done by loading single protein markers on the sucrose gradient in same condition.

5.5.4 Homo oligomerization of Vam7p

Vam7p is a Q-SNARE protein. Vam7p does not contain any TMD. It is attached to membrane by N-terminal PX-domain, which is bound to phosphatidylinositol 3-phosphate. In Figure 29 sucrose gradient separation of Vam7p (42 kDa) showed that it is mostly monomer.

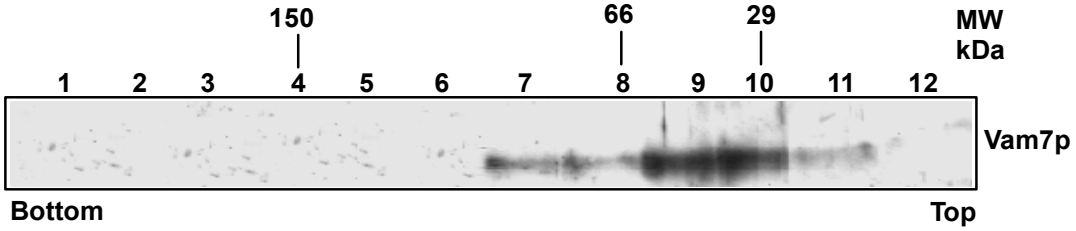

Figure 29. **Self-interaction of Vam7p**. Vam7p analyzed in 15-60% linear sucrose gradient. Sucrose gradient was prepared in 25 mM HEPES pH 7.6, 1 M NaCl, 10 mM β-mercaptoethanol and 1% (v/v) Thesit. Fractions were collected from the bottom to top. Molecular weight estimation was done by loading single protein markers on the sucrose gradient in same condition.

5.5.5 Homo oligomerization of Ykt6p

Ykt6p is an R-SNARE protein. Ykt6p was produced as GST-tagged or His_6-tagged fusion protein. His_6-tagged protein was produced for the CD experiment. Here, the self-interaction of these different Ykt6p fusion proteins was analyzed. Results obtained (Figure 30) show that in sucrose gradient separation GST-Ykt6p (48kDa) is mostly dimeric but in equilibrium with the monomeric form, while GST under same condition did not show any dimeric form. Sucrose gradient separation of His_6-tagged Ykt6p showed mostly monomeric with some protein being distributed in all twelve fractions. This suggests that the homodimerization of GST-Ykt6 is due to weak interaction of Ykt6 while some unspecific aggregation in the absence of the soluble GST-tag.

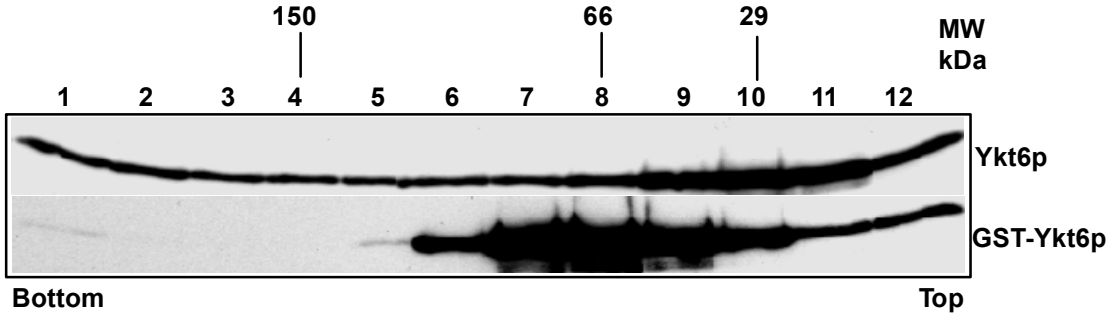

Figure 30. **Self-interaction of Ykt6p**. A GST-Ykt6p and His-ykt6 analyzed in 15-60% linear sucrose gradient. Sucrose gradient was prepared in 25 mM HEPES, pH 7.6, 1 M NaCl, 10 mM β-mercaptoethanol and 1% (v/v) Thesit. Fractions were collected from the bottom to top. Molecular weight estimation was done by loading single protein markers on the sucrose gradient in same condition.

5.5.6 Assessment of self-interaction of SNARE proteins

In summary the results obtained for self-interaction of SNARE proteins are presented in Table 7. In particular synaptobrevin II, a neuronal SNARE protein, is forming a dimer that is better preserved in urea SDS-PAGE than in SDS-PAGE in mild condition. The vacuolar Q-SNARE protein, Vam3p forms a dimer that is dependent on its TMD. Nyv1p and Vti1p dimers are not mediated by their TMD, but in case of Nyv1pAla21 and Vti1pAla23 mutants the equilibrium is shifted towards monomer

form. Vam7p is only monomer form, while in case of Ykt6p the protein is mostly in dimeric form.

Table 7 Summary of self-interaction of SNARE proteins

Protein	Monomer	Dimer	Aggregation
Synaptobrevin II	+++	++	
Vam3p	+	++++	+
Vam3pΔTMD	++++	+	+
Vam3pA4	++++	+	+
Vam3pA4bb	+++	++	+
Vam3pC274A	+	++++	+
Vam3pAla20	+++	++	+
Nyv1p	+++	++	
Nyv1pΔTMD	+++	++	
Nyv1pAla21	+++	+	
Vti1p	++	+++	
Vti1pΔTMD	++	++	
vti1Ala23	+++	+	
Vam7p	+++		
GST-Ykt6p	++	++++	
His_6-Ykt6p	+++	++	++

5.6 *In vitro* assembly of vacuolar SNARE complex

Crucial step in membrane fusion is the formation of the SNARE complex, in which conserved regions, called 'SNARE motif' from the individual SNAREs associate and form a core complex (Hanson et al., 1995; Hay and Scheller, 1997), which consist of a parallel coiled coil. The neuronal SNARE complex is a heterotrimer of vesicular (R) SNARE synaptobrevin II and two plasma membrane (Q) SNAREs syntaxin 1A and SNAP-25. Later the crystal structure of the neuronal SNARE complex and endosomal SNARE complex was clarified and it was shown that three Q-SNARE proteins form a complex with one R-SNARE (Antonin et al., 2002; Sutton et al., 1998).

Here, *in vitro* SNARE complex assembly of yeast vacuolar SNARE proteins was studied. Previous studies show that alterations in the TMD clearly affected the stability of the *cis*-SNARE complex during the priming step and *trans*-SNARE pairing (Rohde et al., 2003). In the previous chapter, the self-interaction studies also showed that Vam3p homodimer is mediated by TMD, suggesting an important role of the TMD in vacuolar SNARE protein interaction. Different combinations of SNARE proteins and their mutants are studied here *in vitro*, in order to clarify the importance of their TMD in the yeast vacuolar SNARE protein assembly.

5.6.1 *In vitro* SNARE complex assembly corresponding to *trans*-SNARE complex

In yeast vacuolar fusion four SNARE proteins are involved in the last step of membrane fusion (Dietrich et al., 2004; Dietrich and Ungermann, 2004; Rohde et al., 2003) – Vam3p, Nyv1p, Vam7p and Vti1p. Among these proteins, Nyv1p is an R-SNARE and the rest are Q-SNAREs. The proteins were mixed together and incubated overnight. The mixture was gently pipetted onto the top of 15-60% linear sucrose gradient and it was centrifuged at high speed. Twelve fractions were collected from the bottom to the top and fractions were precipitated with TCA and analyzed by SDS-PAGE followed by Western blot with specific antibodies. Results are presented in Figure 31. For comparison panel A shows again self-interaction of the individual proteins (of Figure 26, 27, 28, 29). Panel B shows the result upon mixing the four SNARE proteins. In comparison with single protein separation on

sucrose gradient, some of the proteins (e.g. Nyv1p and Vti1p) are shifted towards higher molecular weight fractions (fraction 7–9) (Figure 31, panel B), whereas others behave similarly as in homomeric assembly (Vam3 and Vamp7). This result suggests some heterophilic interaction between Nyv1p/Vti1p proteins. In order to exclusively detect those proteins bound to Vam3p, each fraction of sucrose gradient was co-immunoprecipitated with rabbit anti-Vam3p antibody (Figure 31, panel C). As shown in Figure 31, panel C after co-immunoprecipitation it is possible to detect a complex, co-migrating with the 150 kDa marker, that may represent the quaternary SNARE complex (calculated molecular weight 141 kDa) (fraction 3–5). Other binary and ternary complexes appear to be present at lower molecular weight.

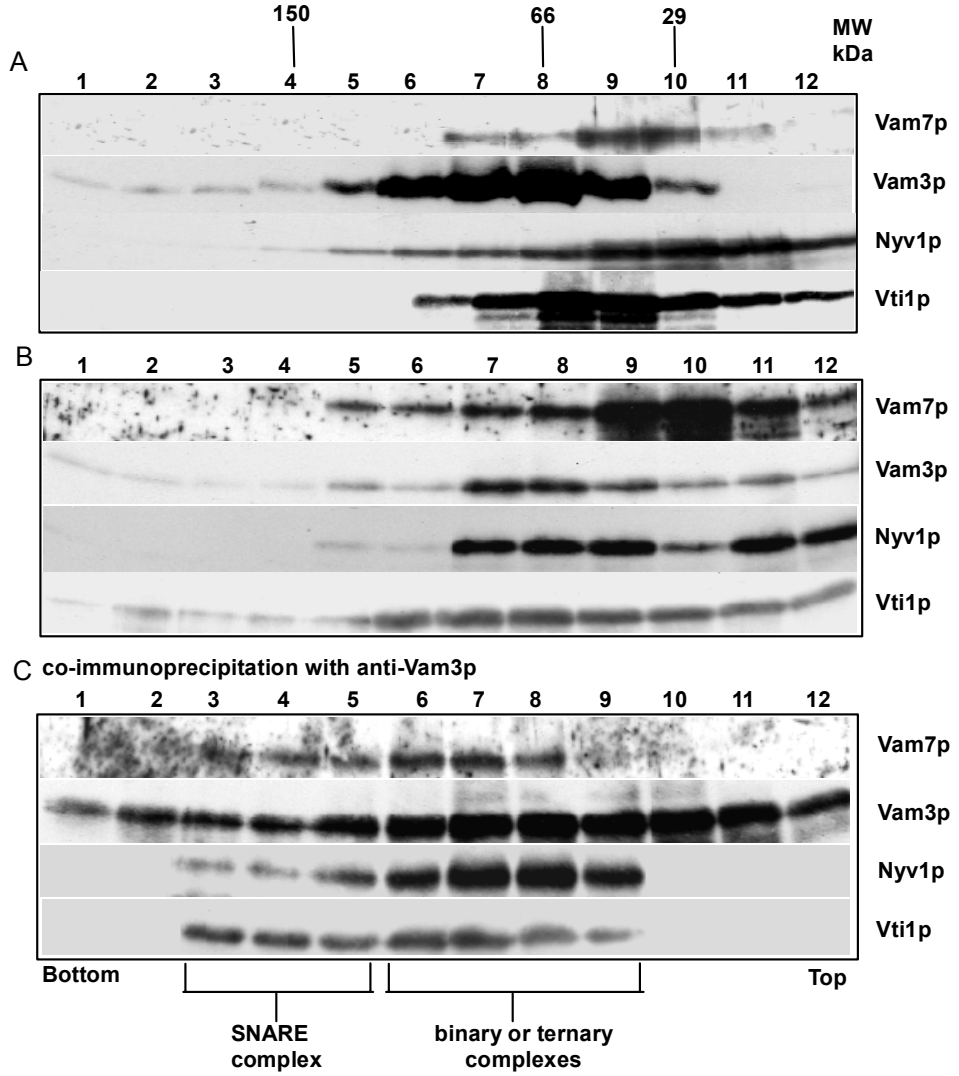

Figure 31. ***In vitro* vacuolar SNARE complex assembly**. SNARE complex assembly was analyzed by sucrose gradient. A 15-60% linear sucrose gradient was prepared with 25 mM HEPES pH 7.6, 1% (v/v) Thesit, 1 M NaCl, 10 mM β-mercaptoethanol. The fractions were collected from bottom to top and analyzed by SDS-PAGE and Western blot with specific antibodies. A, Individual protein (as reproduce from the Figure 26, 27, 28, 29) in sucrose gradient; B, SNARE protein mixture on sucrose gradient, C, fractions analyzed upon co-immunoprecipitation with rabbit anti-Vam3p.

5.6.2 Disassembly of SNARE complex

Sec17p and Sec18p (Graham and Emr, 1991; Haas and Wickner, 1996; Hicke et al., 1997; Mayer et al., 1996; Wickner, 2002) are α-SNAP and NSF homologs respectively. They are present in yeast to disrupt *cis*-SNARE protein complex, thus preparing the individual SNARE proteins for the formation of *trans*-SNARE complexes (see Figure 2, the "SNARE cycle" described in introduction). Here SNARE complex as identified by sucrose gradient and co-immunoprecipitation, was disassembled by Sec17p and Sec18p in presence of ATP (Horsnell et al., 2002; Sollner et al., 1993a). The SNARE protein overnight incubated mixture was incubated with recombinant Sec17p and Sec18p with $MgCl_2$ and ATP or ATPγS for 30 min at 4^{o}C. The mixture was subjected to sucrose gradient, and analyzed as described in the previous section. The results (Figure 32, panel A & B) show that when SNARE protein mixture was incubated with Sec17p and Sec18p in presence of ATP, all proteins are localized at the monomeric position (Figure 32, panel A fraction 9–12), but when the non-hydrolyzable ATPγS was used instead of ATP for control the SNARE protein assembly was not disrupted, as the proteins could be found in higher molecular weight fractions (Figure 32, panel B fraction 4-6), like the predicted SNARE complex shown in Figure 31, panel B. Therefore, the results obtained show that *in vitro* SNARE protein complex, as well as the homodimers, can be specifically disassembled by NSF and α-SNAP in presence of ATP and $MgCl_2$. Thus the complex corresponds to a biologically relevant form rather than to an unspecific aggregate.

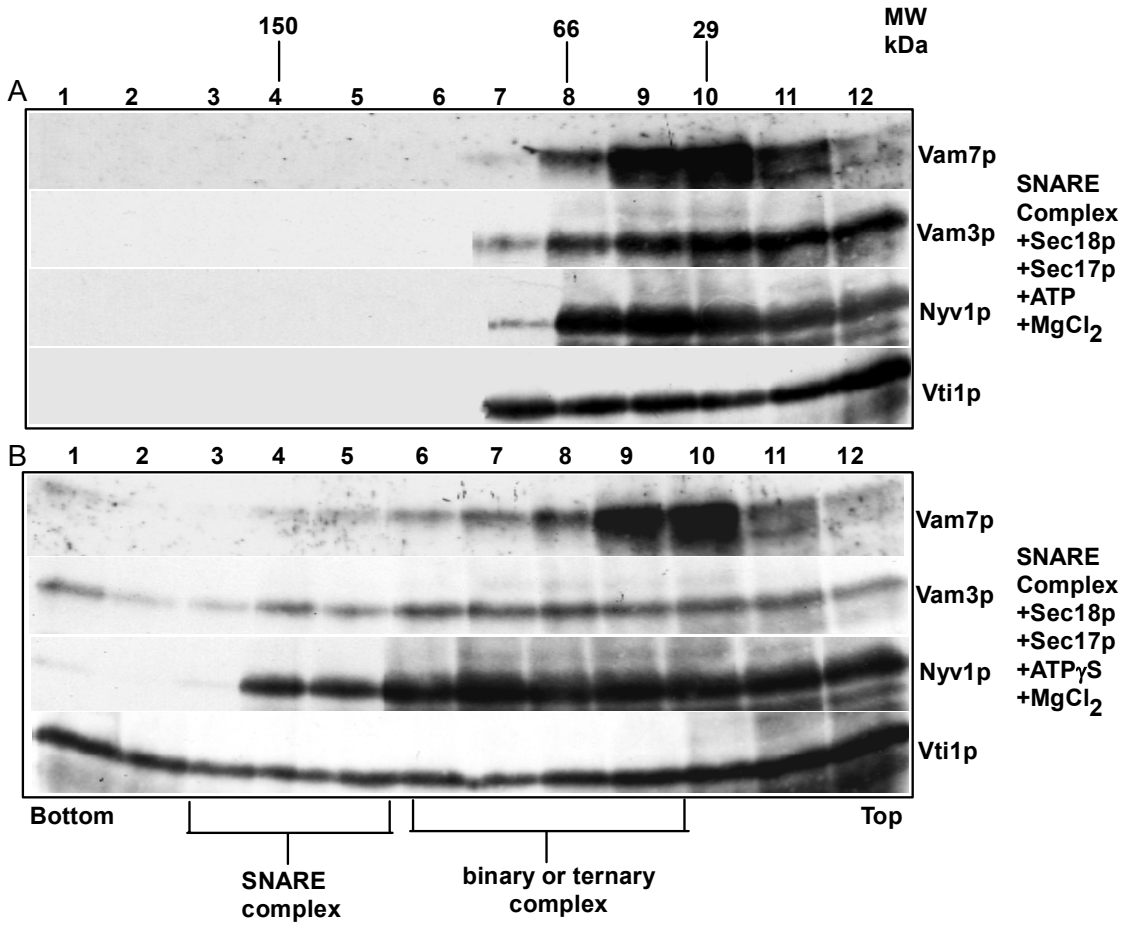

Figure 32. **SNARE protein complex disassembly.** SNARE complex assembly and disassembly were analyzed by sucrose gradient. A 15-60% linear sucrose gradient was prepared with 25 mM HEPES pH 7.6, 1% (v/v) Thesit, 1 M NaCl, 10 mM β-mercaptoethanol. The fractions were collected from bottom to top and analyzed by SDS-PAGE and Western blot with specific antibodies. A, SNARE protein mixture, incubated with Sec17p, Sec18p, ATP and $MgCl_2$, B, SNARE protein mixture, incubated with Sec17p, Sec18p, ATPγS and $MgCl_2$.

5.6.3 SNARE complex assembly with Vam3p TMD mutants

SNARE complex with Vam3p TMD mutants was also studied. It was shown in the previous section that Vam3p self-interaction is dependent on its TMD. The mutants, studied for Vam3p self-interaction, had previously been studied in *in vitro* vacuolar fusion assay ((Rohde et al., 2003) and J. Rohde and C. Ungermann, unpublished data). It has been shown that Vam3pA4 and Vam3pΔTMD fuse less efficiently than wild type, Vam3pA4bb fusion efficiency is similar to wild type (Rohde, 2002). The *in vitro* SNARE complex with Vam3p TMD mutants were analyzed by sucrose gradient separation followed by co-immunoprecipitation with rabbit Vam3p antibody and visualized by SDS-PAGE and Western blot with specific antibodies. The results

obtained are shown in Figure 33. Figure 33, panel A shows the *in vitro* SNARE complex with Vam3pΔTMD. Figure 33, panel B shows the SNARE complex formation with Vam3pA4. SNARE complex formation with Vam3pA4bb is shown in Figure 33, panel C, while the SNARE complex formation with Vam3pAla20 is presented in Figure 33, panel D. In comparison with wild type complex (Figure 31, panel C) Vam3pΔTMD and Vam3pAla20 are forming a SNARE complex (fractions 3-5) with some higher oligomers (fractions 1-2) (Figure 33, panel A&D). The other mutants Vam3pA4 and Vam3pA4bb are not forming any higher oligomers (Figure 33, panel B&D) but have a similar pattern like wild type complex of proteins (fraction 3-5).

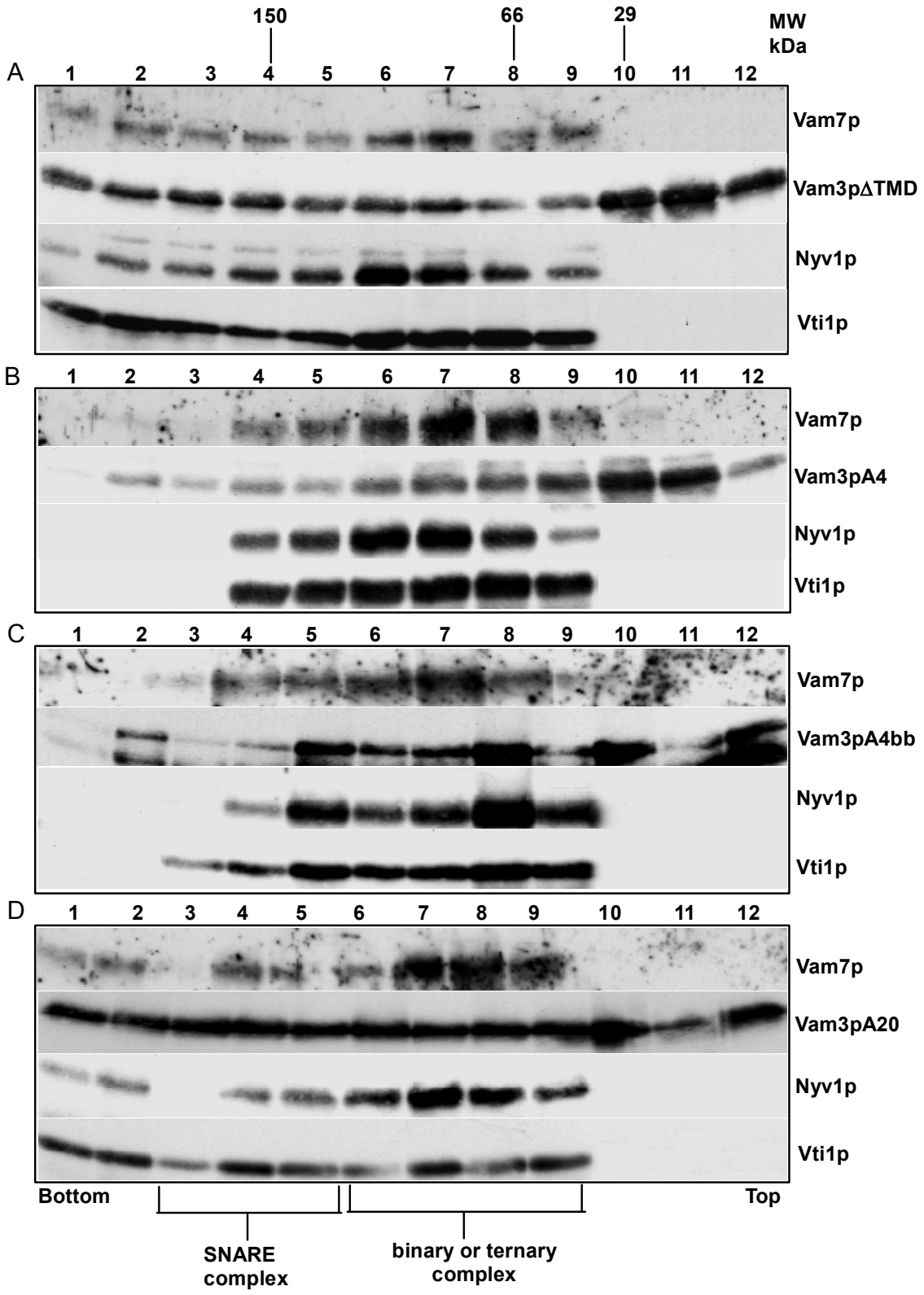

Figure 33. ***In vitro* vacuolar SNARE complex assembly with Vam3pTMD mutants**. SNARE complex assembly with Vam3p TMD mutants was analyzed by sucrose gradient. A 15-60% linear sucrose gradient was prepared with 25 mM HEPES pH 7.6, 1% (v/v) Thesit, 1 M NaCl, 10 mM β-mercaptoethanol. The fractions were collected from bottom to top and co-immunoprecipitated with rabbit anti-Vam3p. The eluted proteins were then analyzed by SDS-PAGE and Western blot with specific antibodies. A, SNARE complex with Vam3pΔTMD; B, SNARE complex with Vam3pA4; C, SNARE complex with Vam3pA4bb; D, SNARE complex with Vam3pAla20.

5.6.4 SNARE complex assembly with cytoplasmic part of the SNARE proteins

The yeast vacuolar SNARE proteins, Vam3p, Vti1p and Nyv1p, were also expressed without TMD (as ΔTMD), but containing the full SNARE cytosolic domain. Since Vam7p is without TMD, the wild type protein was used. The *in vitro* assembly of these mutant SNARE proteins was studied with sucrose gradient separation, followed by co-immunoprecipitation with rabbit anti Vam3p and visualized by SDS-PAGE and Western blot with specific antibodies as described earlier. The results obtained are shown in Figure 34. Individual proteins on sucrose gradient are shown in Figure 34, panel A and in comparison the SNARE complex, as co-immunoprecipitated with Vam3p, is shown in Figure 34, panel B. The individual ΔTMD mutants are mostly monomeric or in equilibrium of monomers and dimers (Figure 34, panel A). When these proteins were mixed for complex formation, most of the proteins were shifted to higher molecular weight fractions (Figure 34, panel B fractions 1-5), thus suggesting SNARE complex formation (fraction 3-5) of the mutants containing only the cytoplasmic domains whereas supernatant after co-immunoprecipitation indicates that the major parts of SNARE proteins (Vam7p, Nyv1pΔTMD and Vti1pΔTMD) are not bound with Vam3pΔTMD (Figure 34, panel C). In conclusion, deletion of TMD does not prevent formation of the SNARE complex.

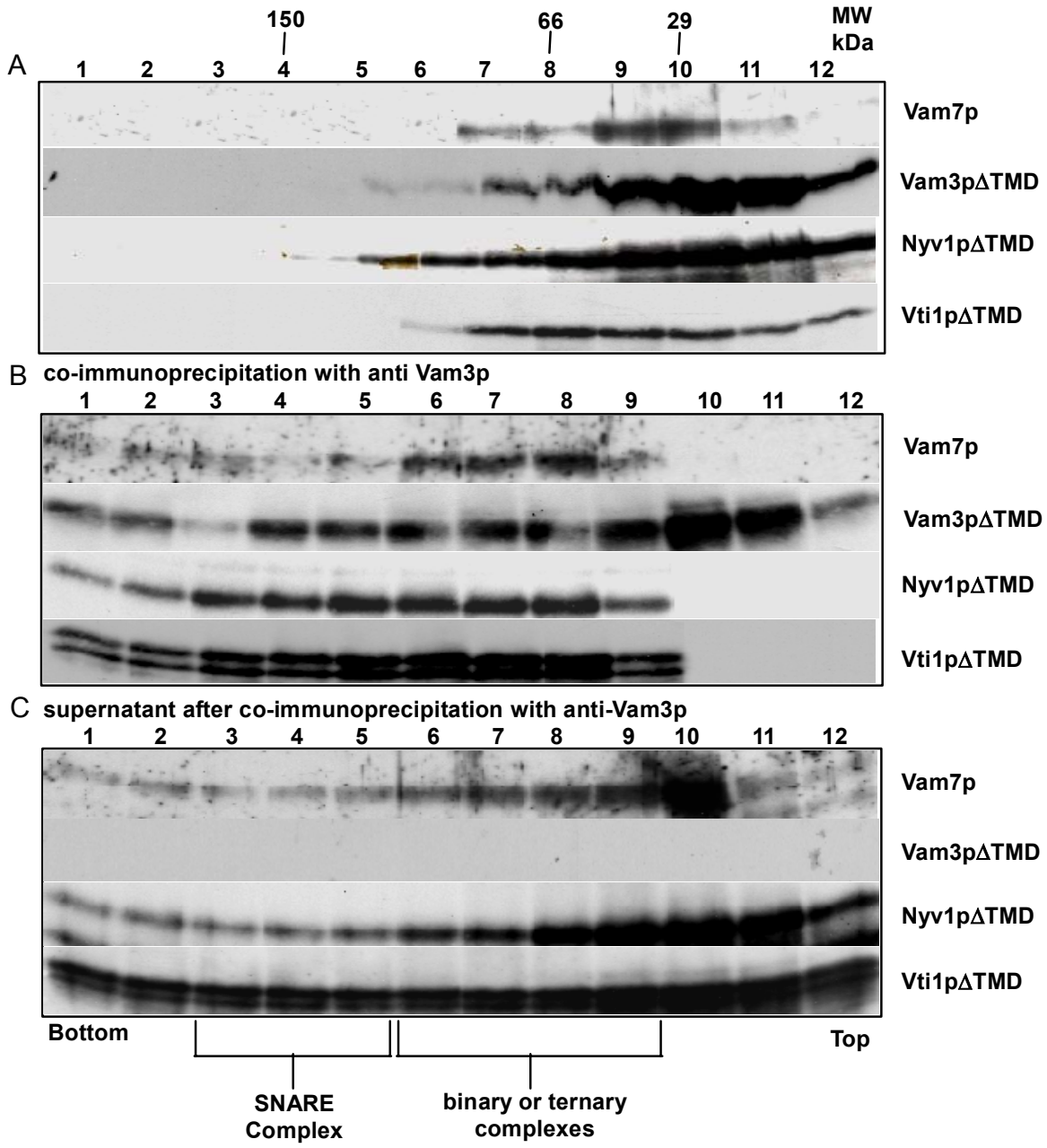

Figure 34. ***In vitro* vacuolar SNARE complex assembly with cytoplasmic domains**. SNARE complex assembly with ΔTMD mutants was analyzed by sucrose gradient. A 15-60% linear sucrose gradient was prepared with 25 mM HEPES pH 7.6, 1% (v/v) Thesit, 1 M NaCl, 10 mM β-mercaptoethanol. The fractions were collected from bottom to top and analyzed by SDS-PAGE and Western blot with specific antibodies. A, individual ΔTMD protein in sucrose gradient (reproduced from Figure 26, 27, 28, 29); B, co-immunoprecipitation of sucrose gradient fractions with rabbit anti-Vam3p; C, supernatant after co-immunoprecipitation with rabbit anti-Vam3p.

5.6.5 SNARE complex assembly with alanine TMD mutants of the SNARE proteins

The mutants of Vam3p, Vti1p and Nyv1p, in which the TMD was replaced by oligo alanine, were used for *in vitro* SNARE complex assembly. Since Vam7p does not contain TMD, the wild type Vam7p was used for complex formation. Therefore, all the proteins contain an intact SNARE domain and N-terminal domain, while the C-terminal TMD is changed to alanine stretch. All the mutant proteins were mixed and incubated overnight at 4^{o}C. The protein mixture was subjected to sucrose gradient centrifugation. Twelve fractions were collected from the bottom to top, individually co-immunoprecipitated with rabbit anti-Vam3p and analyzed on SDS-PAGE and Western blot with specific antibodies (Figure 35). Figure 35, panel A shows that the individual alanine mutants after sucrose gradient separation are mainly in monomeric form. Figure 35, panel B shows the SNARE complex with alanine TMD mutants. In comparison with the individual mutant proteins, the protein mixture shows a shift to higher molecular weight fractions (fraction 1–5) for all the mutant proteins except for Vam7p, which is detected only in the fraction 6-9, indicating that probably Vam7p is forming a binary complex with Vam3p as major part of Vam7p is detected in the supernatant after co-immunoprecipitation with anti-Vam3p (Figure 35, panel C). In the presence of TMD alanine mutant proteins a full SNARE complex is not detected, probably less specific interactions are occurring between Nyv1p, Vam3p and Vti1p mutants.

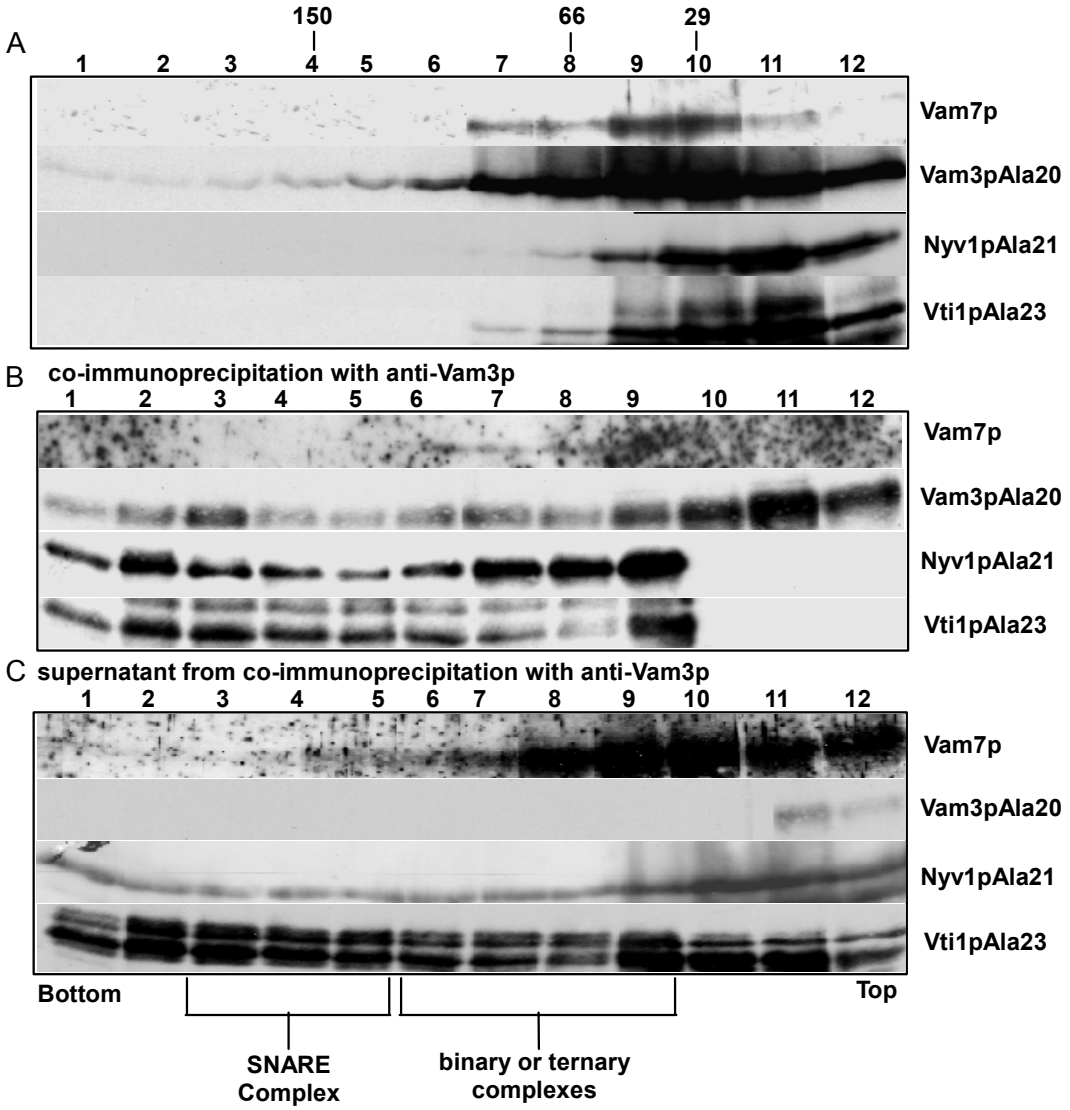

Figure 35. ***In vitro* vacuolar SNARE complex assembly with alanine mutants**. SNARE complex with alanine TMD mutants was analyzed by sucrose gradient. A 15-60% linear sucrose gradient was prepared with 25 mM HEPES pH 7.6, 1% (v/v) Thesit, 1 M NaCl, 10 mM β-mercaptoethanol. The fractions were collected from bottom to top and analyzed by SDS-PAGE and Western blot with specific antibodies. A, individual alanine TMD proteins in sucrose gradient (reproduced from Figure 26, 27, 28, 29); B, co-immunoprecipitation of sucrose gradient fractions with rabbit anti-Vam3p; C, supernatant after co-immunoprecipitation with anti-Vam3p.

5.6.6 SNARE complex assembly corresponding to *cis*-SNARE complex

In yeast vacuole a pentameric *cis*-SNARE complex formed by Vam3p, Nyv1p, Vti1p, Vam7p and Ykt6p has been described (Ungermann et al., 1999a). For this pentameric complex assembly Ykt6p was used as GST fusion protein. The proteins were mixed together and incubated overnight at 4^{o}C and then subjected to sucrose gradient separation. Twelve fractions were collected from the bottom to top. The fractions were analyzed by SDS-PAGE and Western blot with specific antibodies

(Figure 36). In Figure 36, panel A, the separation of the individual proteins shows that Ykt6p, Vam3p, Vti1p and Nyv1p are detected as monomer and dimer form, while Vam7p is mainly monomeric. Figure 36, panel B shows the separation of the SNARE complex assembly with all the five SNARE proteins on sucrose gradient. In comparison with the single proteins, the four proteins Vam3p, Nyv1p, Vti1p and Vam7p are detected in higher molecular weight fractions (fraction 4–6), but not Ykt6p, thus indicating that Ykt6p is not a part of full SNARE complex. Probably the more stabilized homodimeric form of GST-Ykt6p (as found in Figure 30) does not allow it to form complex. A more sensitive detection by co-immunoprecipitation was not possible because GST-Ykt6p is recognized by all antibodies against SNARE proteins.

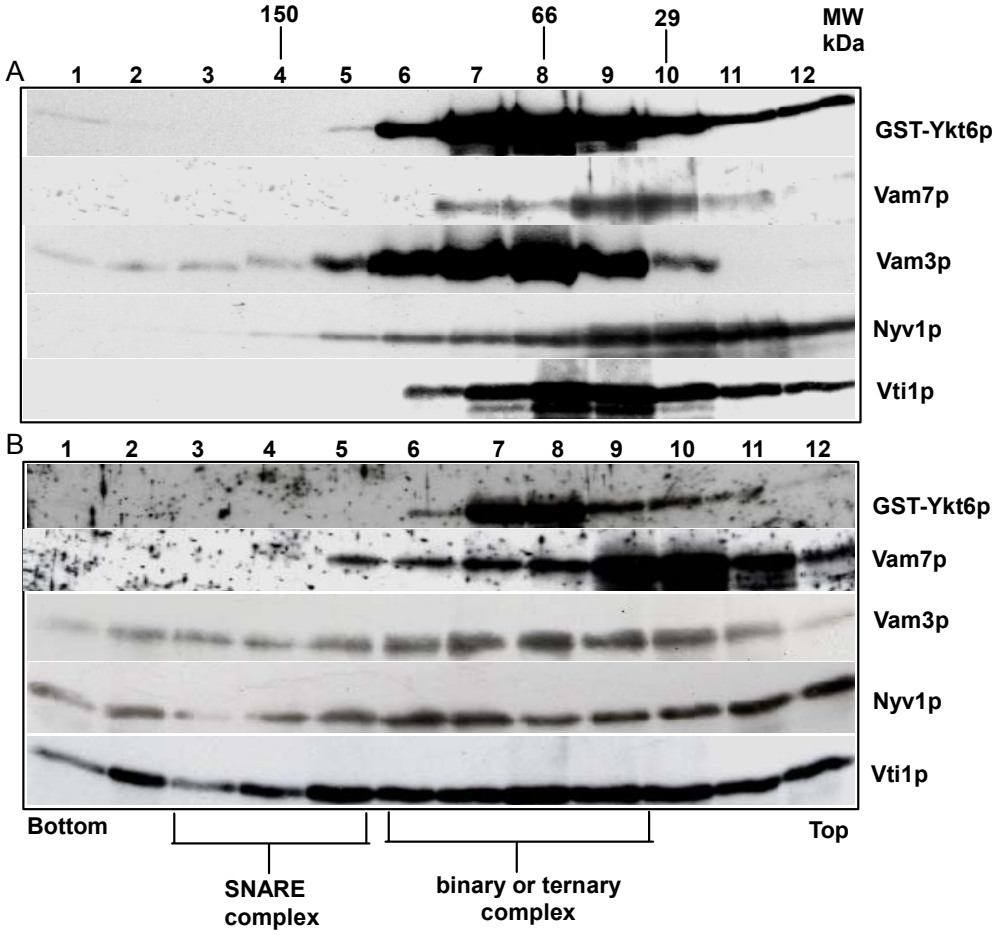

Figure 36. ***In vitro* vacuolar SNARE complex assembly corresponding to *cis*-SNARE complex**. SNARE complex assembly was analyzed by sucrose gradient. A 15-60% linear sucrose gradient was prepared with 25 mM HEPES pH 7.6, 1% (v/v) Thesit, 1 M NaCl, 10 mM β-mercaptoethanol. The fractions were collected from bottom to top and analyzed by SDS-PAGE and Western blot with specific antiobodies. A, individual proteins in sucrose gradient (reproduced from Figure 25, 26, 27, 28, 29, 30); B, SNARE protein mixture on sucrose gradient.

6 Discussion

The aim of this study was to investigate the role of TMD in SNARE protein interactions *in vitro*. In the first part, self-interaction of neuronal SNARE protein synaptobrevin II is discussed and in the second part the interaction of yeast vacuolar SNARE proteins is commented.

6.1 Self-interaction of synaptobrevin II

Synaptobrevin II is a v-SNARE or R-SNARE protein, localized in synaptic vesicles. Previous studies from our laboratory showed that synaptobrevin II has two interaction domains, cytosolic domain and C-terminal transmembrane domain (TMD). The TMD is important for synaptobrevin homodimerization (Laage and Langosch, 1997), as well as for heterophilic interaction with syntaxin 1A, whereas the cytosolic domain is important only for heterophilic interaction (Laage et al., 2000; Margittai et al., 1999). Here, homodimerization of synaptobrevin II was carefully re-examined by two different methods: “mild” SDS-PAGE and “urea” SDS-PAGE. The aim was to pinpoint the effect of urea, previously used in interaction analysis (Laage and Langosch, 1997; Laage et al., 2000). “Mild” SDS-PAGE was done according to the method described by Bowen et al. (Bowen et al., 2002). Results obtained here (Figure 25) show that by mild SDS-PAGE only small amount of synaptobrevin II homodimer can be detected. On the contrary, significant amount of dimer is detected by urea SDS-PAGE (Figure 25) (Roy et al., 2004). In our experimental conditions urea can thus preserve the homodimerized form of synaptobrevin II. Generally urea is used to unfold proteins, though the mechanism is still unknown. According to one hypothesis, urea disorder the water structure around the hydrophobic domains of unfolded proteins, thus weakening the strength of the hydrophobic effect in protein folding (Dill and Shortle, 1991). Here, the secondary structure analysis of synaptobrevin II TMD peptide revealed similar helical content in detergent solution with and without 6 M urea (Table 2). This demonstrates that urea does not denature this helix and suggests specificity of this protein-protein interaction since urea is also known to suppress unspecific aggregation of membrane proteins in SDS-PAGE (Soulie et al., 1996). Possibly urea is required to fully denature the nuclease fusion domain (Flanagan et al., 1992; From and Bowler, 1998) in this construct, since low-level of dimerization can also be seen in the absence of urea when the nuclease

fusion domain is missing (Bowen et al., 2002; Margittai et al., 1999) or proteolytically cleaved (Laage and Langosch, 2001). In addition to that, urea is known to affect the behavior of detergents by increasing the water solubility of its acyl moieties (Walter et al., 2000) and might thus induce formation of larger and less tightly packed micelles.

Homodimerization of native synaptobrevin II was also observed when it is cross-linked with DSS and iodine in isolated synaptic vesicles (Roy et al., 2004). DSS, which primarily reacts with lysine side chains localized within the soluble part of the proteins, showed that synaptobrevin II forms heterodimers with synaptophysin along with homodimer but no cross-linked products were detected with syntaxin 1A or SNAP-25 (Calakos and Scheller, 1994; Edelmann et al., 1995; Washbourne et al., 1995). On the contrary, iodine leads to intermolecular disulfide bridge formation of the whole protein, that is, to cysteine 103 within the TMD (Figure 20, sequence of synaptobrevin II TMD sequence). Since disulfide formation requires spatial proximity of cysteines, the detection of iodine cross-linked synaptobrevin II homodimers suggested that homodimerization in synaptic vesicles involves TMD–TMD interface (Laage and Langosch, 1997; Laage et al., 2000). This agrees well with the model computed by Fleming and Engelman (Fleming and Engelman, 2001) where cysteine 103 represents the site of closest contact within the TMD–TMD interface. Accordingly, the cross-linkable synaptobrevin molecules must contain an unmodified cysteine residue. Nevertheless, the intriguing possibility remains that part of native synaptobrevin is palmitoylated at cysteine 103, as found by Veit et al., although it could not be acylated in synaptic vesicles from embryonic brain (Veit et al., 2000) and therefore it could not form homodimer via TMD–TMD interaction when it is acylated. One may therefore speculate that synaptobrevin II homodimerization *in vivo* is regulated by this covalent modification that is known to be reversible and frequently regulated in a highly specific way (Veit et al., 2000; Veit et al., 2001).

Synaptobrevin II TMD–TMD self-assembly was further shown by ToxR assay (Roy et al., 2004). The degrees of interaction were comparable to that of membrane-spanning leucine zipper (Gurezka et al., 1999) and lower than the glycophorin A TMD (Brosig and Langosch, 1998; Langosch et al., 1996). Glycophorin A adopts a negative packing angle as indicated by mutagenesis (Laage and Langosch, 1997;

Laage et al., 2000; Langosch et al., 1996; Lemmon et al., 1992; Mingarro et al., 1996), model building (Adams et al., 1996; Fleming and Engelman, 2001) and NMR spectroscopy (MacKenzie et al., 1997; Smith et al., 2001) and its TMD interface harbors a critical GxxxG motif. This motif is thought to drive TMD–TMD packing by formation of a flat helix surface, by limiting entropy loss that is normally associated with the freezing of side chain conformations upon protein-protein interaction (Russ and Engelman, 2000), or by facilitating hydrogen bond formation between C_α-hydrogens and the backbone of the partner helix (Senes et al., 2001) or by a combination of these. It is not surprising, therefore, that the synaptobrevin II TMD self-interacts with a lower affinity than that of glycophorin A (Roy et al., 2004).

Thus, synaptobrevin appears to exist in different forms – that is, as a monomer, as a homodimer, or bound to synaptophysin or to other SNAREs – at the various stages of the synaptic vesicle cycle. Synaptobrevin II TMD–TMD self-assembly may have to be of sufficiently low affinity to allow for rapid interconversion of these complexes during neurotransmitter release (Roy et al., 2004).

6.2 Self-interaction of vacuolar SNARE proteins

Five SNARE proteins were found in yeast vacuole (Darsow et al., 1997; Nichols et al., 1997; Ungermann et al., 1998a; Ungermann et al., 1998b; Ungermann et al., 1999a) – Vam3p, Nyv1p, Vam7p, Vti1p and Ykt6p, where Vam3p, Vam7p and Vti1p are Q-SNAREs and Nyv1p and Ykt6p are R-SNAREs (Darsow et al., 1997; Dilcher et al., 2001; Fischer von Mollard and Stevens, 1999; Fischer von Mollard et al., 1997; Kweon et al., 2003; Nichols et al., 1997; Sato et al., 1998; Wickner and Haas, 2000). Among them Vam3p, Nyv1p and Vti1p contain a C-terminal TMD, while Vam7p and Ykt6p do not contain a TMD. Ykt6p is attached to the membrane via prenyl-anchor at the C-terminal (McNew et al., 1997) and Vam7p via an N-terminus PX-domain, which interacts with phosphatidylinositol 3-phosphate (Boeddinghaus et al., 2002). Rohde et al. observed that replacement of TMD from Vam3p by an isoprenoid anchor causes poor vacuole fusion. This functional defect was associated with stabilization of the *cis*-complex, since an extra amount of Sec18p was required to disrupt it and to release the individual SNARE proteins. Surprisingly, a higher amount of *trans*-complex was detected in cells expressing this Vam3p mutant compared to the wild type. Further, when the cytosolic SNARE motif is mutated in

Vam3p, the mutant did not show vacuolar fusion due to lack of trans-SNARE pairing. In contrast, isoprenoid mutant of Vam3p showed trans-complex formation but was deficient in fusion. These results indicate that Vam3p TMD is crucial at a stage of membrane fusion after *trans*-SNARE pairing (Rohde et al., 2003). Moreover mutations in the TMD of Vam3p are affecting vacuole fusion to a greater degree when they affect one helix interface (i.e. Vam3pA4), compared to mutations at the opposite side (i.e.Vam3pA4bb) (Rohde, 2002).

Here, we characterized homophilic interactions of all recombinantly expressed yeast vacuolar SNARE proteins by sucrose gradient to assess the role of the TMD. Self-interaction studies of Vam3p and its mutants show (Figure 26) that Vam3p wild type is mainly in dimer form, whereas the deletion of TMD (Vam3pΔTMD) or its mutation (Vam3pA4 and Vam3pA4bb) causes a shift towards the monomeric form. The homodimerization of Vam3p is not mediated by the cysteine at 274, as the Vam3pC274A mutant showed a dimeric form in sucrose gradient similar to wild type Vam3p. The deletion of TMD of Vam3p or mutation in TMD did not change the secondary structure of the Vam3p full length protein (Table 3). For a detailed characterization, also the corresponding TMD peptides were analysed via CD spectroscopy. The wild type Vam3pTMD peptide is highly α-helical in TFE (~80%) as well as in detergent solution (59%). Also the Vam3pA4 TMD peptide shows highly α-helical secondary structure in TFE (~80%) as well as in detergent solution (68%) (Table 3). Strikingly the full length Vam3pA4 protein in sucrose gradient is in monomeric form (Figure 26), suggesting that sequence specific interaction of TMD is required for dimers. The TMD peptide of Vam3pA4bb is less α-helical (39%) than that of wild type or Vam3pA4 and its β-sheet content is increased to 14% (Table 3). This structural perturbation may be due to the mutation of two leucines into alanines (Figure 14), as leucine is known to stabilize α-helical structure (Hofmann et al., 2004; Minor and Kim, 1994; Street and Mayo, 1999). The mutant protein Vam3pA4bb is distributed between monomeric and dimeric forms in sucrose gradient probably because the helical nature of TMD is compromised severely. The TMD of Vam3p was also substituted by 20 alanines and this mutant protein in sucrose gradient shows a monomeric and dimeric distribution (Figure 26). This dimer may be due to the weak interaction of the 20 alanine repeat although it was found previously that 16 alanine gives very weak interaction (Gurezka et al., 1999). In summary, results

showed that Vam3p is mainly in dimeric form by sucrose gradient analysis and mutations or deletion of the TMD can disrupt its self-interaction, thus supporting that Vam3p dimer formation is mediated by the TMD. Vam3p, a syntaxin analog in yeast vacuole, has therefore two interaction domains: SNARE domain and C-terminal TMD, like syntaxin 1A and synaptobrevin II.

Similarly, the self-interactions of other SNARE proteins were studied by sucrose gradient. Results obtained show that Nyv1p and Nyv1pΔTMD are mainly monomeric and possibly in equilibrium with small amounts of dimeric forms, while in case of Nyv1pAla21 the protein exists only in monomeric form (Figure 27). In sucrose gradient separation Vti1p and Vti1pΔTMD are mainly in dimeric form, while Vti1pAla23 is mainly in monomeric form (Figure 28). Therefore in case of Vti1p and Nyv1p the dimerization seems not to be mediated by the TMD of these proteins but probably by the SNARE domain. A recent study with Vti1p revealed that homo-oligomerization of the cytoplasmic domain produced hexamers or higher molecular weight oligomer depending on the glycerol (0–15 %) and salt (0–200 mM NaCl) concentration of the buffer (pH 5.6–8). It seems that oligomerization of Vti1p cytoplasmic domain may be favored under dehydrating conditions and by the electrostatic effect (Tishgarten et al., 1999). Here, in the presented experimental condition (25 mM HEPES, pH 7.6, 1 M NaCl, 10% glycerol) higher molecular weight oligomers of full length Vti1p were also observed with different detergents (Triton X-100 and CHAPS as shown in Table 1) in sucrose gradient. It was mentioned earlier that full length Vti1p could not be stabilized in solution less than 1 M NaCl, thus the other mutants of Vti1p were solubilized in 1 M NaCl. Moreover Tishgarten et al. found 76% α-helical content of Vti1pΔTMD at higher concentration of protein (Tishgarten et al., 1999) and a little less than the result obtained here (84% α-helical, Table 5). It could be, therefore, possible that the higher oligomers obtained by Tishgarten et al. are due to unspecific aggregation. However, the decreased amounts of dimeric form of Nyv1pAla21 and Vti1pAla23 remain unclear. Structural analysis showed the wild type as well as the alanine mutants have similar secondary structures (Table 4 & 5). Probably the dimerization of Nyv1p and Vti1p is mediated by SNARE domain, which is somehow perturbed in these alanine repeat mutants.

Self-interactions of Vam7p and Ykt6p were also examined by sucrose gradient. In particular Vam7p is monomeric (Figure 29), while ykt6 GST fusion protein is mainly in dimeric form even with a certain amount of monomeric form (Figure 30). As control, the GST protein itself did not show any dimeric form in this condition. Probably GST-Ykt6p fusion protein dimerizes due to weak self-affinity of Ykt6p supported by weak GST dimerization. However Ykt6p without any soluble fusion protein (His_6-Ykt6p) formed monomer plus unspecific aggregates (Figure 30). Structural analysis of Ykt6p showed less α-helical and more β-sheet content compared to other SNARE partners (Table 6). Crystal structure of the N-terminus of Ykt6p revealed five β-sheet strands, which are sandwiched by one α-helix on one side and two α-helices on the other side (Dietrich et al., 2003; Tochio et al., 2001). In summary, Vam3p dimerization is mediated by TMD and Vti1p dimer seems not to be dependent on TMD whereas Nyv1p is mainly monomer with a small amount of dimer and that is not affected upon deletion of TMD. The other SNARE protein Vam7p shows monomer and GST-Ykt6p is dimer in sucrose gradient.

6.3 SNARE complex assembly

In yeast vacuole fusion the *trans*-SNARE complex forms during the docking step, which is the second step before membrane fusion. Insights into *trans*-SNARE complex formation can help in understanding how SNARE protein interactions lead to membrane fusion. In vacuolar membrane fusion only four proteins are participating in the *trans*-SNARE complex – Vam3p, Nyv1p, Vam7p and Vti1p (Dietrich et al., 2004; Rohde, 2002; Rohde et al., 2003) following the general stoichiometry rule for SNARE complex formation: three Q-SNARE proteins and one R-SNARE protein. Here, all four vacuolar SNARE proteins were mixed to detect, after sucrose gradient separation, formation of a high molecular weight complex indicative of the formation of the tetrameric SNARE complex (Figure 31). To separate Vam3p associated proteins from free SNAREs, each fraction of sucrose gradient was first co-immunoprecipitated with anti-Vam3p antibody and reprobed with all the other specific antibodies in a Western blot. Results obtained (Figure 31) show that part of all four proteins co-migrated at a molecular weight of 150 kDa after co-immunoprecipitation, showing the partial formation of the full SNARE complex (fraction 3-5). Other intermediate complexes like binary or ternary complexes with Vam3p, [e.g. interaction of Vam3p and Vam7p or Vam3p with other SNARE proteins]

are also detected. As shown in Figure 32, in the presence of Sec18p, Sec17p and ATP the SNARE complex is completely disassembled (Figure 32), indicating that the complexes are not representing unspecific aggregation of the SNARE proteins.

Previous results obtained with *in vitro* fusion assay showed that Vam3p TMD is important for vacuolar membrane fusion (Rohde, 2002; Rohde et al., 2003), since TMD deletion leads to a significant decrease in fusion efficiency. *In vitro* analysis of the different SNARE complexes containing mutants with deleted or mutated TMDs is a good strategy for understanding the involvement of TMD in SNARE protein-protein interactions. In this study, *in vitro* SNARE complex assembly with Vam3p mutants plus the other wild type SNARE proteins shows that both complexes containing Vam3pΔTMD and Vam3pAla20 are forming higher molecular weight multimers in addition to the complexes seen in wild type (Figure 33), suggesting partial loss in specificity of protein-protein interactions. The formation of these oligomers may account for the described accumulation of the mutant *trans*-SNARE complex upon docking *in vitro* of respective yeast vacuole (Rohde et al., 2003). Vam3pA4 mutant, in which four amino acids were mutated into alanine, showed less fusion efficiency in *in vitro* fusion assay (unpublished). Sucrose gradient result shows that Vam3pA4 has a similar SNARE complex assembly as wild type (Figure 33, fraction 4-5). On the other hand when the alanine mutation (Vam3pA4bb) was carried out on the backside of the helix, in *in vitro* fusion assay the fusion efficiency was between wild type and Vam3pA4. Here sucrose gradient result shows that Vam3A4bb forms a similar SNARE complex (Figure 33) like wild type or A4 mutant. Probably these mutants are affecting membrane fusion after post docking stage like Vam3p isoprenoid mutant (Rohde et al., 2003).

Considering all the result of the self-interaction and the ternary complex formation with different Vam3p TMD mutants of yeast vacuolar SNARE proteins the possible interactions cycle could be summarized as (Figure 37) – i) Vam3p and Vti1p are stabilized as dimer, ii) Vam3p is in binary or ternary complex with other SNARE proteins as intermediate complexes, iii) SNARE proteins form tetrameric full complex which is completely zipped till TMD.

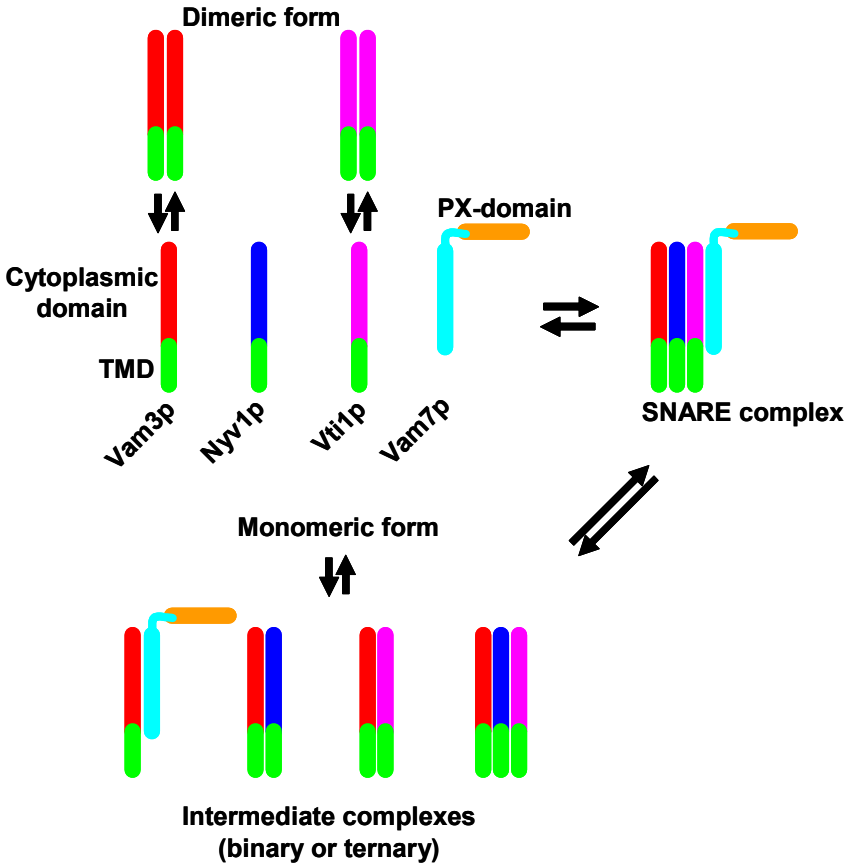

Figure 37. **Possible interaction cycle of yeast vacuolar SNARE proteins**. The individual yeast vacuolar SNARE proteins are present in monomeric forms that are in equilibrium with dimeric (homo- or hetero-dimers) forms and ternary forms. The monomeric vacuolar SNARE proteins and the intermediate complexes are also in equilibrium with the full tetrameric vacuolar SNARE complex. Unspecific multimers are not considered in this picture.

SNARE complex formation was also studied with the only cytoplasmic domains of all the SNARE proteins. Co-immunoprecipitation results show the formation of multimeric aggregates of SNARE complexes in addition to smaller complexes (Figure 34). This result confirm the possibility of SNARE complex formation via SNARE motif without the C-terminal TMD as found by other investigators (Fasshauer et al., 1999; Yang et al., 1999).

SNARE complex was assembled also with vacuolar SNARE protein mutants, in which the TMD had been substituted by alanine repeats. The results obtained here by sucrose gradient separation show that Vam3pAla20, Nyv1pAla21 and Vti1pAla23 interact to form complexes, but a full SNARE complex with all the four proteins can

not be detected as Vam7p is not found in fraction 3-5 (Figure 35), whereas most of the Vam7p was detected in the supernatant of the immunoprecipitated fractions.

Since a pentameric *cis*-complex, made by Vam3p, Nyv1p, Vti1p, Vam7p and Ykt6p, was described in yeast vacuole (Ungermann et al., 1999a) I incubated all these five SNAREs for *in vitro* complex formation. The sucrose gradient separation of the mixture of five SNARE proteins shows that Ykt6p is not detected in the high molecular weight fractions, as the other four proteins (fraction 3-5) (Figure 36), indicating the formation of SNARE complex without Ykt6p. A more sensible detection by co-immunoprecipitation was not achievable because GST-Ykt6p is recognized by all the antibodies used. In our experimental conditions it was not possible to detect a pentameric complex, possibly due to: i) the very unstable Ykt6p interaction with other SNARE proteins, or ii) the stabilization of dimeric form in GST-Ykt6p, or iii) the autoinhibitory effect of Ykt6p N-terminus domain (Tochio et al., 2001). It has been shown that Ykt6p is responsible of Vac8p palmitoylation and it is released during the priming step of vacuole fusion, when cis-complex is disrupted (Dietrich et al., 2004).

7 Conclusions

In summary, it can be concluded from the work presented here that synaptobrevin II homodimerization was successfully detected by urea SDS-PAGE and urea is not hampering the secondary structure of the synaptobrevin II TMD.

Studies on yeast vacuolar SNARE proteins showed that Vam3p self-interaction is mediated by the TMD. Mutations in Vam3p TMD or deletion of the Vam3p TMD disrupt the Vam3p homo interaction. The other yeast vacuolar SNARE proteins: Nyv1p and Vti1p form homo dimers, but they are not mediated by their TMD. Probably the homo dimers of Nyv1p and Vti1p are mediated by the SNARE domain of these proteins. Also soluble Ykt6p shows homo dimer in sucrose gradient separation. The other vacuolar SNARE Vam7p is monomer in native condition.

Results obtained here show for the first time the isolation of an *in vitro* complex of the full length vacuolar SNARE proteins – Vam3p, Nyv1p, Vti1p and Vam7p. SNARE complex can be disrupted by Sec18p and Sec17p in the presence of ATP and $MgCl_2$, confirming that it is a specific SNARE complex and not an unspecific aggregation of the proteins. Vam3p TMD has a key role in SNARE complex, since its exchange or deletion is strongly affecting SNARE complex assembly, leading to the partial formation of probably unspecific multimeric complexes. Deletion of all the TMDs of SNARE proteins or their mutations into alanine stretch leads to the formation of same unspecific multimeric complexes. In our experimental condition a pentameric SNARE complex with Vam3p, Nyv1p, Vti1p, Vam7p and Ykt6p could not be identified, but other binary or ternary interactions of Ykt6p with other SNARE proteins can not be ruled out.

8 Future outlooks

The results presented here showed the importance of vacuolar SNARE proteins TMD in their homo interactions and complex formation, though several aspects need to be addressed to elucidate a more precise picture of the SNARE complex and membrane fusion. Results presented here showed that Vam3p TMD is important for self-interaction and SNARE protein interaction and membrane fusion. Alanine scanning mutagenesis can be carried out to reveal the important amino acids for Vam3p TMD-TMD interaction. The binary and ternary interactions of SNARE proteins can reveal more insight about the composition of *cis*-SNARE complexes and the importance of TMD in the SNARE proteins interactions. Mutations in the other part of the SNARE proteins also can be carried out to know the importance in mediating interaction.

9 References

Adams, P. D., Engelman, D. M., and Brünger, A. T. (1996). Improved prediction for the structure of the dimeric transmembrane domain of glycophorin A obtained through global searching. Proteins *26*, 257-261.

Almers, W., and Tse, F. W. (1990). Transmitter release from synapses: does a preassembled fusion pore initiate exocytosis? Neuron *4*, 813-818.

Antonin, W., Fasshauer, D., Becker, S., Jahn, R., and Schneider, T. R. (2002). Crystal structure of the endosomal SNARE complex reveals common structural principles of all SNAREs. Nat Struct Biol *9*, 107-111.

Banerjee, A., Barry, V. A., DasGupta, B. R., and Martin, T. F. (1996). N-Ethylmaleimide-sensitive factor acts at a prefusion ATP-dependent step in Ca2+-activated exocytosis. J Biol Chem *271*, 20223-20226.

Barrowman, J., Sacher, M., and Ferro-Novick, S. (2000). TRAPP stably associates with the Golgi and is required for vesicle docking. EMBO J *19*, 862-869.

Baumert, M., Maycox, P. R., Navone, F., De Camilli, P., and Jahn, R. (1989). Synaptobrevin: an integral membrane protein of 18,000 daltons present in small synaptic vesicles of rat brain. EMBO J *8*, 379-384.

Bennett, M. K., Calakos, N., and Scheller, R. H. (1992). Syntaxin: a synaptic protein implicated in docking of synaptic vesicles at presynaptic active zones. Science *257*, 255-259.

Bennett, M. K., and Scheller, R. H. (1993). The molecular machinery for secretion is conserved from yeast to neurons. Proc Natl Acad Sci USA *90*, 2559-2563.

Bittner, M. A., and Holz, R. W. (1992). A temperature-sensitive step in exocytosis. J Biol Chem *267*, 16226-16229.

Boeddinghaus, C., Merz, A. J., Laage, R., and Ungermann, C. (2002). A cycle of Vam7p release from and PtdIns 3-P-dependent rebinding to the yeast vacuole is required for homotypic vacuole fusion. J Cell Biol *157*, 79-89.

Bohm, G., Muhr, R., and Jaenicke, R. (1992). Quantitative analysis of protein far UV circular dichroism spectra by neural networks. Protein Eng *5*, 191-195.

Bowen, M. E., Engelman, D. M., and Brunger, A. T. (2002). Mutational analysis of synaptobrevin transmembrane domain oligomerization. Biochemistry *41*, 15861-15866.

Bradford, M. M. (1976). A rapid and sensitive method for the quantitation of microgram quantities of protein utilizing the principle of protein-dye binding. Anal Biochem *72*, 248-254.

Broadie, K., Prokop, A., Bellen, H. J., O'Kane, C. J., Schulze, K. L., and Sweeney, S. T. (1995). Syntaxin and synaptobrevin function downstream of vesicle docking in Drosphila. Neuron *15*, 663-673.

Brosig, B., and Langosch, D. (1998). The dimerization motif of the glycophorin A transmembrane segment in membranes: importance of glycine residues. Protein Sci *7*, 1052-1056.

Brugger, B., Nickel, W., Weber, T., Parlati, F., McNew, J. A., Rothman, J. E., and Sollner, T. (2000). Putative fusogenic activity of NSF is restricted to a lipid mixture whose coalescence is also triggered by other factors. EMBO J *19*, 1272-1278.

Burri, L., and Lithgow, T. (2004). A complete set of SNAREs in yeast. Traffic *5*, 45-52.

Calakos, N., and Scheller, R. H. (1994). Vesicle-associated membrane protein and synaptophysin are associated on the synaptic vesicle. J Biol Chem *269*, 24534-24537.

Catlett, N. L., and Weisman, L. S. (2000). Divide and multiply: organelle partitioning in yeast. Curr Opin Cell Biol *12*, 509-516.

Cheever, M. L., Sato, T. K., de Beer, T., Kutateladze, T. G., Emr, S. D., and Overduin, M. (2001). Phox domain interaction with PtdIns(3)P targets the Vam7 t-SNARE to vacuole membranes. Nat Cell Biol *3*, 613-618.

Chen, Y. A., Scales, S. J., Patel, S. M., Doung, Y.-C., and Scheller, R. H. (1999). SNARE complex formation is triggered by Ca^{2+} and drives membrane fusion. Cell *97*, 165-174.

Chen, Y. A., and Scheller, R. H. (2001). SNARE-mediated membrane fusion. Nat Rev Mol Cell Biol *2*, 98-106.

Chernomordik, L. V., Melikyan, G. B., and Chizmadzhev, Y. A. (1987). Biomembrane fusion: a new concept derived from model studies using two interacting planar lipid bilayers. Biochim Biophys Acta *906*, 309-352.

Christoforidis, S., McBride, H. M., Burgoyne, R. D., and Zerial, M. (1999). The Rab5 effector EEA1 is a core component of endosome docking. Nature *397*, 621-625.

Clary, D. O., Griff, I. C., and Rothman, J. E. (1990). SNAPs, a family of NSF attachment proteins involved in intracellular membrane fusion in animals and yeast. Cell *61*, 709-721.

Clary, D. O., and Rothman, J. E. (1990). Purification of three related peripheral membrane proteins needed for vesicular transport. J Biol Chem *265*, 10109-10117.

Conradt, B., Haas, A., and Wickner, W. (1994). Determination of four biochemically distinct, sequential stages during vacuole inheritance in vitro. J Cell Biol *126*, 99-110.

Conradt, B., Shaw, J., Vida, T., Emr, S., and Wickner, W. (1992). In vitro reactions of vacuole inheritance in Saccharomyces cerevisiae. J Cell Biol *119*, 1469-1479.

Cowan, S. W., Schirmer, T., Rummel, G., Steiert, M., Ghosh, R., Pauptit, R. A., Jansonius, J. N., and Rosenbusch, J. P. (1992). Crystal structures explain functional properties of two E. coli porins. Nature *358*, 727-733.

Darsow, T., Rieder, S. E., and Emr, S. D. (1997). A multispecificity syntaxin homologue, Vam3p, essential for autophagic and biosynthetic protein transport to the vacuole. J Cell Biol *138*, 517-529.

Dietrich, L. E., Boeddinghaus, C., LaGrassa, T. J., and Ungermann, C. (2003). Control of eukaryotic membrane fusion by N-terminal domains of SNARE proteins. Biochim Biophys Acta *1641*, 111-119.

Dietrich, L. E., Gurezka, R., Veit, M., and Ungermann, C. (2004). The SNARE Ykt6 mediates protein palmitoylation during an early stage of homotypic vacuole fusion. EMBO J *23*, 45-53.

Dietrich, L. E., and Ungermann, C. (2004). On the mechanism of protein palmitoylation. EMBO Rep *5*, 1053-1057.

Dilcher, M., Kohler, B., and von Mollard, G. F. (2001). Genetic interactions with the yeast Q-SNARE VTI1 reveal novel functions for the R-SNARE YKT6. J Biol Chem *276*, 34537-34544.

Dill, K. A., and Shortle, D. (1991). Denatured states of proteins. Annu Rev Biochem *60*, 795-825.

Dougan, D. A., Mogk, A., and Bukau, B. (2002). Protein folding and degradation in bacteria: to degrade or not to degrade? That is the question. Cell Mol Life Sci *59*, 1607-1616.

Doyle, D. A., Morais Cabral, J., Pfuetzner, R. A., Kuo, A., Gulbis, J. M., Cohen, S. L., Chait, B. T., and MacKinnon, R. (1998). The structure of the potassium channel: molecular basis of K+ conduction and selectivity. Science *280*, 69-77.

Dulubova, I., Yamaguchi, T., Wang, Y., Sudhof, T. C., and Rizo, J. (2001). Vam3p structure reveals conserved and divergent properties of syntaxins. Nat Struct Biol *8*, 258-264.

Edelmann, L., Hanson, P. I., Chapman, E. R., and Jahn, R. (1995). Synaptobrevin binding to synaptophysin: a potential mechanism for controlling the exocytotic fusion machine. EMBO J *14*, 224-231.

Fasshauer, D. (2003). Structural insights into the SNARE mechanism. Biochim Biophys Acta *1641*, 87-97.

Fasshauer, D., Antonin, W., Margittai, M., Pabst, S., and Jahn, R. (1999). Mixed and non-cognate SNARE complexes. Characterization of assembly and biophysical properties. J Biol Chem *274*, 15440-15446.

Fasshauer, D., Antonin, W., Subramaniam, V., and Jahn, R. (2002). SNARE assembly and disassembly exhibit a pronounced hysteresis. Nat Struct Biol *9*, 144-151.

Fasshauer, D., Bruns, D., Shen, B., Jahn, R., and Brunger, A. T. (1997a). A structural change occurs upon binding of syntaxin to SNAP-25. J Biol Chem *272*, 4582-4590.

Fasshauer, D., Eliason, W. K., Brunger, A. T., and Jahn, R. (1998a). Identification of a minimal core of the synaptic SNARE complex sufficient for reversible assembly and disassembly. Biochemistry *37*, 10354-10362.

Fasshauer, D., Otto, H., Eliason, W. K., Jahn, R., and Brunger, A. T. (1997b). Structural changes are associated with soluble N-ethylmaleimide-sensitive fusion protein attachment protein receptor complex formation. J Biol Chem *272*, 28036-28041.

Fasshauer, D., Sutton, R. B., Brunger, A. T., and Jahn, R. (1998b). Conserved structural features of the synaptic fusion complex: SNARE proteins reclassified as Q- and R-SNAREs. Proc Natl Acad Sci USA *95*, 15781-15786.

Fernandez, I., Ubach, J., Dulubova, I., Zhang, X., Sudhof, T. C., and Rizo, J. (1998). Three-dimensional structure of an evolutionarily conserved N-terminal domain of syntaxin 1A. Cell *94*, 841-849.

Fischer von Mollard, G., and Stevens, T. H. (1999). The Saccharomyces cerevisiae v-SNARE Vti1p is required for multiple membrane transport pathways to the vacuole. Mol Biol Cell *10*, 1719-1732.

Fischer von Mollard, G. F., Nothwehr, S. F., and Stevens, T. H. (1997). The yeast v-SNARE Vti1p mediates two vesicle transport pathways through interactions with the t-SNAREs Sed5p and Pep12p. J Cell Biol *137*, 1511-1524.

Flanagan, J. M., Kataoka, M., Shortle, D., and Engelman, D. M. (1992). Truncated staphylococcal nuclease is compact but disordered. Proc Natl Acad Sci USA *89*, 748-752.

Fleming, K. G., and Engelman, D. M. (2001). Computation and mutagenesis suggest a right-handed structure for the synaptobrevin transmembrane dimer. Proteins *45*, 313-317.

From, N. B., and Bowler, B. E. (1998). Urea denaturation of staphylococcal nuclease monitored by Fourier transform infrared spectroscopy. Biochemistry *37*, 1623-1631.

Fukasawa, M., Varlamov, O., Eng, W. S., Sollner, T. H., and Rothman, J. E. (2004). Localization and activity of the SNARE Ykt6 determined by its regulatory domain and palmitoylation. Proc Natl Acad Sci USA *101*, 4815-4820.

Gonzalez, L. C., Jr., Weis, W. I., and Scheller, R. H. (2001). A novel snare N-terminal domain revealed by the crystal structure of Sec22b. J Biol Chem *276*, 24203-24211.

Gorvel, J. P., Chavrier, P., Zerial, M., and Gruenberg, J. (1991). rab5 controls early endosome fusion in vitro. Cell *64*, 915-925.

Graham, T. R., and Emr, S. D. (1991). Compartmental organization of Golgi-specific protein modification and vacuolar protein sorting events defined in a yeast sec18 (NSF) mutant. J Cell Biol *114*, 207-218.

Grote, E., Baba, M., Ohsumi, Y., and Novick, P. J. (2000). Geranylgeranylated SNAREs are dominant inhibitors of membrane fusion. J Cell Biol *151*, 453-466.

Guo, W., Sacher, M., Barrowman, J., Ferro-Novick, S., and Novick, P. (2000). Protein complexes in transport vesicle targeting. Trends Cell Biol *10*, 251-255.

Gurezka, R., Laage, R., Brosig, B., and Langosch, D. (1999). A heptad motif of leucine residues found in membrane proteins can drive self-assembly of artificial transmembrane segments. J Biol Chem *274*, 9265-9270.

Haas, A., and Wickner, W. (1996). Homotypic vacuole fusion requires Sec17p (yeast alpha-SNAP) and Sec18p (yeast NSF). EMBO J *15*, 3296-3305.

Hanson, P. I., Heuser, J. E., and Jahn, R. (1997a). Neurotransmitter release - four years of SNARE complexes. Curr Opin Neurobiol *7*, 310-315.

Hanson, P. I., Otto, H., Barton, N., and Jahn, R. (1995). The N-ethylmaleimide-sensitive fusion protein and alpha-SNAP induce a conformational change in syntaxin. J Biol Chem *270*, 16955-16961.

Hanson, P. I., Roth, R., Morisaki, H., Jahn, R., and Heuser, J. E. (1997b). Structure and conformational changes in NSF and its membrane receptor complexes visualized by quick-freeze/deep-etch electron microscopy. Cell *90*, 523-535.

Hartl, F. U., and Hayer-Hartl, M. (2002). Molecular chaperones in the cytosol: from nascent chain to folded protein. Science *295*, 1852-1858.

Hay, J. C., and Scheller, R. H. (1997). SNAREs and NSF in targeted membrane fusion. Curr Opin Cell Biol *9*, 505-512.

Hess, D. T., Slater, T. M., Wilson, M. C., and Skene, J. H. (1992). The 25 kDa synaptosomal-associated protein SNAP-25 is the major methionine-rich polypeptide in rapid axonal transport and a major substrate for palmitoylation in adult CNS. J Neurosci *12*, 4634-4641.

Hicke, L. (1999). Gettin' down with ubiquitin: turning off cell-surface receptors, transporters and channels. Trends Cell Biol *9*, 107-112.

Hicke, L., Zanolari, B., Pypaert, M., Rohrer, J., and Riezman, H. (1997). Transport through the yeast endocytic pathway occurs through morphologically distinct compartments and requires an active secretory pathway and Sec18p/N-ethylmaleimide-sensitive fusion protein. Mol Biol Cell *8*, 13-31.

High, S., and Dobberstein, B. (1992). Mechanisms that determine the transmembrane disposition of proteins. Curr Opin Cell Biol *4*, 581-586.

Hofmann, M. W., Weise, K., Ollesch, J., Agrawal, P., Stalz, H., Stelzer, W., Hulsbergen, F., de Groot, H., Gerwert, K., Reed, J., and Langosch, D. (2004). De novo design of conformationally flexible transmembrane peptides driving membrane fusion. Proc Natl Acad Sci USA *101*, 14776-14781.

Hohl, T. M., Parlati, F., Wimmer, C., Rothman, J. E., Sollner, T. H., and Engelhardt, H. (1998). Arrangement of subunits in 20 S particles consisting of NSF, SNAPs, and SNARE complexes. Mol Cell *2*, 539-548.

Horsnell, W. G. C., Steel, G. J., and Morgan, A. (2002). Analysis of NSF mutants reveals residues involved in SNAP binding and ATPase stimulation. Biochemistry *41*, 5230-5235.

Hunt, J. M., Bommert, K., Charlton, M. P., Kistner, A., Habermann, E., Augustine, G. J., and Betz, H. (1994). A post-docking role for synaptobrevin in synaptic vesicle fusion. Neuron *12*, 1269-1270.

Ibaraki, K., Horikawa, H. P., Morita, T., Mori, H., Sakimura, K., Mishina, M., Saisu, H., and Abe, T. (1995). Identification of four different forms of syntaxin 3. Biochem Biophys Res Commun *211*, 997-1005.

Inoue, H., Nojima, H., and Okayama, H. (1990). High efficiency transformation of Escherichia coli with plasmids. Gene *96*, 23-28.

Jahn, R. (1999). Recycling of synaptic vesicle membrane within nerve terminals. Brain Res Bull *50*, 313-314.

Jahn, R. (2000). Sec1/Munc18 proteins: mediators of membrane fusion moving to center stage. Neuron *27*, 201-204.

Jahn, R. (2004). Principles of exocytosis and membrane fusion. Ann N Y Acad Sci *1014*, 170-178.

Jahn, R., and Grubmuller, H. (2002). Membrane fusion. Curr Opin Cell Biol *14*, 488-495.

Jahn, R., Lang, T., and Sudhof, T. C. (2003). Membrane fusion. Cell *112*, 519-533.

Jahn, R., and Sudhof, T. C. (1999). Membrane fusion and exocytosis. Annu Rev Biochem *68*, 863-911.

Klionsky, D. J., Herman, P. K., and Emr, S. D. (1990). The fungal vacuole: composition, function, and biogenesis. Microbiol Rev *54*, 266-292.

Kozlov, M. M., and Markin, V. S. (1983). [Possible mechanism of membrane fusion]. Biofizika *28*, 242-247.

Kweon, Y., Rothe, A., Conibear, E., and Stevens, T. H. (2003). Ykt6p is a multifunctional yeast R-SNARE that is required for multiple membrane transport pathways to the vacuole. Mol Biol Cell *14*, 1868-1881.

Laage, R., and Langosch, D. (1997). Dimerization of the synaptic vesicle protein synaptobrevin (vesicle-associated membrane protein) II depends on specific residues within the transmembrane segment. Eur J Biochem *249*, 540-546.

Laage, R., and Langosch, D. (2001). Strategies for prokaryotic expression of eukaryotic membrane proteins. Traffic *2*, 99-104.

Laage, R., Rohde, J., Brosig, B., and Langosch, D. (2000). A conserved membrane-spanning amino acid motif drives homomeric and supports heteromeric assembly of presynaptic SNARE proteins. J Biol Chem *275*, 17481-17487.

Laage, R., and Ungermann, C. (2001). The N-terminal domain of the t-SNARE Vam3p coordinates priming and docking in yeast vacuole fusion. Mol Biol Cell *12*, 3375-3385.

Laemmli, U. K. (1970). Cleavage of structural proteins during the assembly of the head of bacteriophage T4. Nature *227*, 680-685.

Langosch, D., Crane, J. M., Brosig, B., Hellwig, A., Tamm, L. K., and Reed, J. (2001). Peptide mimics of SNARE transmembrane segments drive membrane fusion depending on their conformational plasticity. J Mol Biol *311*, 709-721.

Langosch, D. L., Brosig, B., Kolmar, H., and Fritz, H.-J. (1996). Dimerisation of the glycophorin A transmembrane segment in membranes probed with the ToxR transcription activator. J Mol Biol *263*, 525-530.

Lemmon, M. A., Flanagan, J. M., Treutlein, H. R., Zhang, J., and Engelman, D. M. (1992). Sequence specificity in the dimerization of transmembrane alpha-helices. Biochemistry *31*, 12719-12725.

Lerman, J. C., Robblee, J., Fairman, R., and Hughson, F. M. (2000). Structural analysis of the neuronal SNARE protein syntaxin-1A. Biochemistry *39*, 8470-8479.

Lindau, M., and Almers, W. (1995). Structure and function of fusion pores in exocytosis and ectoplasmic membrane fusion. Curr Opin Cell Biol *7*, 509-517.

Littleton, J. T., Chapman, E. R., Kreber, R., Garment, M. B., Carlson, S. D., and Ganetzky, B. (1998). Temperature-sensitive paralytic mutations demonstrate that synaptic exocytosis requires SNARE complex assembly and disassembly. Neuron *21*, 401-413.

Liu, Y., and Barlowe, C. (2002). Analysis of Sec22p in endoplasmic reticulum/Golgi transport reveals cellular redundancy in SNARE protein function. Mol Biol Cell *13*, 3314-3324.

Lu, J., Garcia, J., Dulubova, I., Sudhof, T. C., and Rizo, J. (2002). Solution structure of the Vam7p PX domain. Biochemistry *41*, 5956-5962.

MacKenzie, K. R., Prestegard, J. H., and Engelman, D. M. (1997). A transmembrane helix dimer: structure and implications. Science *276*, 131-133.

Margittai, M., Fasshauer, D., Jahn, R., and Langen, R. (2003). The Habc domain and the SNARE core complex are connected by a highly flexible linker. Biochemistry *42*, 4009-4014.

Margittai, M., Otto, H., and Jahn, R. (1999). A stable interaction between syntaxin 1a and synaptobrevin 2 mediated by their transmembrane domains. FEBS Lett *446*, 40-44.

Martinez-Arca, S., Alberts, P., Zahraoui, A., Louvard, D., and Galli, T. (2000). Role of tetanus neurotoxin insensitive vesicle-associated membrane protein (TI-VAMP) in vesicular transport mediating neurite outgrowth. J Cell Biol *149*, 889-900.

Mayer, A. (1999). Intracellular membrane fusion: SNAREs only? Curr Opin Cell Biol *11*, 447-452.

Mayer, A. (2001). What drives membrane fusion in eukaryotes? Trends Biochem Sci *26*, 717-723.

Mayer, A. (2002). Membrane fusion in eukaryotic cells. Annu Rev Cell Dev Biol *18*, 289-314. Epub 2002 Apr 2002.

Mayer, A., and Wickner, W. (1997). Docking of yeast vacuoles is catalyzed by the Ras-like GTPase Ypt7p after symmetric priming by Sec18p (NSF). J Cell Biol *136*, 307-317.

Mayer, A., Wickner, W., and Haas, A. (1996). Sec18p (NSF)-driven release of Sec17p (alpha-SNAP) can precede docking and fusion of yeast vacuoles. Cell *85*, 83-94.

McNew, J. A., Parlati, F., Fukuda, R., Johnston, R. J., Paz, K., Paumet, F., Sollner, T. H., and Rothman, J. E. (2000). Compartmental specificity of cellular membrane fusion encoded in SNARE proteins. Nature *407*, 153-159.

McNew, J. A., Sogaard, M., Lampen, N. M., Machida, S., Ye, R. R., Lacomis, L., Tempst, P., Rothman, J. E., and Sollner, T. H. (1997). Ykt6p, a prenylated SNARE essential for endoplasmic reticulum-Golgi transport. J Biol Chem *272*, 17776-17783.

Mingarro, I., Whitley, P., Lemmon, M. A., and von Heijne, G. (1996). Ala-insertion scanning mutagenesis of the glycophorin A transmembrane helix: a rapid way to map helix-helix interactions in integral membrane proteins. Protein Sci *5*, 1339-1341.

Minor, D. L., Jr., and Kim, P. S. (1994). Measurement of the beta-sheet-forming propensities of amino acids. Nature *367*, 660-663.

Monck, J. R., Oberhauser, A. F., and Fernandez, J. M. (1995). The exocytotic fusion pore interface: a model of the site of neurotransmitter release. Mol Membr Biol *12*, 151-156.

Mujacic, M., Cooper, K. W., and Baneyx, F. (1999). Cold-inducible cloning vectors for low-temperature protein expression in Escherichia coli: application to the production of a toxic and proteolytically sensitive fusion protein. Gene *238*, 325-332.

Munson, M., Chen, X., Cocina, A. E., Schultz, S. M., and Hughson, F. M. (2000). Interactions within the yeast t-SNARE Sso1p that control SNARE complex assembly. Nat Struct Biol *7*, 894-902.

Neiman, A. M. (1998). Prospore membrane formation defines a developmentally regulated branch of the secretory pathway in yeast. J Cell Biol *140*, 29-37.

Neiman, A. M., Katz, L., and Brennwald, P. J. (2000). Identification of domains required for developmentally regulated SNARE function in Saccharomyces cerevisiae. Genetics *155*, 1643-1655.

Nichols, B. J., Ungermann, C., Pelham, H. R., Wickner, W. T., and Haas, A. (1997). Homotypic vacuolar fusion mediated by t- and v-SNAREs. Nature *387*, 199-202.

Nicholson, K. L., Munson, M., Miller, R. B., Filip, T. J., Fairman, R., and Hughson, F. M. (1998). Regulation of SNARE complex assembly by an N-terminal domain of the t-SNARE Sso1p. Nat Struct Biol *5*, 793-802.

Nonet, M. L., Saifee, O., Zhao, H., Rand, J. B., and Wei, L. (1998). Synaptic transmission deficits in Caenorhabditis elegans synaptobrevin mutants. J Neurosci *18*, 70-80.

Novick, P., and Zerial, M. (1997). The diversity of Rab proteins in vesicle transport. Curr Opin Cell Biol *9*, 496-504.

Oyler, G. A., Higgins, G. A., Hart, R. A., Battenberg, E., Billingsley, M., Bloom, F. E., and Wilson, M. C. (1989). The identification of a novel synaptosomal-associated protein, SNAP-25, differentially expressed by neuronal subpopulations. J Cell Biol *109*, 3039-3052.

Pelham, H. R. (2001). SNAREs and the specificity of membrane fusion. Trends Cell Biol *11*, 99-101.

Peters, C., and Mayer, A. (1998). Ca2+/calmodulin signals the completion of docking and triggers a late step of vacuole fusion. Nature *396*, 575-580.

Poirier, M. A., Hao, J. C., Malkus, P. N., Chan, C., Moore, M. F., King, D. S., and Bennett, M. K. (1998a). Protease resistance of syntaxin.SNAP-25.VAMP complexes. Implications for assembly and structure. J Biol Chem *273*, 11370-11377.

Poirier, M. A., Xiao, W., Macosko, J. C., Chan, C., Shin, Y. K., and Bennett, M. K. (1998b). The synaptic SNARE complex is a parallel four-stranded helical bundle. Nat Struct Biol *5*, 765-769.

Price, A., Seals, D., Wickner, W., and Ungermann, C. (2000a). The docking stage of yeast vacuole fusion requires the transfer of proteins from a cis-SNARE complex to a Rab/Ypt protein. J Cell Biol *148*, 1231-1238.

Price, A., Wickner, W., and Ungermann, C. (2000b). Proteins needed for vesicle budding from the Golgi complex are also required for the docking step of homotypic vacuole fusion. J Cell Biol *148*, 1223-1229.

Qing, G., Ma, L. C., Khorchid, A., Swapna, G. V., Mal, T. K., Takayama, M. M., Xia, B., Phadtare, S., Ke, H., Acton, T.*, et al.* (2004). Cold-shock induced high-yield protein production in Escherichia coli. Nat Biotechnol *22*, 877-882. Epub 2004 Jun 2013.

Rohde, J. (2002) Analysis of SNARE transmembrane domains in membrane fusion, Ph. D. Thesis, University of Heidelberg.

Rohde, J., Dietrich, L., Langosch, D., and Ungermann, C. (2003). The transmembrane domain of Vam3 affects the composition of cis- and trans-SNARE complexes to promote homotypic vacuole fusion. J Biol Chem *278*, 1656-1662. Epub 2002 Nov 1608.

Rothman, J. E. (1994a). Intracellular membrane fusion. Adv Second Messenger Phosphoprotein Res *29*, 81-96.

Rothman, J. E. (1994b). Mechanisms of intracellular protein transport. Nature *372*, 55-63.

Roy, R., Laage, R., and Langosch, D. (2004). Synaptobrevin transmembrane domain dimerization-revisited. Biochemistry *43*, 4964-4970.

Russ, W. P., and Engelman, D. M. (2000). The GxxxG motif: a framework for transmembrane helix-helix association. J Mol Biol *296*, 911-919.

Sacher, M., and Ferro-Novick, S. (2001). Purification of TRAPP from Saccharomyces cerevisiae and identification of its mammalian counterpart. Methods Enzymol *329*, 234-241.

Sacher, M., Jiang, Y., Barrowman, J., Scarpa, A., Burston, J., Zhang, L., Schieltz, D., Yates, J. R., 3rd, Abeliovich, H., and Ferro-Novick, S. (1998). TRAPP, a highly conserved novel complex on the cis-Golgi that mediates vesicle docking and fusion. EMBO J *17*, 2494-2503.

Saifee, O., Wei, L., and Nonet, M. L. (1998). The Caenorhabditis elegans unc-64 locus encodes a syntaxin that interacts genetically with synaptobrevin. Mol Biol Cell *9*, 1235-1252.

Sato, T. K., Darsow, T., and Emr, S. D. (1998). Vam7p, a SNAP-25-like molecule, and Vam3p, a syntaxin homolog, function together in yeast vacuolar protein trafficking. Mol Cell Biol *18*, 5308-5319.

Sato, T. K., Overduin, M., and Emr, S. D. (2001). Location, location, location: membrane targeting directed by PX domains. Science *294*, 1881-1885.

Sato, T. K., Rehling, P., Peterson, M. R., and Emr, S. D. (2000). Class C Vps protein complex regulates vacuolar SNARE pairing and is required for vesicle docking/fusion. Mol Cell *6*, 661-671.

Scales, S. J., Chen, Y. A., Yoo, B. Y., Patel, S. M., Doung, Y. C., and Scheller, R. H. (2000). SNAREs contribute to the specificity of membrane fusion. Neuron *26*, 457-464.

Schulze, K. L., Broadie, K., Perin, M. S., and Bellen, H. J. (1995). Genetic and electrophysiological studies of Drosophila syntaxin-1A demonstrate its role in nonneuronal secretion and neurotransmission. Cell *80*, 311-320.

Seals, D. F., Eitzen, G., Margolis, N., Wickner, W. T., and Price, A. (2000). A Ypt/Rab effector complex containing the Sec1 homolog Vps33p is required for homotypic vacuole fusion. Proc Natl Acad Sci USA *97*, 9402-9407.

Senes, A., Ubarretxena-Belandia, I., and Engelman, D. M. (2001). The Ca-H...O hydrogen bond: A determinant of stability and specifity in transmembrane helix interactions. Proc Natl Acad Sci *98*, 9056-9061.

Smith, S. O., Song, D., Shekar, S., Groesbeek, M., Ziliox, M., and Aimoto, S. (2001). Structure of the Transmembrane Dimer Interface of Glycophorin A in Membrane Bilayers. Biochemistry *40*, 6553-6558.

Sollner, T., Bennett, M. K., Whiteheart, S. W., Scheller, R. H., and Rothman, J. E. (1993a). A protein assembly-disassembly pathway in vitro that may correspond to sequential steps of synaptic vesicle docking, activation, and fusion. Cell *75*, 409-418.

Sollner, T., Whiteheart, S. W., Brunner, M., Erdjument-Bromage, H., Geromanos, S., Tempst, P., and Rothman, J. E. (1993b). SNAP receptors implicated in vesicle targeting and fusion. Nature *362*, 318-324.

Soulie, S., Moller, J. V., Falson, P., and le Maire, M. (1996). Urea reduces the aggregation of membrane proteins on sodium dodecyl sulfate-polyacrylamide gel electrophoresis. Anal Biochem *236*, 363-364.

Springer, S., and Schekman, R. (1998). Nucleation of COPII vesicular coat complex by endoplasmic reticulum to Golgi vesicle SNAREs. Science *281*, 698-700.

Srivastava, A., and Jones, E. W. (1998). Pth1/Vam3p is the syntaxin homolog at the vacuolar membrane of Saccharomyces cerevisiae required for the delivery of vacuolar hydrolases. Genetics *148*, 85-98.

Street, A. G., and Mayo, S. L. (1999). Intrinsic beta-sheet propensities result from van der Waals interactions between side chains and the local backbone. Proc Natl Acad Sci USA *96*, 9074-9076.

Sutton, R. B., Fasshauer, D., Jahn, R., and Brunger, A. T. (1998). Crystal structure of a SNARE complex involved in synaptic exocytosis at 2.4 A resolution. Nature *395*, 347-353.

Thorngren, N., Collins, K. M., Fratti, R. A., Wickner, W., and Merz, A. J. (2004). A soluble SNARE drives rapid docking, bypassing ATP and Sec17/18p for vacuole fusion. EMBO J *23*, 2765-2776.

Tishgarten, T., Yin, F. F., Faucher, K. M., Dluhy, R. A., Grant, T. R., Fischer von Mollard, G., Stevens, T. H., and Lipscomb, L. A. (1999). Structures of yeast vesicle trafficking proteins. Protein Sci *8*, 2465-2473.

Tochio, H., Tsui, M. M., Banfield, D. K., and Zhang, M. (2001). An autoinhibitory mechanism for nonsyntaxin SNARE proteins revealed by the structure of Ykt6p. Science *293*, 698-702.

Trimble, W. S., Cowan, D. M., and Scheller, R. H. (1988). VAMP-1: a synaptic vesicle-associated integral membrane protein. Proc Natl Acad Sci USA *85*, 4538-4542.

Ungar, D., and Hughson, F. M. (2003). SNARE protein structure and function. Annu Rev Cell Dev Biol *19*, 493-517.

Ungermann, C., Nichols, B. J., Pelham, H. R., and Wickner, W. (1998a). A vacuolar v-t-SNARE complex, the predominant form in vivo and on isolated vacuoles, is disassembled and activated for docking and fusion. J Cell Biol *140*, 61-69.

Ungermann, C., Sato, K., and Wickner, W. (1998b). Defining the functions of trans-SNARE pairs. Nature *396*, 543-548.

Ungermann, C., von Mollard, G. F., Jensen, O. N., Margolis, N., Stevens, T. H., and Wickner, W. (1999a). Three v-SNAREs and two t-SNAREs, present in a pentameric cis-SNARE complex on isolated vacuoles, are essential for homotypic fusion. J Cell Biol *145*, 1435-1442.

Ungermann, C., and Wickner, W. (1998). Vam7p, a vacuolar SNAP-25 homolog, is required for SNARE complex integrity and vacuole docking and fusion. EMBO J *17*, 3269-3276.

Ungermann, C., Wickner, W., and Xu, Z. (1999b). Vacuole acidification is required for trans-SNARE pairing, LMA1 release, and homotypic fusion. Proc Natl Acad Sci USA *96*, 11194-11199.

Veit, M., Becher, A., and Ahnert-Hilger, G. (2000). Synaptobrevin 2 Is Palmitoylated in Synaptic Vesicles Prepared from Adult, But Not from Embryonic Brain. Mol Cell Neurosci *15*, 408-416.

Veit, M., Laage, R., Dietrich, L., Wang, L., and Ungermann, C. (2001). Vac8p release from the SNARE complex and its palmitoylation are coupled and essential for vacuole fusion. EMBO J *20*, 3145-3155.

Vida, T. A., and Emr, S. D. (1995). A new vital stain for visualizing vacuolar membrane dynamics and endocytosis in yeast. J Cell Biol *128*, 779-792.

Wada, Y., Nakamura, N., Ohsumi, Y., and Hirata, A. (1997). Vam3p, a new member of syntaxin related protein, is required for vacuolar assembly in the yeast Saccharomyces cerevisiae. J Cell Sci *110*, 1299-1306.

Walter, A., Kuehl, G., Barnes, K., and VanderWaerdt, G. (2000). The vesicle-to-micelle transition of phosphatidylcholine vesicles induced by nonionic detergents: effects of sodium chloride, sucrose and urea. Biochim Biophys Acta *1508*, 20-33.

Walter, S., and Buchner, J. (2002). Molecular chaperones--cellular machines for protein folding. Angew Chem Int Ed Engl *41*, 1098-1113.

Wang, Y. X., Catlett, N. L., and Weisman, L. S. (1998). Vac8p, a vacuolar protein with armadillo repeats, functions in both vacuole inheritance and protein targeting from the cytoplasm to vacuole. J Cell Biol *140*, 1063-1074.

Washbourne, P., Schiavo, G., and Montecucco, C. (1995). Vesicle-associated membrane protein-2 (synaptobrevin-2) forms a complex with synaptophysin. Biochem J *305*, 721-724.

Weber, T., Zemelman, B. V., McNew, J. A., Westermann, B., Gmachl, M., Parlati, F., Sollner, T. H., and Rothman, J. E. (1998). SNAREpins: minimal machinery for membrane fusion. Cell *92*, 759-772.

Wegele, H., Muller, L., and Buchner, J. (2004). Hsp70 and Hsp90--a relay team for protein folding. Rev Physiol Biochem Pharmacol *151*, 1-44.

Weimbs, T., Low, S. H., Chapin, S. J., Mostov, K. E., Bucher, P., and Hofmann, K. (1997). A conserved domain is present in different families of vesicular fusion proteins: a new superfamily. Proc Natl Acad Sci USA *94*, 3046-3051.

Weisman, L. S. (2003). Yeast vacuole inheritance and dynamics. Annu Rev Genet *37*, 435-460.

Weisman, L. S., Bacallao, R., and Wickner, W. (1987). Multiple methods of visualizing the yeast vacuole permit evaluation of its morphology and inheritance during the cell cycle. J Cell Biol *105*, 1539-1547.

Weisman, L. S., Wickner, W., and Ballou, C. E. (1988). Intervacuole exchange in the yeast zygote: a new pathway in organelle communication Methanol production by Mycobacterium smegmatis. Science *241*, 589-591.

Wessel, D., and Flugge, U. I. (1984). A method for the quantitative recovery of protein in dilute solution in the presence of detergents and lipids. Anal Biochem *138*, 141-143.

Whiteheart, S. W., Brunner, M., Wilson, D. W., Wiedmann, M., and Rothman, J. E. (1992). Soluble N-ethylmaleimide-sensitive fusion attachment proteins (SNAPs) bind to a multi-SNAP receptor complex in Golgi membranes. J Biol Chem *267*, 12239-12243.

Whiteheart, S. W., Griff, I. C., Brunner, M., Clary, D. O., Mayer, T., Buhrow, S. A., and Rothman, J. E. (1993). SNAP family of NSF attachment proteins includes a brain-specific isoform. Nature *362*, 353-355.

Wickner, W. (2002). Yeast vacuoles and membrane fusion pathways. EMBO J *21*, 1241-1247.

Wickner, W., and Haas, A. (2000). Yeast homotypic vacuole fusion: a window on organelle trafficking mechanisms. Annu Rev Biochem *69*, 247-275.

Wilson, D. W., and Rothman, J. E. (1992). Expression and purification of recombinant N-ethylmaleimide-sensitive fusion protein from Escherichia coli. Methods Enzymol *219*, 309-318.

Wilson, D. W., Whiteheart, S. W., Wiedmann, M., Brunner, M., and Rothman, J. E. (1992). A multisubunit particle implicated in membrane fusion. J Cell Biol *117*, 531-538.

Wishart, M. J., Taylor, G. S., and Dixon, J. E. (2001). Phoxy lipids: revealing PX domains as phosphoinositide binding modules. Cell *105*, 817-820.

Yang, B., Gonzalez, L., Prekeris, R., Steegmaier, M., Advani, R. J., and Scheller, R. H. (1999). SNARE interactions are not selective - Implications for membrane fusion specificity. J Biol Chem *274*, 5649-5653.

Zerial, M., and McBride, H. (2001). Rab proteins as membrane organizers. Nat Rev Mol Cell Biol *2*, 107-117.

10 Abbreviations

A	Ala	Alanine
C	Cys	Cysteine
D	Asp	Aspartate
E	Glu	Glutamine
F	Phe	Phenylalanine
G	Gly	Glycine
H	His	Histidine
I	Ile	Isoleucine
K	Lys	Lysine
L	Leu	Leucine
M	Met	Methionine
N	Asn	Asparagine
P	Pro	Proline
Q	Gln	Glutamine
R	Arg	Arginine
S	Ser	Serine
T	Thr	Threonine
V	Val	Valine
W	Trp	Tryptophane
Y	Tyr	Tyrosine

Amp	Ampicillin
APS	Ammonium persulfate
BSA	Bovine serum albumin
CD	Circular dichroism
C.elegans	*Caenorhabditis elegans*
CHAPS	3-3[(3-cholamidopropyl)dimethylammonio]-1-propane-sulfonate
Cm	Chloramphenicol
Da	Dalton
DMP	Dimethylepimilidate

DMSO	Dimethylesulfoxide
DNA	Deoxyribonucleic acid
DNase	Deoxyribonuclease
dNTP	deoxynucleoside (5'-) triphosphate
ddNTP	di deoxynucleoside (5'-) triphosphate
ds DNA	double strand DNA
DTT	1,4-dithiothretol
E.coli	*Escherichia coli*
EDTA	Ethylenediamine-N-N-N'-N'-tetraacetic acid
EtOH	Ethanol
g	Acceleration of free fall (9.81 m/sec^2)
GST	Glutathione S-transferase
hr	Hour
HA	Hemagglutinin
HEPES	4-2(2-hydroxy-ethyl)-1-piperzine-ethanesulfonic acid
His-tag	Hexa-histidine sequence
HRP	Horseradish peroxidase
kDa	kilodalton
l	Liter
LB	Luria-Broth
M	Molar
mA	Miliampete
MeOH	Methanol
mg	Miligram
min	Minute
ml	Mililiter
mM	Milimolar
nm	nanometer (10^{-9} m)
NSF	N-ethylmaleimide sensitive factor
OD	Optical density (absorbance)
PBS	Phosphate buffered saline
PCR	Polymerase chain reaction
PMSF	Phenylmethylsulfonyl fluoride
RNA	Ribonucleic acid

SDS	Sodium dodecyle sulfate
SDS-PAGE	SDS-polyacrylamide gel electrophoresis
sec	Second
SNAP	Soluble N-ethylmaleimide sensitive factor attachment protein
SNAP-25	Synaptosomal associated protein of 25 kDa
SNARE	Soluble NSF attachment protein receptor
TBB	TBS with 0.1% Triton-X 100 and 5% milk powder
TBS	Tris-buffered saline
TEMED	N-N-N'-N'-tetra methylethylenediamide
TMD	Transmembrane domain
Tris	2-amino-2-hydroxymethyl-1,3-propanediol
tRNA	Transfer RNA
TWB	TBS with 0.1% Triton-X 100
µl	Microliter (10^{-6} l)
WT	Wild type